SOUTHERN PLAINS
TRANSPORTATION CENTER

UNDERSTANDING CLIMATE CHANGE IMPACT ON HIGHWAY HYDRAULIC DESIGN PROCEDURES

Anjuman Ara Akhtar, B.Sc.
Armando Esquivel, B.Sc.
Megha Sharma, Ph.D.
Vivek Tandon, Ph.D.

SPTC14.1-97-F

Southern Plains Transportation Center
201 Stephenson Parkway, Suite 4200
The University of Oklahoma
Norman, Oklahoma 73019

DISCLAIMER

The contents of this report reflect the views of the authors, who are responsible for the facts and accuracy of the information presented herein. This document is disseminated under the sponsorship of the Department of Transportation University Transportation Centers Program, in the interest of information exchange. The U.S. Government assumes no liability for the contents or use thereof.

TECHNICAL REPORT DOCUMENTATION PAGE

1. REPORT NO.	2. GOVERNMENT ACCESSION NO.	3. RECIPIENTS CATALOG NO.
SPTC14.1-97-F		

4. TITLE AND SUBTITLE	5. REPORT DATE
Understanding Climate Change Impact on Highway Hydraulic Design Procedures	December 2018
	6. PERFORMING ORGANIZATION CODE

7. AUTHOR(S)	8. PERFORMING ORGANIZATION REPORT
Anjuman Ara Akhtar, B.Sc. Armando Esquivel, B.Sc Megha Sharma, Ph.D. Vivek Tandon, Ph.D.	

9. PERFORMING ORGANIZATION NAME AND ADDRESS	10. WORK UNIT NO.
Center for Transportation Infrastructure Systems The University of Texas at El Paso 500 W. Univ. Ave. El Paso, Texas 79968	11. CONTRACT OR GRANT NO. DTRT13-G-UTC36

12. SPONSORING AGENCY NAME AND ADDRESS	13. TYPE OF REPORT AND PERIOD COVERED
Southern Plains Transportation Center 201 Stephenson Pkwy, Suite 4200 The University of Oklahoma Norman, OK 73019	Final January 2016 – August 2018
	14. SPONSORING AGENCY CODE

15. SUPPLEMENTARY NOTES

University Transportation Center

16. ABSTRACT

The significant change in climate is evident from the records of increased temperature, changed precipitation pattern, increased frequency of extreme weather events like storms, floods, and so forth. Like other infrastructure highway infrastructures also suffer the consequences of these climate change. Since the hydraulic design of these infrastructures is performed using historical climate data, the designs may not be able to provide services because designs are not considering climate change influence especially in terms of precipitation intensity. This study aims at identifying the most accurate source of climate database that predicts future climate change with less uncertainty and links them into the evaluation of vulnerability and risk of the bridges so that the impact of future climate can be incorporated into the design of new infrastructures. In this study, the NARCCAP database has been used to extract the future climate data for different cities of SPTC representing states. Climate models have predicted as high as 10.2% increase in precipitation for Houston, Texas, which leads to an increase in the intensity of streamflow in that region. A hydraulic model has been established using HEC-RAS for streamflow modeling. Overtopping depth and scour depth have been estimated as the primary vulnerability stressors of the bridge. This study has estimated the range of the return periods of the floods for which bridge may fail under the predicted future climate scenarios. The annual economic loss has been calculated for the bridges, and possible adaptation strategies have been suggested using HYRISK software.

17. KEYWORDS	18. DISTRIBUTION STATEMENT
Flooding, Climate Change, Bridge, Hydraulic	No restrictions. This publication is available at www.sptc.org and from the NTIS.

19. SECURITY CLASSIF. (OF THIS REPORT)	20. SECURITY CLASSIF. (OF THIS PAGE)	21. NO. OF PAGES	22. PRICE
Unclassified	Unclassified	129	

SI* (MODERN METRIC) CONVERSION FACTORS

APPROXIMATE CONVERSIONS TO SI UNITS

SYMBOL	WHEN YOU KNOW	MULTIPLY BY	TO FIND	SYMBOL
		LENGTH		
in	inches	25.4	millimeters	mm
ft	feet	0.305	meters	m
yd	yards	0.914	meters	m
mi	miles	1.61	kilometers	km
		AREA		
in^2	square inches	645.2	square millimeters	mm^2
ft^2	square feet	0.093	square meters	m^2
yd^2	square yard	0.836	square meters	m^2
ac	acres	0.405	hectares	ha
mi^2	square miles	2.59	square kilometers	km^2
		VOLUME		
fl oz	fluid ounces	29.57	milliliters	mL
gal	gallons	3.785	liters	L
ft^3	cubic feet	0.028	cubic meters	m^3
yd^3	cubic yards	0.765	cubic meters	m^3
		NOTE: volumes greater than 1000 L shall be shown in m^3		
		MASS		
oz	ounces	28.35	grams	g
lb	pounds	0.454	kilograms	kg
T	short tons (2000 lb)	0.907	megagrams (or "metric ton")	Mg (or "t")
		TEMPERATURE (exact degrees)		
^oF	Fahrenheit	5 (F-32)/9 or (F-32)/1.8	Celsius	^oC
		ILLUMINATION		
fc	foot-candles	10.76	lux	lx
fl	foot-Lamberts	3.426	candela/m^2	cd/m^2
		FORCE and PRESSURE or STRESS		
lbf	poundforce	4.45	newtons	N
lbf/in^2	poundforce per square inch	6.89	kilopascals	kPa

APPROXIMATE CONVERSIONS FROM SI UNITS

SYMBOL	WHEN YOU KNOW	MULTIPLY BY	TO FIND	SYMBOL
		LENGTH		
mm	millimeters	0.039	inches	in
m	meters	3.28	feet	ft
m	meters	1.09	yards	yd
km	kilometers	0.621	miles	mi
		AREA		
mm^2	square millimeters	0.0016	square inches	in^2
m^2	square meters	10.764	square feet	ft^2
m^2	square meters	1.195	square yards	yd^2
ha	hectares	2.47	acres	ac
km^2	square kilometers	0.386	square miles	mi^2
		VOLUME		
mL	milliliters	0.034	fluid ounces	fl oz
L	liters	0.264	gallons	gal
m^3	cubic meters	35.314	cubic feet	ft^3
m^3	cubic meters	1.307	cubic yards	yd^3
		MASS		
g	grams	0.035	ounces	oz
kg	kilograms	2.202	pounds	lb
Mg (or "t")	megagrams (or "metric ton")	1.103	short tons (2000 lb)	T
		TEMPERATURE (exact degrees)		
^oC	Celsius	1.8C+32	Fahrenheit	^oF
		ILLUMINATION		
lx	lux	0.0929	foot-candles	fc
cd/m^2	candela/m^2	0.2919	foot-Lamberts	fl
		FORCE and PRESSURE or STRESS		
N	newtons	0.225	poundforce	lbf
kPa	kilopascals	0.145	poundforce per square inch	lbf/in^2

**SI is the symbol for the International System of Units. Appropriate rounding should be made to comply with Section 4 of ASTM E380.*

(Revised March 2003)

UNDERSTANDING CLIMATE CHANGE IMPACT ON HIGHWAY HYDRAULIC DESIGN PROCEDURES

Conducted for

Southern Plains Transportation Center

Final Research Report 14.1-97

2018

Department of Civil Engineering

The University of Texas at El Paso

El Paso, TX 79968

(915) 747-6924

ACKNOWLEDGEMENT

Authors would like to acknowledge the financial support from the Southern Plains Transportation Center, the U.S. DOT, and the Center for Transportation Infrastructure Systems.

TITLE PAGE

Abstract

The significant change in climate is evident from the records of increased temperature, changed precipitation pattern, increased frequency of extreme weather events like storms, floods, and so forth. Like other infrastructure highway infrastructures also suffer the consequences of these climate change. Since the hydraulic design of these infrastructures is performed using historical climate data, the designs may not be able to provide services because designs are not considering climate change influence especially in terms of precipitation intensity. This study aims at identifying the most accurate source of climate database that predicts future climate change with less uncertainty and links them into the evaluation of vulnerability and risk of the bridges so that the impact of future climate can be incorporated into the design of new infrastructures. In this study, the NARCCAP database has been used to extract the future climate data for different cities of SPTC representing states. Climate models have predicted as high as 10.2% increase in precipitation for Houston, Texas, which leads to an increase in the intensity of streamflow in that region. A hydraulic model has been established using HEC-RAS for streamflow modeling. Overtopping depth and scour depth have been estimated as the primary vulnerability stressors of the bridge. This study has estimated the range of the return periods of the floods for which bridge may fail under the predicted future climate scenarios. The annual economic loss has been calculated for the bridges, and possible adaptation strategies have been suggested using HYRISK software.

TABLE OF CONTENTS

LIST OF FIGURES

LIST OF TABLES

1. INTRODUCTION

1.1 ADDRESSING THE PROBLEM

Although the influence of climate change on highway infrastructure needs to be evaluated, the aggregation of complex and interdependent competing factors to predict the impact of climate change on transportation infrastructure is challenging. On the contrary, in action will leave infrastructure vulnerable to climate change. However, it is very likely that the impact of individual factors like the impact of precipitation on transportation infrastructure can be evaluated. According to climate scientists (Intergovernmental Panel on Climate Change, 2013), the increase in greenhouse gas (GHG) emissions will lead to higher humidity that will eventually lead to higher precipitation rates. Although the change in mean precipitation levels seems to have less impact on transportation infrastructure, the increase in the intensity and frequency of precipitation can impact on transportation infrastructure such as slope instability, reduced bearing capacity due to saturation, and so forth. Similarly, the runoff resulting from increased precipitation could also lead to increased peak streamflow especially if rivers are swollen from, and soils are already saturated with the previous storm. The increased runoff would require a change in the sizing requirement for bridges and gutters (Warren et al., 2004).

The prediction of intensity and frequency of precipitation and associated runoff due to climate change can be estimated using historical weather database or using climate models developed by various agencies (NOAA, USGS, etc.) that predict future global climate conditions. The climate prediction models are downscaled using statistical or dynamic downscaling approach to predict climate conditions at the regional or local levels. Since global models have inherent variability associated with their prediction capabilities, the downscaling further enhances levels of uncertainty associated with future predictions. The compound influence of uncertainty may lead to erroneous sizing requirements in the event climate predictions are inaccurate. Therefore, overestimating climate event can result in costly oversizing of infrastructure while underestimating climate event will leave infrastructure vulnerable. Therefore, vulnerability and risk assessment need to be performed to identify cost-effective adoption solutions.

Based on the above discussion, there is a need to evaluate the impact of intensity and frequency of precipitation on existing infrastructure and propose cost-effective solutions to enhance the service life of highway infrastructure by making them resilient to the climate change.

1.2 OBJECTIVES AND SCOPES OF THE STUDY

The following objectives have been formulated in understanding the climate change impacts on the hydraulic design of bridge infrastructures:

1) To identify the primary climatic stressor for the hydraulic bridge design.

2) To recognize and analyze the future change in the climate factor, predicted by climate model simulation.

3) To evaluate the bridge hydraulic design criteria for future climate through risk and vulnerability assessment.

4) To suggest possible adaptation strategies.

Laying focus on the objectives stated above the research has been conducted within the scope of the following tasks:

1) Theoretical Review on the bridge hydraulic design practices followed by different State and Federal agencies.

2) Extracting simulated future climate data from climate models from NARCCAP (North American Regional Climate Change Assessment Program) and modified with an appropriate method.

3) Developing a hydraulic model for the studied bridges using HEC-RAS (Hydraulic Engineering Center-River Analysis System) and communicate the climatic factor to the hydraulic model.

1.3 ORGANIZATION OF THE REPORT

The report is organized in six chapters. It includes various aspects of bridge vulnerability assessment and adaptation techniques to mitigate the impact of climate change.

- Chapter 1 provides the brief introduction to the nature of the problem and objectives and scopes of the study.
- Chapter 2 contains the literature review of different climate models and previous works done in the field of climate change impact on highway infrastructures. This chapter also contains a review of bridge hydraulic design practices by different Department of Transportations (DOTs).
- Chapter 3 contains the extracted climate data from different climate models.
- Selection of climatic stressors and communicating those stressors to the hydraulic model have been discussed in Chapter 4.
- Chapter 5 describes the vulnerability and risk analysis of the bridge from overtopping and scour and the possible adaptation techniques.
- In chapter 6, a framework has been presented to compute the scour depth using Machine Learning platform.
- The report ends with Chapter 7 that contains a summary, conclusion, and recommendations for further research.

- References
- Appendix A contains the bias-corrected climate data for cities of Texas, New Mexico, Louisiana, Oklahoma, and Arkansas.

2. LITERATURE

2.1. REVIEW OF LITERATURE

Climate scientists have been conducting studies on the recognition of the pattern change in different climatic variables and their impacts on the earth systems. In their fifth assessment report, published in 2013, Intergovernmental Panel on Climate Change (IPCC) has been reported an increase of global mean temperature by 0.780 C and rising of the sea level by 7.5 inches, over the past century. U.S. Climate Change Science Program (CCSP) 2008, a report by the U.S climate change program, provides evidence of changes in weather and climate extremes such as temperature, precipitation which includes droughts, heavy precipitation, tropical storms and cyclones, winter storms, etc. According to CCSP 2008 report, in the continental U.S. intense precipitation (the heaviest 1% of the daily precipitation totals) has been increased by about 20% over the past 100 years, while total precipitation increased by only 7%.

A clear indication of climate change leads many agencies to conduct climate change impact studies, such as the Gulf Coast study (Phase I & Phase II). This study includes the impact of climate change on transportation infrastructures. Like other infrastructure systems, transportation infrastructures are also vulnerable to change in different climatic variables like heavy precipitation, rising temperature, increase in sea levels, the frequency of extreme events like hurricanes and storm surges, etc. Agencies like the United States Department of Transportation (USDOT) and Federal Highway Administration (FHWA) has done several studies on the impact of the climate change on the transportation infrastructures.

USDOT Gulf Coast Study Phase I (Savonis, Burkett and Potter, 2008), has been done for U.S. central Gulf Coast between Galveston, Texas, and Mobile, Alabama. This study showed the vulnerability of the transportation infrastructure to the temperature increase, flooding due to rising sea level and changed precipitation patterns. According to this study, 27% of the major roads, 9% of the rail lines, and 72% of the ports are built on the land which is below 122 cm (4 feet) in elevation and is more vulnerable to frequent or permanent inundation due to change in precipitation pattern. It also reported, more than half of the area's major highways, rail lines, 29

airports and lower elevation ports are in danger of damage due to inundation during hurricane storm surges.

To quantify the vulnerability of the transportation infrastructures to the changing climate, USDOT has developed some tools and approaches in their second phase of the Gulf Coast Study (Hayhoe and Stoner, 2012), which is done in Mobile, Alabama. This study has analyzed the impacts based on future climate data collected from climate models. They have developed a sensitivity matrix to identify potential climate stressors in transportation components. They have also created Vulnerability Assessment Scoring Tool (VAST) which qualitatively evaluate the assets vulnerability.

In 2010 to 2011, different DOTs and Metropolitan Planning Organizations (MPOs) have conducted five climate change resilient pilots, to assess the climate change impacts on different transportation assets. These studies have been conducted based on FHWA's conceptual risk assessment model (FHWA website).

Metropolitan Transportation Commission: San Francisco Bay (FHWA,2012) has developed inundation maps for the coast region using future projection climate data. They reported nearly all the shoreline assets would be inundated with the extreme sea level rise scenario. The future projection shows minor flooding in mid-century, but the end of the century will face major flooding which will require drastic adaptation strategies. A pilot study done by the New Jersey Transportation Planning Authority (FHWA,2012), showed the impact of increased heat on transportation assets and the rise of sea level to infrastructures near the shoreline. It was reported that temperatures higher than 95°F would increase the risk of rail kinks and during extreme heat overhead wires may sag or experience pulley failures.

In 2013-2015, FHWA has done 19 pilot studies with the help of different DOTs and MPOs based on the 'Climate Change and Extreme Weather Vulnerability Assessment Framework, 2012', which has been later modified in the 3rd edition of the report (Filosa et al.,2017). In these studies, different agencies worked on climate change impact on different transportation assets. They have used the FHWA's framework to assess the vulnerability of the assets and come up with adaptation options and resiliency improvement.

Iowa DOT (Anderson et al.,2015) has conducted a climate change impact study on the vulnerability of bridges, mainly due to the increase in peak streamflow resulted from increased precipitation, predicted by 19 climate models. They have analyzed six bridges in Iowa and suggest possible adaptation strategies. Connecticut DOT (Hogan et al., 2014) have conducted a system-level vulnerability assessment of bridge and culvert for inland flooding resulted from rainfall events. In this study, they evaluated 52 structures for current precipitation data and analyzed their sufficiency in design. 65% of the structure satisfied design criteria. They have shown the connection of precipitation data to a hydraulic model of the channel using USGS regression equations or stream stats.

Moreover, the Minnesota DOT (Almodovar-rosario et al., 2014) have studied bridge and culverts resiliency against flash flooding, predicted for future climate scenarios. They have evaluated structures for three risk level, low, medium and high represented by RCP 4.5, 6.0 and 8.5). The study also analyzed the adaptation options through economic analysis using COAST tool.

Research has been less focused on rectifying the disparity between the output of the climate models and the needed input for bridge hydraulic engineers to incorporate climate change in current design practices. Climate models are generally too coarse spatially and temporally for use in hydraulic design, nor are climate models built with the intent to design new bridges. Hydraulic design techniques rely on rigorous statistical analysis of historical observations whereas climate is based on complex sets of interdependent parameters to describe the physical processes between the atmosphere, ocean, and land. Hydraulic design techniques of bridges look at sets of past data to project the future, whereas climate models are trained on past observations but then are forced by assumed increases in greenhouse gases to predict the future, often in a non-stationary manner. Therefore, this study focuses on draw inferences from climate data to check on the resiliency of the bridge infrastructures for this future climate and identify the possible adaptation techniques.

2.2 CLIMATE MODELS

Initially, climate prediction models were developed based on future emission scenarios commonly known as Special Report on Emission Scenarios or "SRES" (Nakicenovic and Swart, 2000). Various emission scenarios, used in climate models, are summarized in **Table *2-1***.

Table 2-1 SRES based Emission Scenario (IPCC, 2000)

Storyline	**Emission Scenario Description**
A1 storyline	Rapid economic growth, the global population that peaks in mid-century and then declines, and the early introduction of new and more efficient technologies. A1F1, A1T, and A1B.
A2 storyline	A complex world with an increase in the global population at a constant rate. Economic development is primarily regionally oriented, and per capita, economic growth and technological change are more fragmented and slower than in other storylines.
B1 storyline	A convergent world with the same global population as in A1 storyline, but with rapid changes in economic structures and the introduction of clean and resource-efficient technologies.
B2 storyline	Emphasis is on local solutions to economic, social, and environmental sustainability with continuously increasing global population at a rate lower than A2, intermediate levels of economic development, and less rapid and more diverse technological change.

In the last decade, revised scenarios were developed by IPCC for their fifth Assessment Report (IPCC AR5, 2014). The revised scenarios are based on representative concentration pathways (RCPs) that specifies the concentrations and corresponding emissions. The RCP approach uses greenhouse gas (GHG) concentration trajectories instead of emissions to predict climate change (Stocker et al., 2014). The RCP based on radiative forcing utilized for the projection in climate models in **Table *2-2***.

Table 2-2 RCPs as per AR5, 2014

RCP	Radiative Forcing Levels
RCP2.6	Minimal GHG concentration levels. It is radiative forcing level first reaches a value around 3.1 W/m^2 mid-century, returning to 2.6 W/m^2 by 2100. GHG is reduced substantially over time to achieve such radiative forcing levels.
RCP4.5	It is a stabilization scenario where total radiative forcing is stabilized before 2100 by the employment of a range of technologies and strategies for reducing GHG emissions.
RCP6.0	It is a stabilization scenario where total radiative forcing is stabilized after 2100 without overshoot by the employment of a range of technologies and strategies for reducing GHG emissions.
RCP8.5	The RCP 8.5 is characterized by increasing GHG emissions over time representative for scenarios leading to high GHG concentration levels.

The recently developed Global Climate Models (GCMs) and the regional climate models (RCMs) use these different emission scenarios for projecting future climate. The GCMs provide climate data for a large geographical area while the RCMs are developed to generate climate data at a higher fidelity for regional areas. The different climate data sources, available based on emission scenarios, downscaling methods, GCMs, RCMs, and spatial and temporal coverage are summarized in **Table *2-3***.

Table 2-3 Climate Data Sources Based on Different Emission Scenario and Downscaling Methods

Climate Source/ Downscaling Method/ Emission Scenario	Parameters/Spatial Resolution	Climate Models	Coverage
North American Regional Climate Change Assessment Program (NARCCAP) uses Dynamic downscaling and is based on SRES A2. (*Mearns et al., 2007 and 2009*)	**Daily: (table 1)** maximum and minimum daily surface air temperature **3-hourly: (table 2)** precipitation, surface air temperature, cloud fraction, wind speed, relative humidity. **Spatial resolution:** 50x50 km	4 GCMs and 6 RCMs	Phase I, wherein six RCMs use boundary conditions from the NCEP–DOE Reanalysis II (R2) for a 25-yr period (1980–2004), and phase II, wherein the boundary conditions are provided by four AOGCMs for 30 years of current climate (1971–2000) and 30 years of a future climate (2041–70)
Downscaled CMIP3 and CMIP5 Climate and Hydrology Projections uses statistical downscaling. CMIP3 uses SRES B1, A1B, A2 while CMIP5 uses RCP2.6, RCP4.5, RCP6.0, RCP8.5 (*Brekke et al., 2013*)	(a) Monthly projections of total precipitation and monthly-mean daily average temperature; and (b) Daily projections of the precipitation, daily minimum temperature, and daily maximum temperature. **Spatial resolution:** 1/8° (12x12km)	CMIP3 - 16 climate models CMIP5 - 23 climate models	**BCSD: Coverage:** 1950-2099 **resolution:** monthly **BCCA: CMIP3 coverage**: 1961-2000, 2046-2065, 2081-2100 **CMIP5 coverage:** 1950-2099 **resolution:** daily
MACA CMIP5 Archive uses empirical downscaling and has RCP4.5 and RCP8.5 projections.	1) Maximum and Minimum daily temperature near the surface. 2) Maximum and Minimum daily relative humidity 3) Average daily precipitation amount at the surface **Spatial resolution:** 4-6km	20 global climate models of the Coupled Inter-Comparison Project 5 (CMIP5)	Historical: 1950-2005 Future: 2006-2100
NASA NEX DCP30 National Climate Change Viewer (NCCV) uses empirical downscaling and has RCP4.5 and RCP8.5 projections.	Maximum and Minimum Temperature, Precipitation, Runoff **Spatial resolution:** 800-m grid over the CONUS	30 of the Coupled Inter-Comparison Project 5 (CMIP5)	Dataset coverage: 1950-2005, 2025-2049, 2050-2074, and 2075-2099
Program for Climate Model Diagnosis and Intercomparison (PCMDI) CMIP5 Archive. It uses RCP2.6, RCP4.5, RCP6.0, RCP8.5		20 Climate modeling groups	provide projections of climate change on two time scales, near-term (out to about 2035) and long-term (out to 2100 and beyond)

For this study, the North American Regional Climate Change (NARCCAP) that utilizes Special Report on Emission Scenario (SRES) A2 emission scenarios for predicting future climate was selected because of its suitability to hydraulic design procedures. This climate data source uses a dynamic downscaling method to produce the data at the local resolution of 31 x 31 miles (50 x 50 km).

2.3 BRIDGE HYDRAULIC DESIGN PRACTICES

2.3.1 GENERAL BRIDGE HYDRAULICS

Given that hydraulic analysis of bridges depends on a range of factors, like topographic data, river conditions, proper streamflow estimation, accuracy in flow modeling approaches or the floodplain conditions, etc., it is a complicated process. Besides, regulatory requirements set by different agencies (i.e. FHWA, USACE, FEMA, etc.) must be satisfied to choose a proper hydraulic analysis model for bridges (Zevenbergen, Arneson, Hunt and Miller, 2012).

Generally, hydraulic analysis of bridges is performed by computing the energy losses caused by the built structure. So, modeling of bridge section primarily depends on the following factors:

- Bridge cross-section locations
- Flow types at the bridge sites
- Hydraulic flow computation

Bridge cross-section locations:

The performance of hydraulic analysis of the bridge required four cross sections along the river. These cross sections help to capture the characteristics (contraction and expansion) of the flow through bridge opening. ***Figure 2-1*** shows the plan view of the four controlled sections. The first cross-section, the cross-section one should be located sufficiently downstream of the structure. The function of this cross section is to capture the expansion of the flow after passing through the bridge opening. Cross section 2 and three should be located near to the bridge at upstream and downstream respectively. However, they should not be placed at the immediate face of the bridge deck, to let the flow have some expansion and contraction respectively. The cross-section 4 is an upstream cross-section which takes in the distance to capture the contraction characteristic of the flow. In ***Figure 2-1***, the Le and Lc values represent the distance between

two downstream cross-section and upstream cross-section respectively. These values are generally determined from the field observation during the high flows. Although, usually Le value is twice to the Lc value.

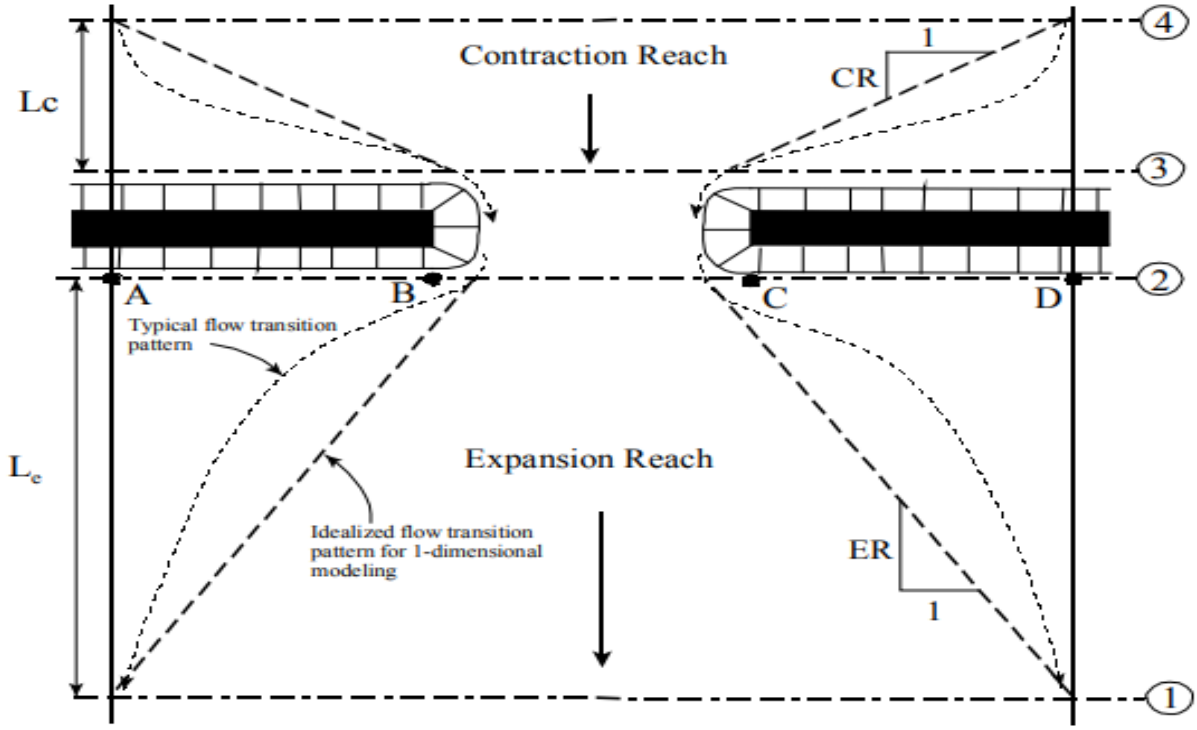

Figure 2-1 Plan View of the Cross-sections needed for Bridge Hydraulics (Brunner et al., 2008)

Flow types of the Bridge Sites:

Understanding the exact flow types that bridge is going to encounter, is one of the significant factors in hydraulic computations of bridges. Flows corresponding to bridge structure can be either a low flow or high flow.

Low flow exists when the flow can pass through the bridge opening. ***Figure 2-2*** shows an example of Low flow condition in the bridge. Low flows are classified (A to C) based on the depth of the flow with respect to the critical depth of the flow. When the depth of the flow exceeds the critical depth (or normal water surface), subcritical flow condition takes place. Similarly, when the depth of flow is below the critical depth supercritical flow condition takes place. Class A low flow is entirely subcritical flow, meaning the flow depth exceeds the critical depth, where gravitational forces dominate, and the flow behaves subtly. Conversely, Class C flow is completely supercritical flow. Class B can be either subcritical or supercritical.

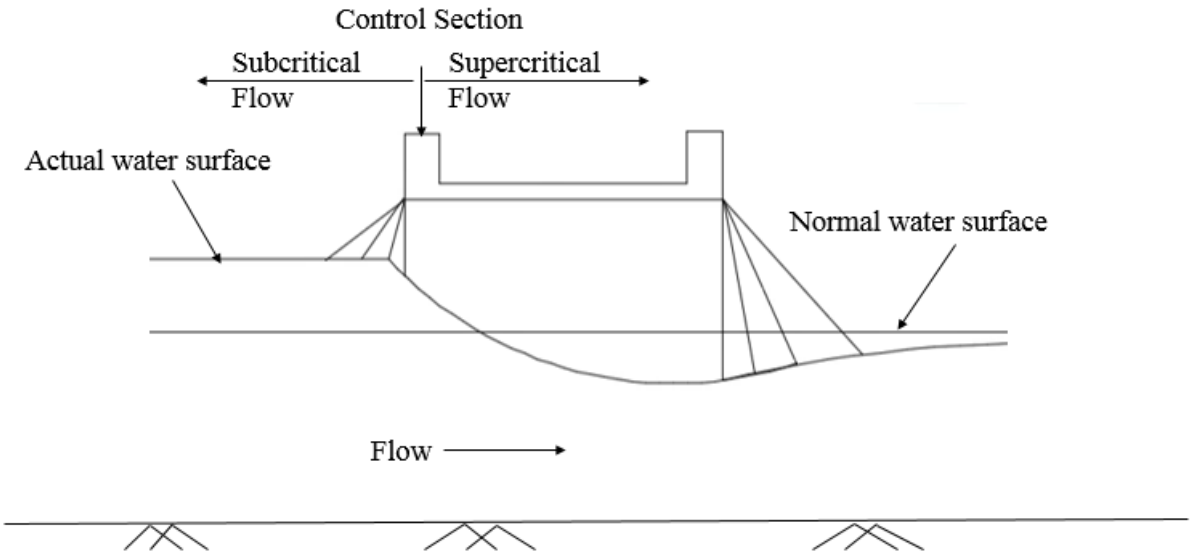

Figure 2-2 An Example of Low Flow in Bridge

High flow occurs when the flow depth exceeds the elevation of the high point of the low chord of the bridge. High flows can be estimated as sluice gate flow, orifice type flow or weir type flow. ***Figure 2-3*** shows the example of the high flows in the bridge.

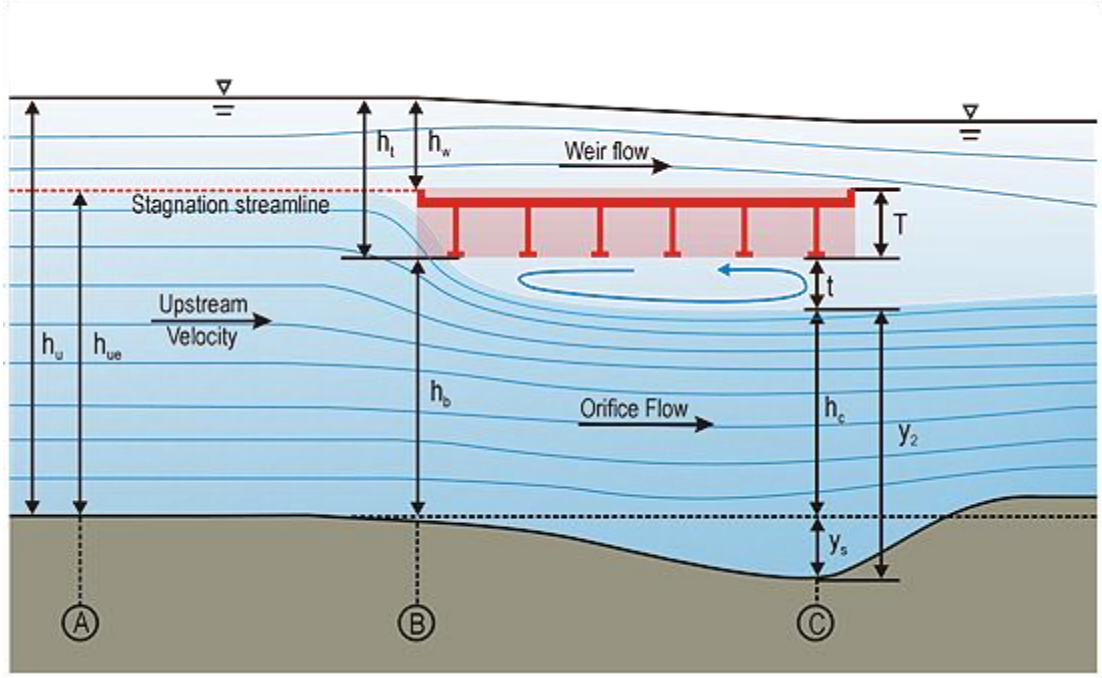

Figure 2-3 An Example of High Flow in Bridge (Shan et al., 2012)

- Sluice gate type flow exists when the water surface is in level with the low chord in upstream and below in the downstream.
- Orifice type flow occurs when low chord at both upstream and downstream is submerged.
- Weir type flow exists when the roadway, even the whole bridge is submerged.

Hydraulic flow computation

The methods available for low flow and high flow conditions are as follows:

For low flow computations:

- Energy Equation or Standard Step Method
- Momentum Balance Method
- Yarnell Equation
- FHWA WSPRO Method

For high flow computations:

- Energy Equation or Standard Step Method
- Pressure Flow Method

2.3.2 OVERTOPPING AND SCOUR ASSESSMENT

The climate change is anticipated to act as a stressor on the transportation infrastructure due to flooding. To evaluate the resilience of transportation infrastructure in the event of the extreme event, a vulnerability assessment needs to determine the impact of climate change on transportation infrastructure before measures can be identified and prioritized. A bridge is vulnerable both regarding overtopping as well as scour criticality during and after an extreme event.

Various transportation agencies have developed methods to identify and locate vulnerable locations in the transportation system (Filosa and Oster, 2015). For instance:

- The Danish Road Directorate follows the Blue Spot method- a four-level analysis to identify roadway locations where the likelihood of floods is high, and consequence of flooding is significant.
- The ROADAPT research project, a joint research effort supported by several European countries, developed a preliminary risk assessment method that can identify vulnerable locations in the transportation network, understand the probabilities and consequences that climate change events could have on these locations, and provide options for adaptation actions.

Scouring can remove the soil from the foundation of the bridge, and in case of heavy loss of soil particle the bridge collapse. According to the researcher (Lagasse et al., 2007, Wardhana and Hadipriono, 2003), 50 % to 60% of the bridge failures in the USA are caused by scouring. In 2003, during a heavy rain of 11 inches, the Loon Mountain Bridge in Lincoln, New Hampshire collapse due to scouring.

According to Bridge Scour Evaluation Program, run by FHWA in 2011 on a total number of 493,473 bridges including Interstate, National Highway System (NHS) and Non-National Highway System bridges. They have reported total 23,034 bridges are scour critical including all three categories, which results in 4.7% of total bridges. **Table *2-4*** shows the status of that report.

Table 2-4 Survey Report of Bridge Scour Evaluation by FHWA (Arneson et al., 2012)

Total Number of Bridges Surveyed	Evaluation Criteria	Interstate Bridges	NHS Bridges	Non-NHS Bridges	Total	Percent of Total
493,473	Needing Evaluation	80	136	3,701	3,917	0.80%
	Foundation Unknown	55	703	40,067	40,825	8.30%
	Scour Critical	937	1,936	20,181	23,034	4.70%

Although it is well known scouring causes failure, the assessment of scouring criticality is a complex process. The principal scour assessment method available for U.S. bridge designers is Hydraulic Engineering Circular No. 18 (HEC-18) published by the FHAWA (Arneson et al., 2012). The currently available version of the documents is the 5th edition which presents the state of knowledge and practices for the design, evaluation, and inspection of bridges for scouring. This document contains updated material from previous editions and combined research by FHWA, state DOTs, and universities.

HEC-18 suggests scouring estimation based on soil and rock criteria along with other geotechnical considerations. The total scour compiles the contraction scour, and local scour as pier and abutment scour. Contraction scour occurs due to the reduction of the flow area of the stream at flood stage by a natural contraction of the channel or by a structure (Arneson et al., 2012). The underlying mechanism causing local scour at piers or abutments is the formation of vortices at their base (Arneson et al., 2012). The steps and equations adopted in HEC-18 for these scour estimations have been summarized in the next section.

Contraction Scour:

Based on the mechanism of the transport of the bed material contraction can be estimated as live-bed sour or clear-bed scour. For the live-bed scour estimation, the following equation has been proposed (a modified version of Laursen (1963) equation):

$$\frac{y_2}{y_1} = (Q_2/Q_1)^{6/7}(W_1/W_2)^{k1} \quad (2\text{-}1)$$

$$y_s = y_2 - y_0 \quad (2\text{-}2)$$

Where,

y_1 = Water depth in the upstream main channel

y_2 = Water depth in the contracted section

y_0 = Existing depth in the contracted section before scour

Q_1 = Flow in the upstream section

Q_2 = Flow in the contracted channel

W_1 = The bottom width of the upstream main channel

W_2 = The bottom width of the contracted main channel

$k1$ = Exponent explaining mode of bed material transport

The equation used for clear-bed contraction scour estimation is stated below (also modified from the Laursen's (1963) equation).

$$y_2 = \left[K_u Q^2/D_m^{2/3} W^2\right]^{3/7} \quad (2\text{-}3)$$

$$y_s = y_2 - y_0 \quad (2\text{-}4)$$

Where,

y_2 = Water depth in the contracted section

y_0 = Existing depth in the contracted section before scour

K_u = 0.0077

Q = Discharge through the bridge

W = Width of the bridge section

D_m = Diameter of the smallest non-transportable bed material

Pier Scour:

For the estimation of the scour on the pier, HEC-18 has adopted the Colorado State University (CSU) equation:

$$\frac{y_s}{a} = 2.0K_1K_2K_3(y_1/a)^{0.35}Fr_1^{0.43} \quad (2\text{-}5)$$

Where,

y_s = Scour depth

y_1 = Flow depth immediately upstream of the pier

a = Pier width

K_1 = Correction factors for pier nose shape

K_2 = Correction factor for the angle of attack of flow

K_3 = Correction factor for bed condition

Fr_1 = Froude number immediately upstream of the pier

Abutment Scour:

HEC-18 suggests the use of Froehlich's (TRB 1989) live bed scour equation or the HIRE equation in HDS 6 (FHWA 2001a) for abutment scour estimation. The Froehlich's equation (based on 170-lab experiments for live bed scour) is:

$$\frac{y_s}{y_a} = 2.27K_1K_2(L'/y_a)^{0.43}Fr^{0.61} + 1 \quad (2\text{-}6)$$

Where,

K_1 = Coefficient for abutment shape

K_2 = Coefficient for the angle of the embankment to flow

L' = Length of active flow obstructed by the embankment

y_a = The average depth of flow on the floodplain

Fr = Froude number of approach flow upstream of the abutment

Based on the field data of scour at the end of spurs in Mississippi River, FHWA derived the following equation, named HIRE equation in 2001:

$$\frac{y_s}{y_1} = 4\ Fr^{0.33}\frac{K_1}{0.55}K_2 \qquad (2\text{-}7)$$

Where,

y_s = Scour depth

y_1 = Depth of flow in the main channel

Fr = Froude number

K_1 = Abutment shape coefficient

K_2 = Coefficient of the skew angle of the abutment to flow

2.3.3 BRIDGE HYDRAULIC DESIGN PRACTICES BY SPTC DOTs

This section discusses the common practices adopted by DOTs of the SPTC representative states: Texas (TxDOT), New Mexico (NMDOT), Louisiana (LDOT), Oklahoma (ODOT) and Arkansas (ArDOT). Although different DOTs have different procedures, they follow a similar principle for hydraulic analysis. The analysis is performed based on the effects of a backwater, flow distribution and velocities and potential scour measurements for a particular flood frequency (TxDOT, 2004; ASHTD, 1982; NMDOT, 1998; LDOT, 2011). According to all DOTs, the risk associated with these parameters should be checked while designing the bridge.

The flood frequency or the annual exceedance probability(AEP) for hydraulic design of a bridge is 50-years or 2% (AEP), preferred by TxDOT but practiced by most DOTs. LDOT prefers 25-years or 50-years AEP based on the local condition. However, design flood frequencies must be justified by risk analysis.

According to AASHTO LRFD (2005), backwater effect should be estimated for 100-year flood as base flood and a 500-year flood. The **Table *2-5*** summarizes the standard design floods for hydraulic, scour and scour countermeasures suggested by FHWA.

Table 2-5 Design Flood Frequencies for Hydraulic Design, Scour Design and Scour Design Countermeasures (Arneson et al., 2012)

Flood Frequency for Hydraulic design	Flood Frequency for Scour	Flood Frequency for Scour Countermeasures
Q_{10}	Q_{25}	Q_{50}
Q_{25}	Q_{50}	Q_{100}
Q_{50}	Q_{100}	Q_{200}
Q_{100}	Q_{200}	Q_{500}

For scour potential measurement, all SPTC DOTs follow the guidelines and regulations of HEC-18 by FHWA while ODOT, NMDOT, and LDOT also follow the AAHSTO LRFD Bridge Design Specifications. The zest of the specifications are as follows:

- HEC-RAS for hydraulic analysis and HEC-18 for scour analysis
- Hydrologic analysis should be done for 2,5,10,25,50,100,200,250 and 500-year floods
- Scour should be estimated for 100-year flood and 500-year flood or overtopping flood if the overtopping flood is less than the 500-year flood.
- Scour depth prediction mainly emphasis on pier and contraction scour
- For abutment scour, countermeasures or armoring is preferred

Given Louisiana has great potential for flooding and migrating, predicted scour depth is the same for all the piers and end bents of main bridges as well as relief bridges.

Although the hydraulic design flood frequency is 100-yr, FHWA increases the standard for scouring design flood from 100-yr to 200-yr floods.

DOTs followed the guidelines proposed in the HEC-23 manual by FHWA for the prevention and protection measures for bridges against scouring or overtopping. For pier scour, the general considerations are:

- Reduced number of piers in the main channel,
- Using circular piles,
- Using drilled shaft foundations,
- Aligning the bents to the flow direction and increasing bridge length for reduced through bridge velocities.

- HEC-23 suggests concrete riprap, stone protection, gabions and grout-filled or sand/ cement filled bags for armoring of pier or abutments to prevent from scouring.

Along with these measures, LDOT also prefers to maintain the slope of the abutment as 3:1, (horizontal to vertical ratio) and minimum total scour depth at 5 feet (LDOT,2011).

3. CLIMATE DATA

3.1 SELECTION OF CLIMATE STRESSOR

The identification of appropriate climatic stressor for the risk and vulnerability assessment of transportation infrastructure is an essential component for the identification of an effective adaptation strategy. The Federal Highway Administration's Climate Change and Extreme Weather Vulnerability Assessment Framework (**Error! Reference source not found.**) will be used in this study to identify the essential climate variables like temperature, extreme precipitation events, sea-level, and coastal storm surge, permafrost thaw, snowmelt hydrology, etc.

Hydraulic design of bridges is based on the risk and vulnerability of bridges to frequency and intensity of flood events. Precipitation is the primary climatic variable that contributes directly to flooding. Although, the temperature is often considered as a climatic factor in bridge vulnerability due to its role in flood events. For instance, a warmer atmosphere can hold more water, and this could lead to bigger storms with increased intensities and frequencies, although warmer atmosphere leads to the drier soil, results in more infiltration, decrease the amount of runoff. So, for this study, precipitation has been chosen as the primary climatic stressor.

3.2 CLIMATE DATA EXTRACTION

Global climate models (GCMs) capture the future trajectories of greenhouse gas emissions and reaction of the global climate system to it. However, GCMs provide information for high spatial regions. For local climate change impact analysis, data from GCMs must be downscaled to the local scale with finer spatial resolution employing downscaling methods. Among the various sources mentioned in the previous chapter, the North American Regional Climate Change Assessment Program (NAARCAP) data source has been used in this study for future climate change projections of different parameters. The reasons behind using this source are as follows:

- **Availability:** The data are easily downloadable given the fact this comes up with grid maps. So, for known coordinates (Latitudes and Longitudes) of the stations, the data can

be retrieved from the portal. In a previous study performed for the TX DOT, the agency has already used the data source and established a MATLAB code to extract the data.

- **Spatial and Temporal resolution:** The source provides data with 50 X 50 km spatial resolution and 3-hr temporal resolution.
- **Downscaling method:** NARCCAP uses the dynamic downscaling for the projection of the future climate data.

NARCCAP program covers the climate change simulations for Conterminous United States (CONUS) and most of Canada (Mearns et al., 2007). This program has been established based on A2 emission scenario set from SRES for climate projections of the 21st century. Using the boundary conditions derived from GCMs, Regional Climate Models (RCMs) have been developed to generate climate data at higher resolution. Climate models established with GCMs and RCMs in this program performs simulation at a spatial resolution of 50 X 50 km.

NARCCAP source uses four GCMs and six RCMs. The used RCMs are: 1) Canadian Regional Climate Model (CRCM); 2) Hadley Regional Model 3 (HadRM3); 3) Mesoscale Model 5 (MM5); 4) the National Center for Atmospheric Research, Weather Research and Forecasting (WRF); 5) RegCM3; and 6) Regional Spectral Model (RSM). The GCMs used in NARCCAP programs are: 1) CCSM; 2) HadCM3; 3) CGM3 and 4) the GFDL model. Thus, twelve climate models were identified and are listed in **Table *3-1***.

NAARCAP program is a two-phase program. Phase I has six RCMs that use boundary conditions from the NCEP-DOE Reanalysis 2 for production of 25 years (1980-2004) simulations. In phase II, NARCCAP uses 4 GCMs and 6 RCMs to run simulations of 30 years (1971-2000) current data and production of 30 years (2041-2070) future data. NARCCAP data are accessible to download for a location using the geographic coordinate system (Latitude and Longitude). Using available grid cell maps within the NARCCAP program, different climate variables from RCMs can be extracted.

Table 3-1 Climate Models in NARCCAP

RCMs	GCMs	Emission Scenario
CRCM	CCSM	A2 Storyline
CRCM	CGM3	A2 Storyline
ECP2	GFDL	A2 Storyline
ECP3	HADCM3	A2 Storyline
HRM3	GFDL	A2 Storyline
HRM3	HADCM3	A2 Storyline
MM5I	CCSM	A2 Storyline
MM5I	CGM3	A2 Storyline
RCM3	GFDL	A2 Storyline
RCM3	CGM3	A2 Storyline
WRFG	CCSM	A2 Storyline
WRFG	CGM3	A2 Storyline

3.3 CLIMATE DATA PLOTS

This study analyzed the climate change phenomenon for all the SPTC representative states (Texas, New Mexico, Louisiana, Oklahoma, and Arkansas). This section presents the future climatic conditions of different cities of different states regarding the change in mean annual precipitation and means annual temperature with respect to existing observed climate data. Mean annual precipitation are the average of annual amount of precipitation for a certain amount of time period, i.e here for 2041-2017. Similarly, mean annual temperature is the average of yearly temperature over a certain time period. Existing temperature and precipitation data have been obtained from AASHTOware pavement ME design software website, which documents the data from North American Regional Reanalysis (NARR) program in NOAA.

Figure *3-1* to **Figure *3-5*** shows the future mean annual precipitation predicted by climate models with a comparison of existing one, for different cities of Texas, New Mexico, Louisiana, Oklahoma and Arkansas. Most of the climate models predict an increase in precipitation for the cities of Texas and New Mexico, where existing mean annual precipitation ranges between 10 to 45 inches and 10 to 15 inches. However, for Louisiana, Oklahoma, and Arkansas, most of the

models predict a decrease in precipitation, where existing precipitation ranges between 50 to 60 inches, 30 to 40 inches and 40 to 50 inches.

Figure *3-6* to **Figure *3-10*** shows the future mean annual temperature predicted by climate models with a comparison of the existing one, for different cities of Texas, New Mexico, Louisiana, Oklahoma and Arkansas. Most of the climate models predict an increase in mean annual temperature for cities of Texas, Louisiana, Oklahoma and Arkansas, but decrease for New Mexico.

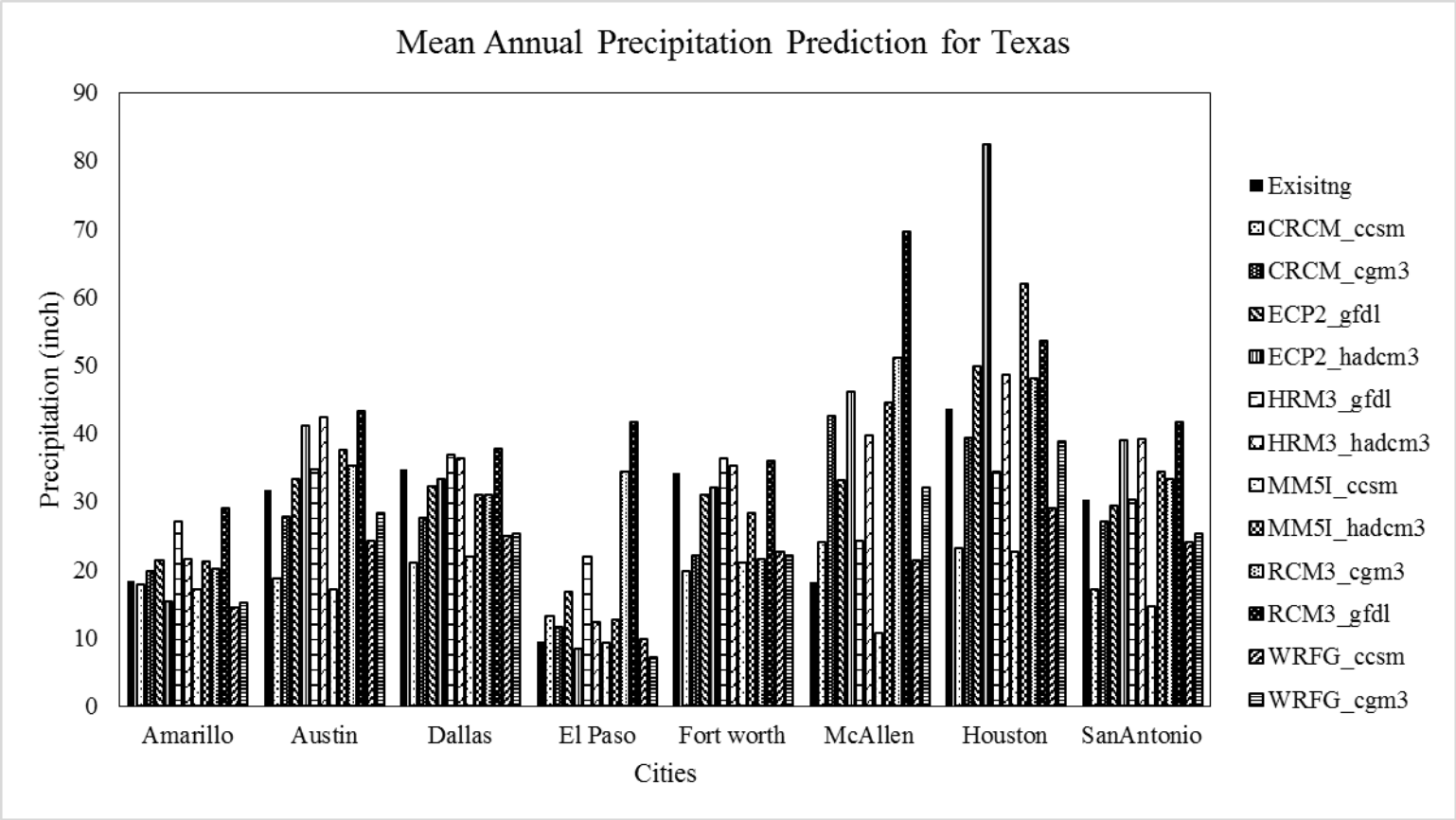

Figure 3-1 Mean Annual Precipitation of Different Cities of Texas for Climate Prediction Models (2041-2070)

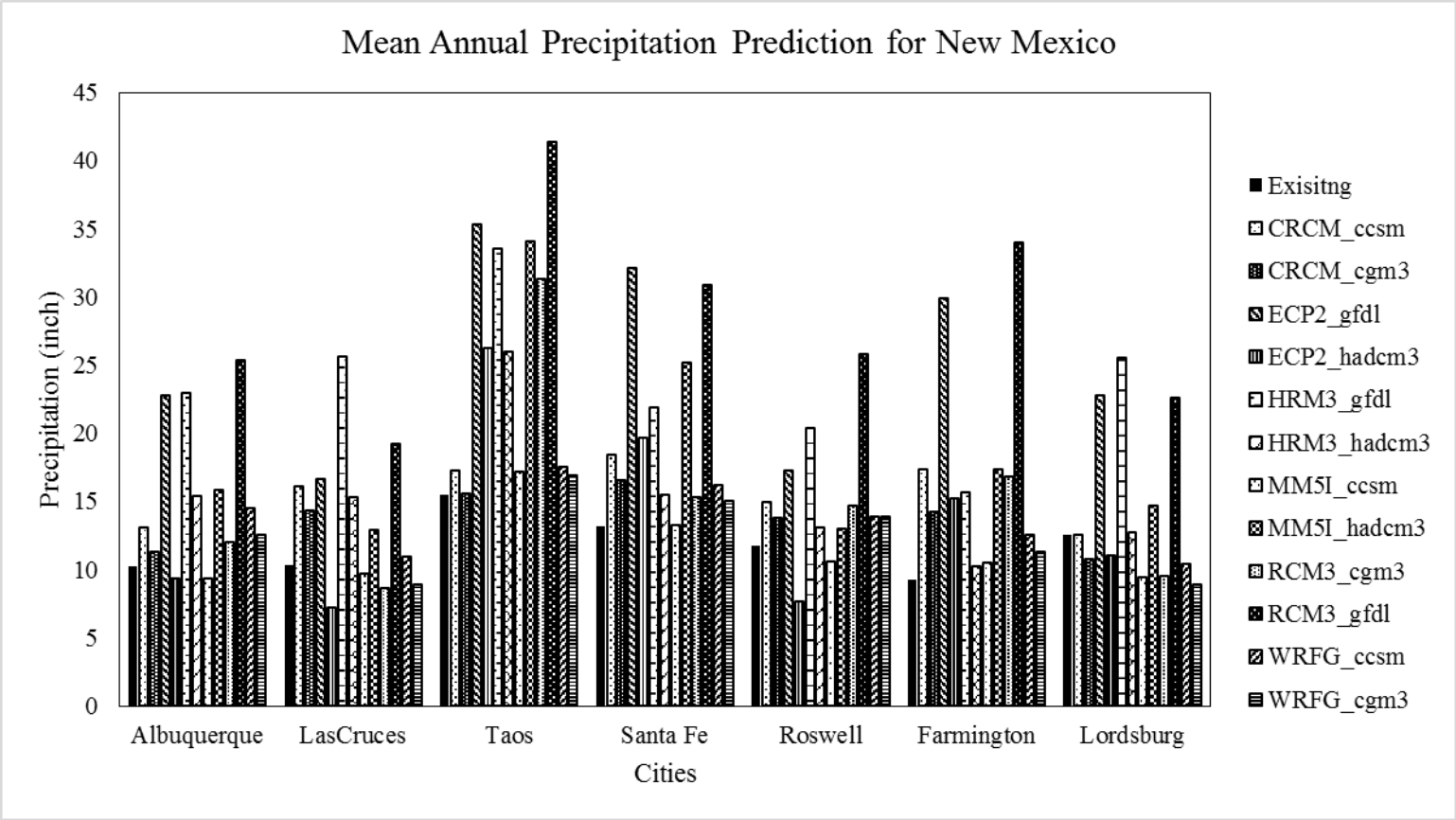

Figure 3-2 Mean Annual Precipitation of Different Cities of New Mexico for Climate Prediction Models (2041-2070)

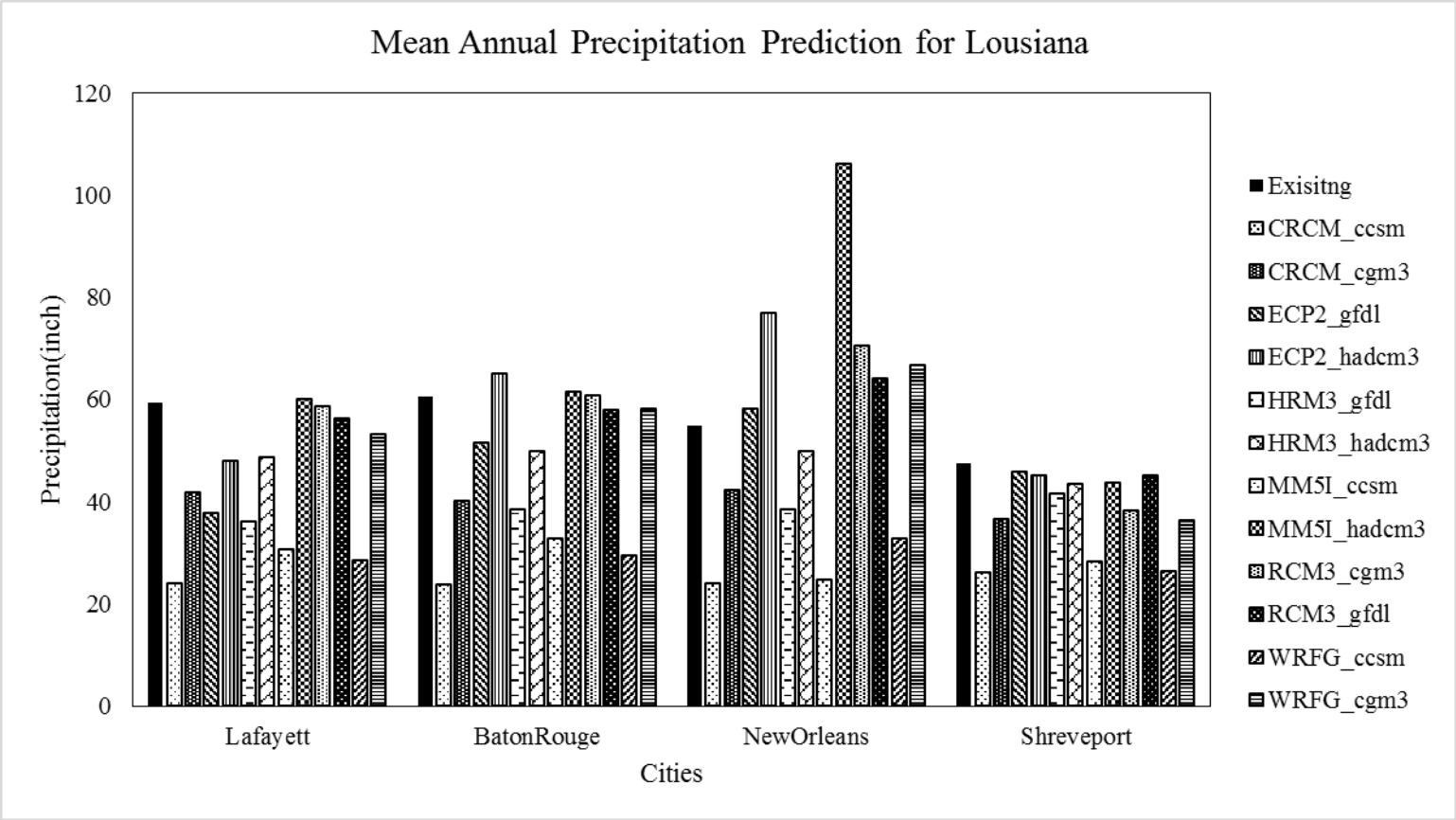

Figure 3-3 Mean Annual Precipitation of Different Cities of Louisiana for Climate Prediction Models (2041-2070)

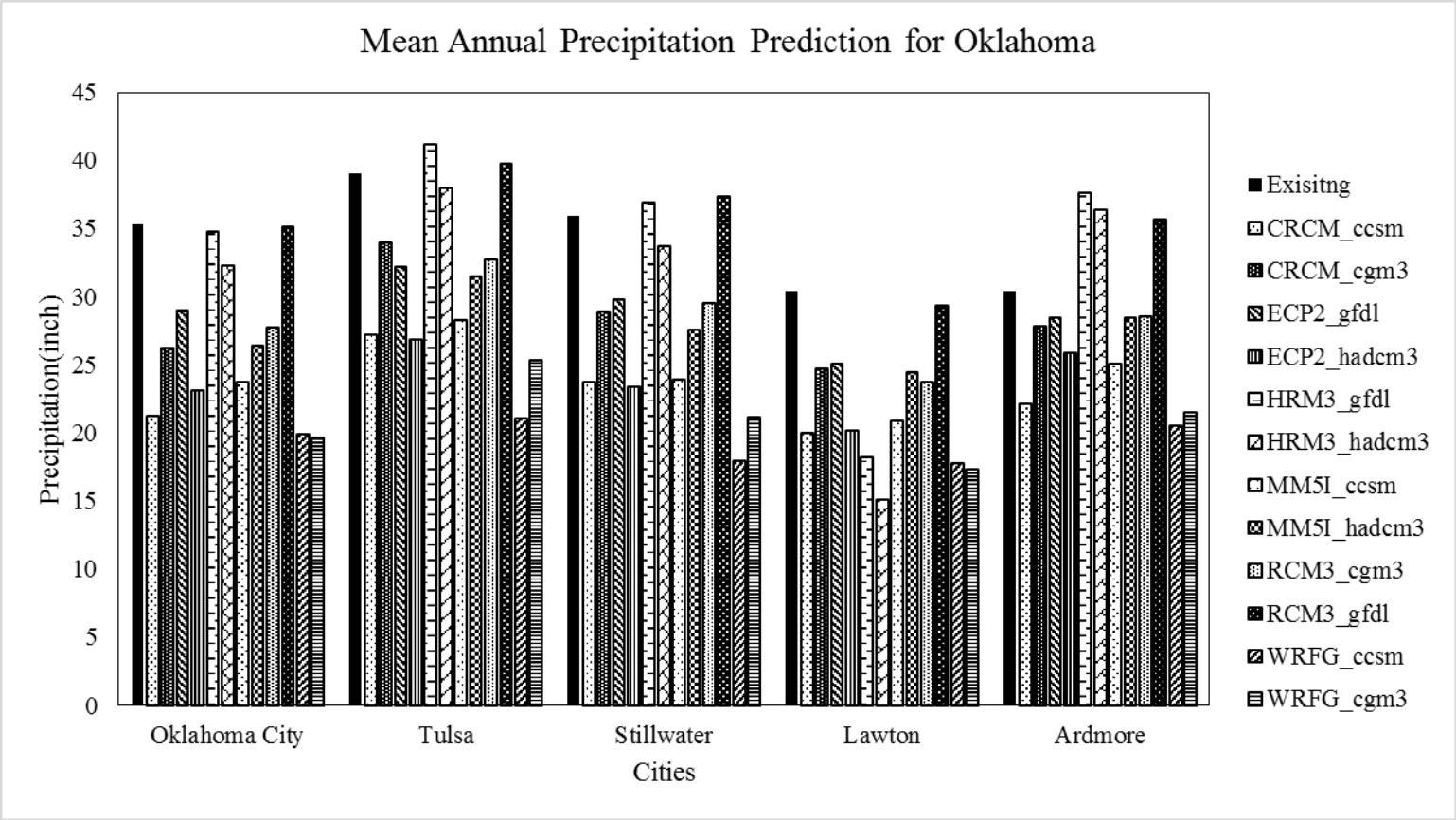

Figure 3-4 Mean Annual Precipitation of Different Cities of Oklahoma for Climate Prediction Models (2041-2070)

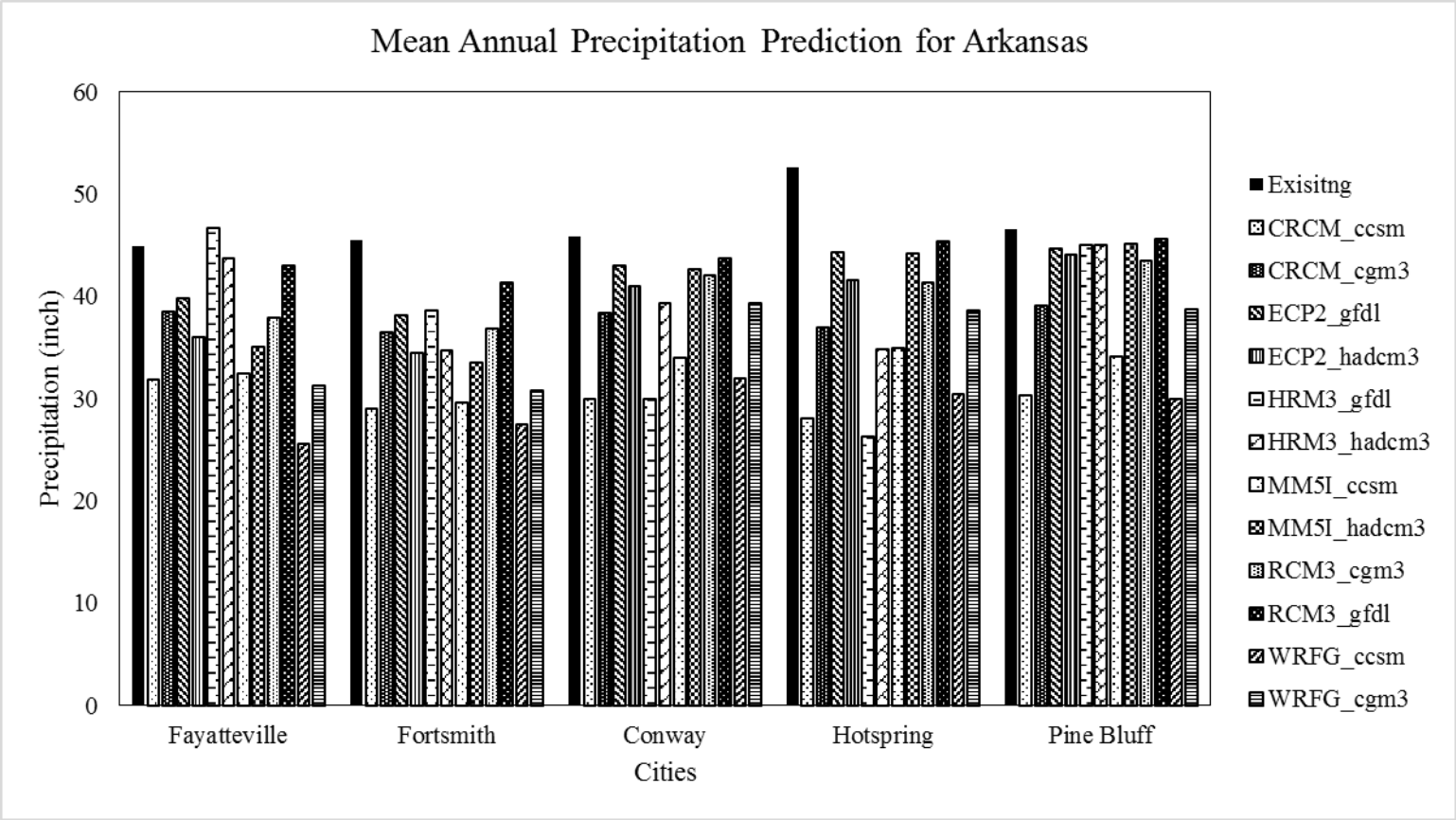

Figure 3-5 Mean Annual Precipitation of Different Cities of Arkansas for Climate Prediction Models (2041-2070)

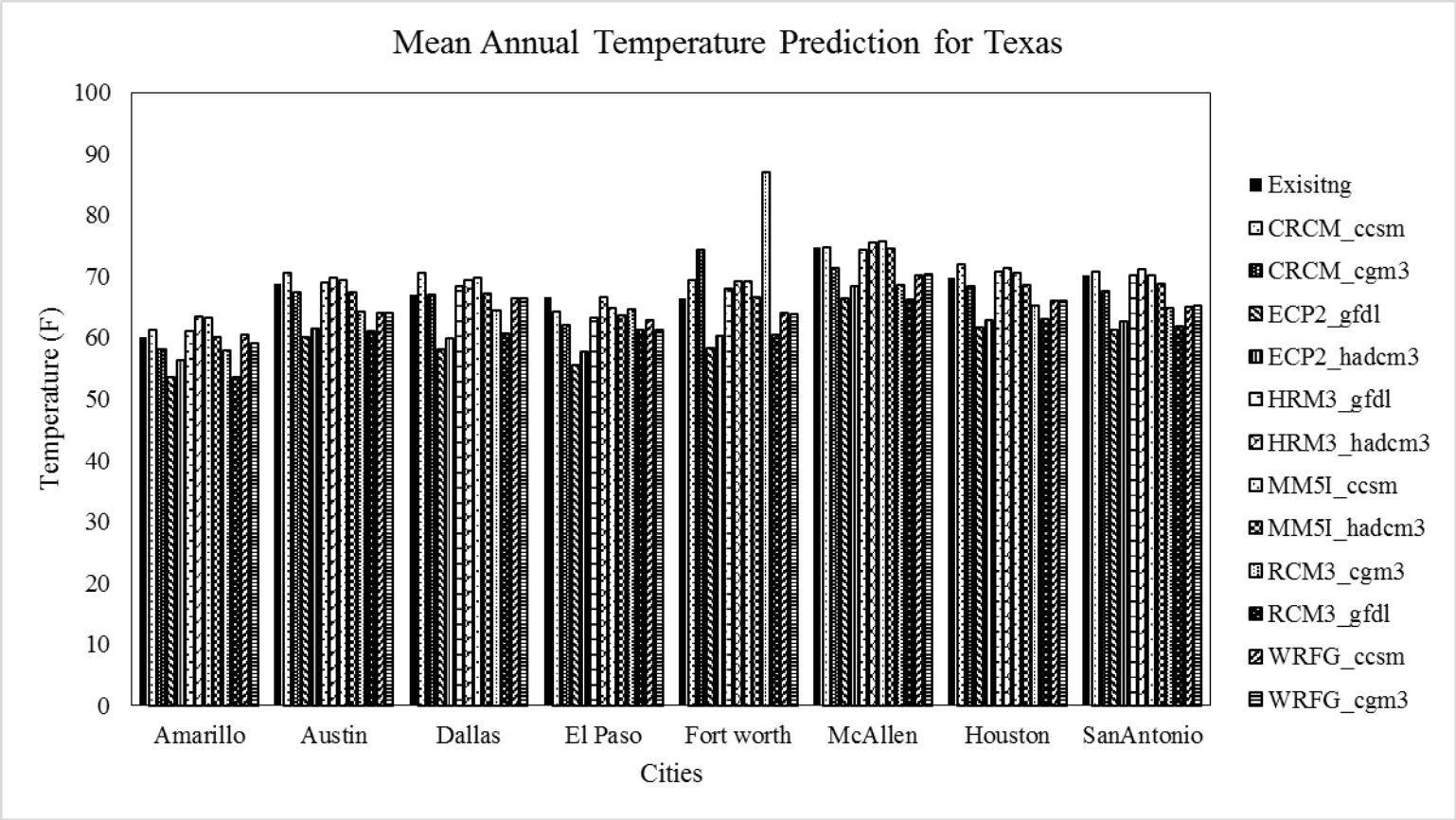

Figure 3-6 Mean Annual Temperature of Different Cities of Texas for Climate Prediction Models (2041-2070)

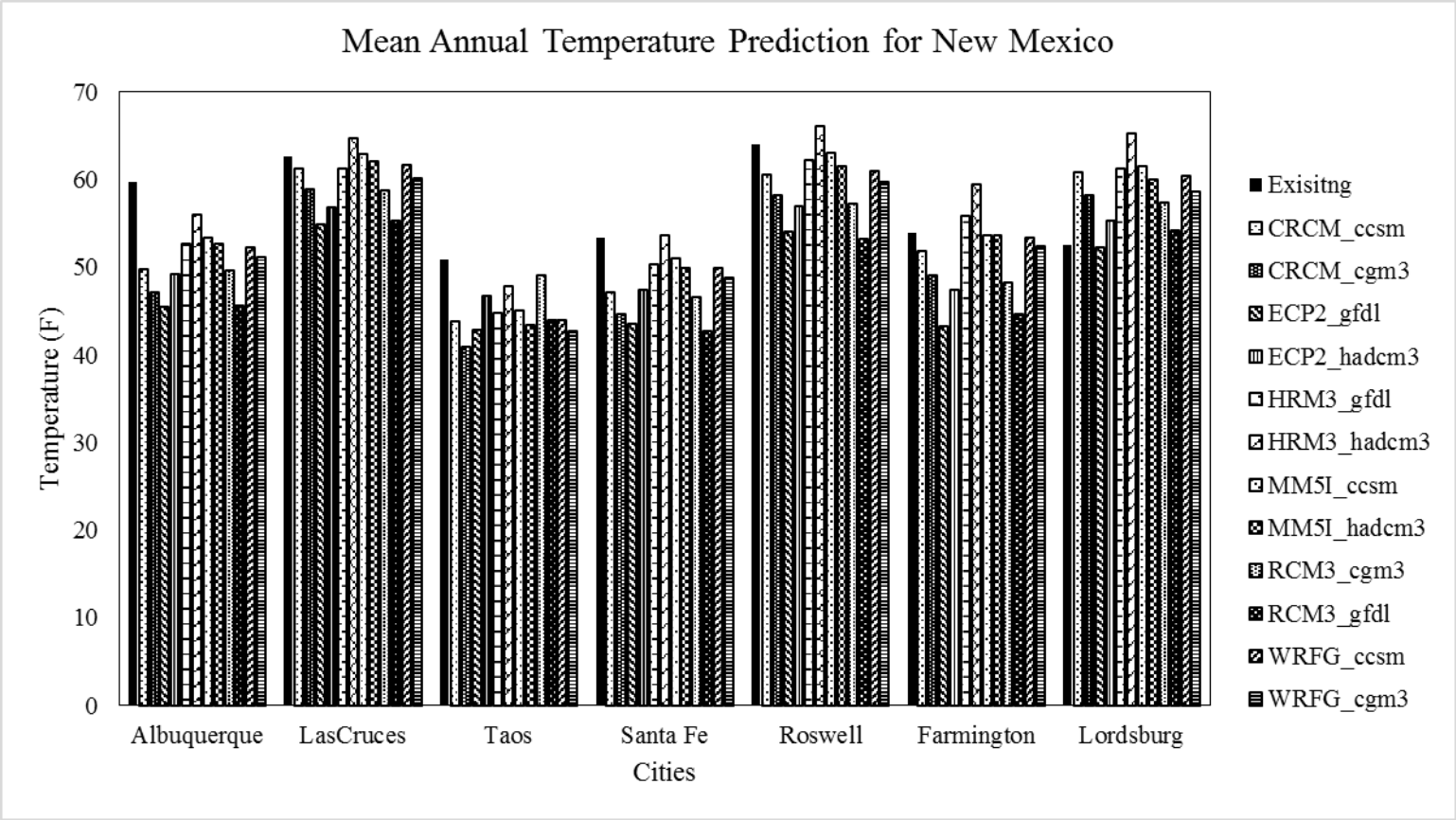

Figure 3-7 Mean Annual Temperature of Different Cities of New Mexico for Climate Prediction Models (2041-2070)

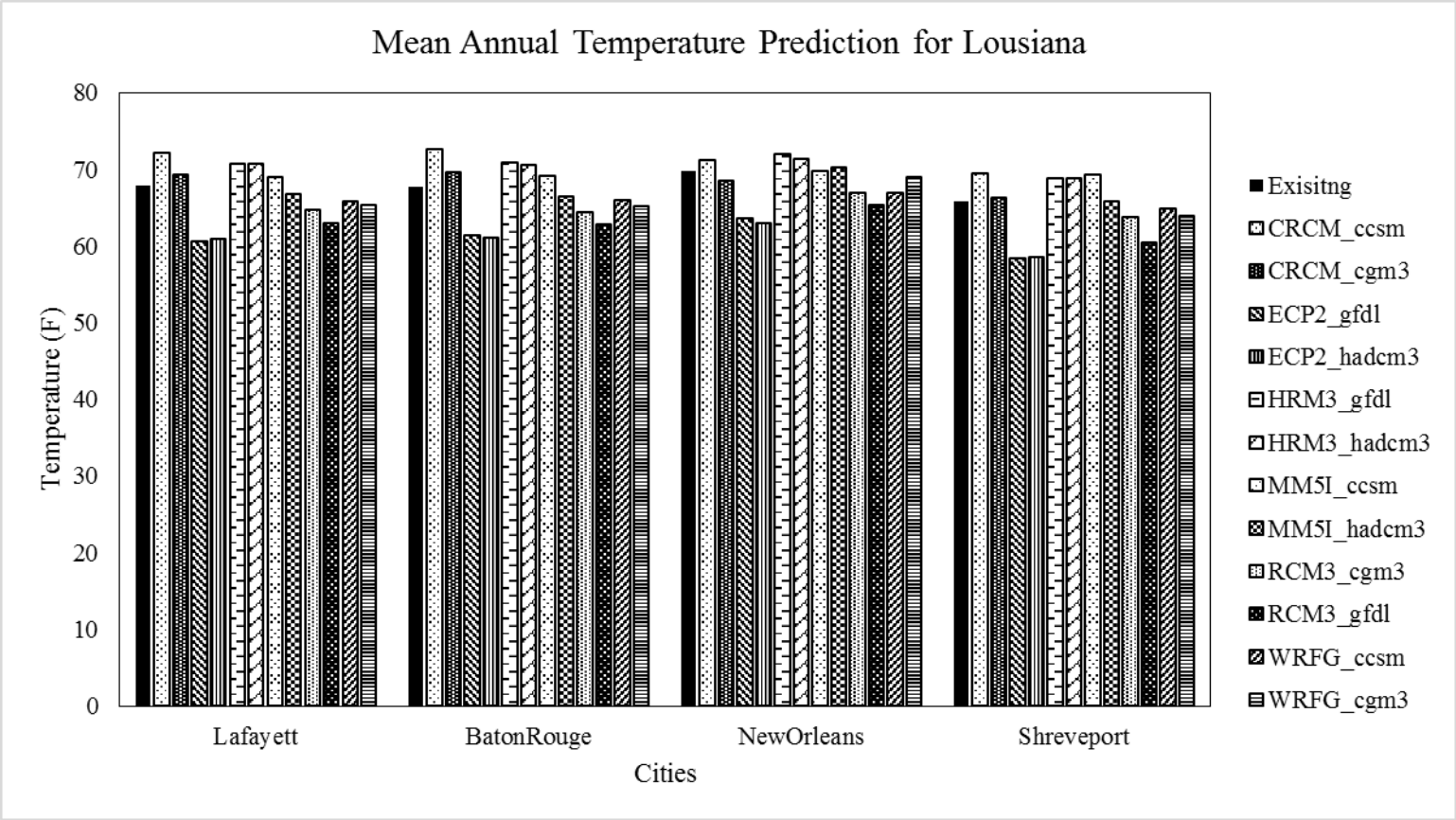

Figure 3-8 Mean Annual Temperature of Different Cities of Louisiana for Climate Prediction Models (2041-2070)

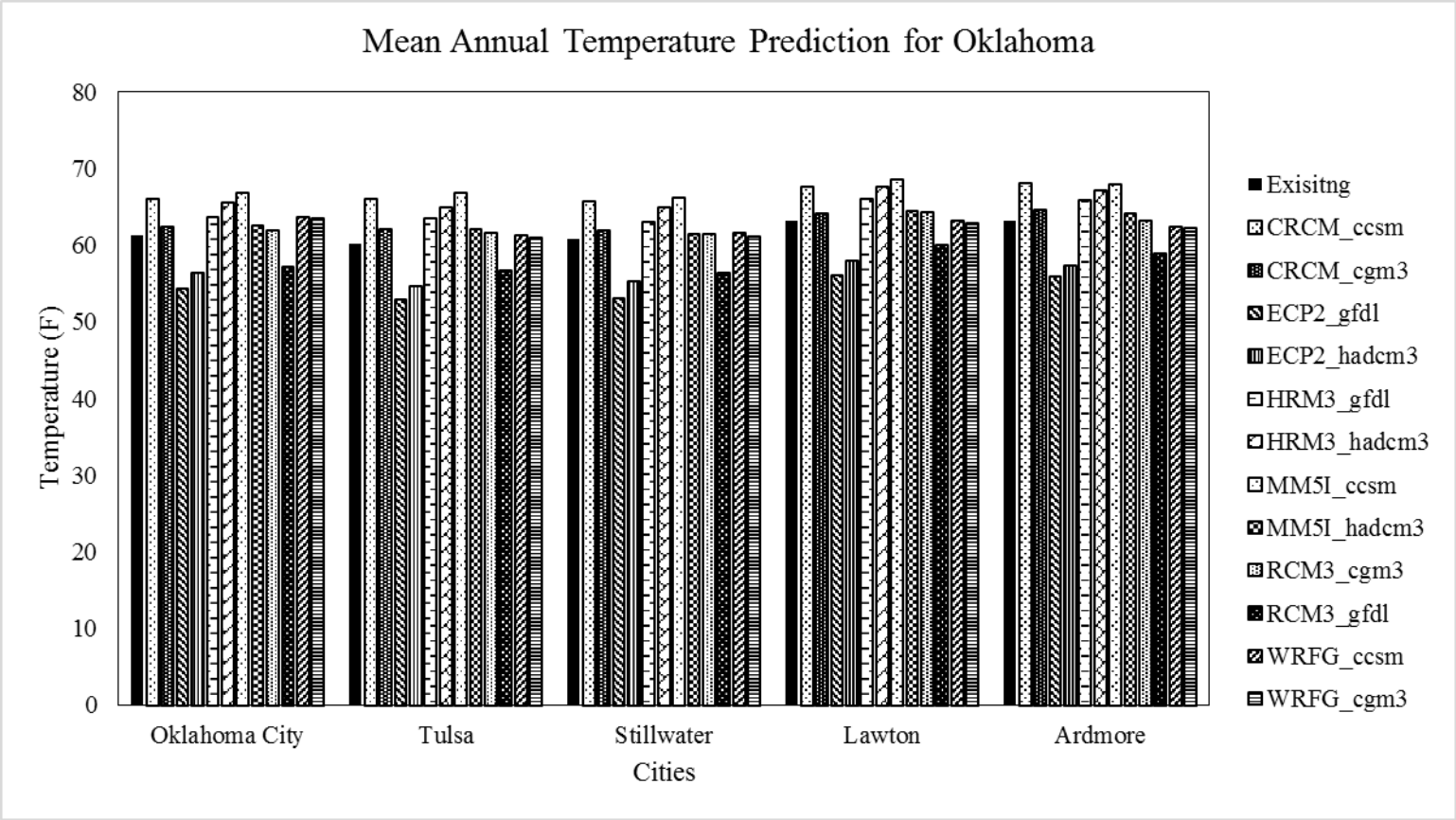

Figure 3-9 Mean Annual Temperature of Different Cities of Oklahoma for Climate Prediction Models (2041-2070)

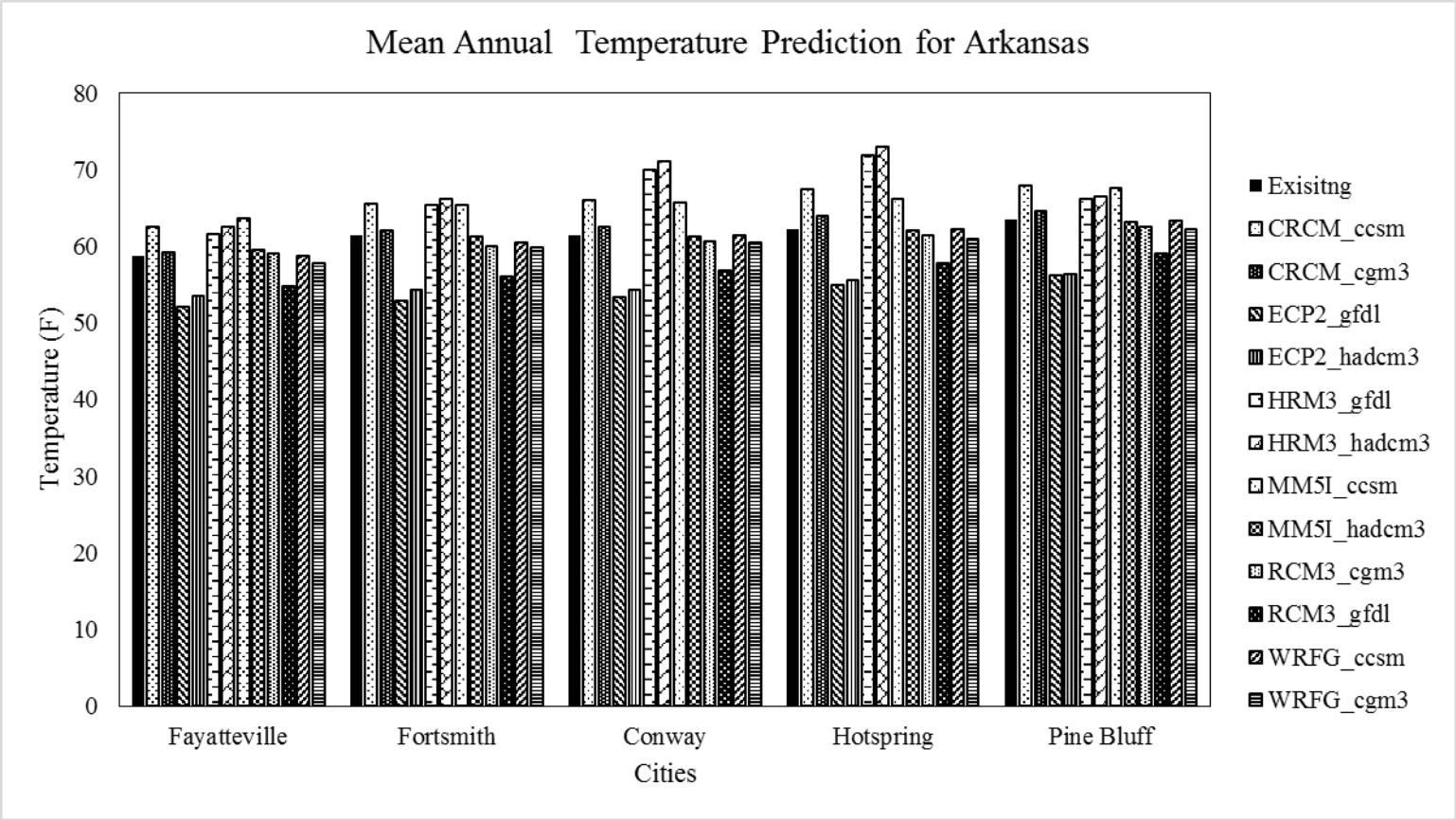

Figure 3-10 Mean Annual Temperature of Different Cities of Arkansas for Climate Prediction Models (2041-2070)

3.4 BIAS CORRECTION

Climate models possess inherent uncertainty. So, here, models simulated climate data has been analyzed with respect to observed climate data (Collected from NOAA) to evaluate the accuracy in the prediction of these models. For this analysis mean annual precipitation data for the period of 1979 to 1999 has been used. ***Figure 3-11*** shows that the model simulated data predict much higher precipitation than the observed values. So, models produced climate data needs to be corrected using bias correction methods before using them in any climate change impact study. The bias correction methods provide adjustment factors to minimize the error between the historical observed data and model produced current climate data (Hempel et al. 2013). Moreover, using that adjustment factor future, climate data also have been adjusted.

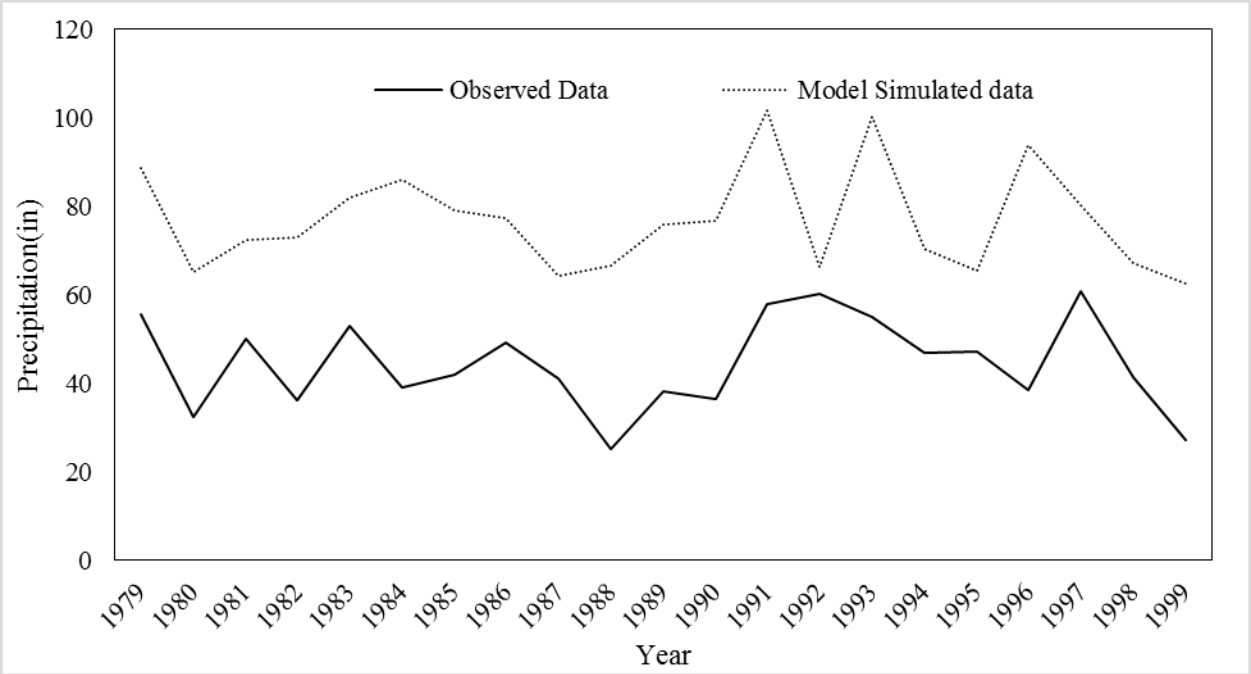

Figure 3-11 Model Simulated and Observed Precipitation Data

While various statistical methods are in practice to adjust the bias of the modeled climate data, in this study the 'delta-change' method has been used. This method is a simple statistical bias correction method. Biases are corrected by taking the difference between observed climate data and model produced current climate data.

Temperature Bias Correction is done using the following equations (3-1 and 3-2), where δ is calculated as the difference between the bserved mean annual temperature ($\overline{T}_{obs}$) and mean model simulated temperature ($\overline{T}_{mod}$). And the bias corrected temperature (T_{bias}) is found just simply adding to the $\overline{T}_{mod}$.

$$\delta = \overline{T}_{obs} - \overline{T}_{mod} \quad (3\text{-}1)$$

$$T_{bias} = T_{mod} + \delta \quad (3\text{-}2)$$

While Precipitation Bias Correction is done using equation 3.3 and 3.4., where δ is calculated by taking the ratio of observed mean annual precipitation ($\overline{P}_{obs}$) to model simulated mean annual precipitation ($\overline{P}_{mod}$). And then the bias corrected mean annual precipitation (P_{bias}) is estimated by multiplying with P_{mod}.

$$\delta = \overline{P}_{obs}/\overline{P}_{mod} \quad (3\text{-}3)$$

$$P_{bias} = P_{mod}\, X\, \delta \quad (3\text{-}4)$$

As the climate models are predicting more changes for precipitation, bias correction has been done for precipitation according to the Delta change method. **Table *3-2*** shows the bias-corrected precipitation data for Houston, Texas, which has been illustrated in **Figure *3-12***.

Table 3-2 Bias Corrected Precipitation Data, Houston, Texas

Climate Models	Future Simulation (in)	Current Simulation (in)	Bias-Corrected (in)
CRCM-CCSM	23.2	25.7	39.4
CRCM-CGCM3	39.4	42.1	40.8
ECP2-GFDL	49.9	56.8	38.2
ECP2-HADCM3	82.4	77.1	46.6
HRM3-GFDL	34.3	37.5	39.8
HRM3-HADCM3	48.1	45.2	44.9
MM5I-CCSM	22.6	25.2	37.9
MM5I-HADCM3	61.9	57.1	48.0
RCM3-CGCM3	48.1	47.1	44.5
RCM3-GFDL	53.6	50.1	46.6
WRFG-CCSM	29.0	28.8	43.9
WRFG-CGCM3	38.8	39.6	42.7

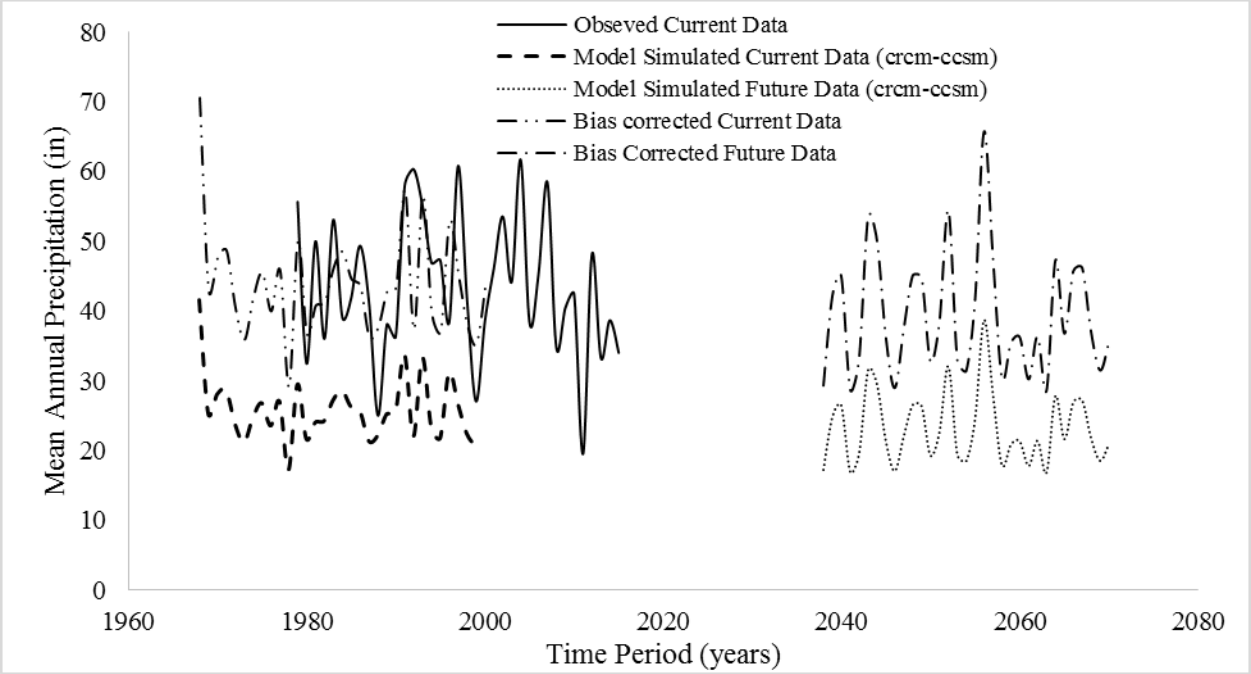

Figure 3-12 Bias Correction for Mean Annual Precipitation, Houston, Texas

Figure *3-12* clearly shows that model (CRCM-CCSM) simulated current data matches the observed data. After the bias correction, the models predict the precipitation increase for Huston as high as 10.2%, which has been predicted by an MM5I-HADCM3 climate model. All the climate model generated future precipitation data of all the cities of SPTC represented states has been bias-corrected and cataloged in Appendix A.

4. HYDRAULIC MODELLING

4.1 COMMUNICATING CLIMATE PREDICTIONS TO HYDRAULIC MODEL

The primary factor influencing bridge infrastructure vulnerability is streamflow, which is affected by climate change event like a change of intensity and frequency of precipitation. So, precipitation is a main climatic stressor. Linking climate projection data to streamflow simulation models is a novel technology in transportation design analysis (Anderson et al., 2015). Some established and widely used precipitation-runoff models in hydrologic and hydraulic are Hydrologic Engineering Centers Rivers Analysis System (HEC-RAS), which was developed by the U.S Army Corps of Engineers (USACE), the Soil and Water Assessment Tool (SWAT), or the U.S. Soil Conservation Service/Natural Resources Conservation Service (NRCS) TR-20 hydrologic model. In this study, Regional regression equations of Texas have been used to perform the hydrologic analysis. Moreover, resulted flow data from these equations have been used as the input for Hydraulic modeling of the bridge, which has been established using HEC-RAS. Both hydrologic and hydraulic modeling for the bridge is discussed in the following sections of this chapter. ***Figure 4-1*** shows the methodology used to incorporate the predicted precipitation data from climate models to the created hydraulic model. After doing the bias correction of climate data as described in previous section, they are feed into the hydrologic model to estimate flood quantiles (flood events for different return periods, i.e 100-year flood). After the computing the flood quantiles, they would be input in the hydraulic model of the bridge. This hydrologic modeling and hydraulic modeling will be discussed in the following sections.

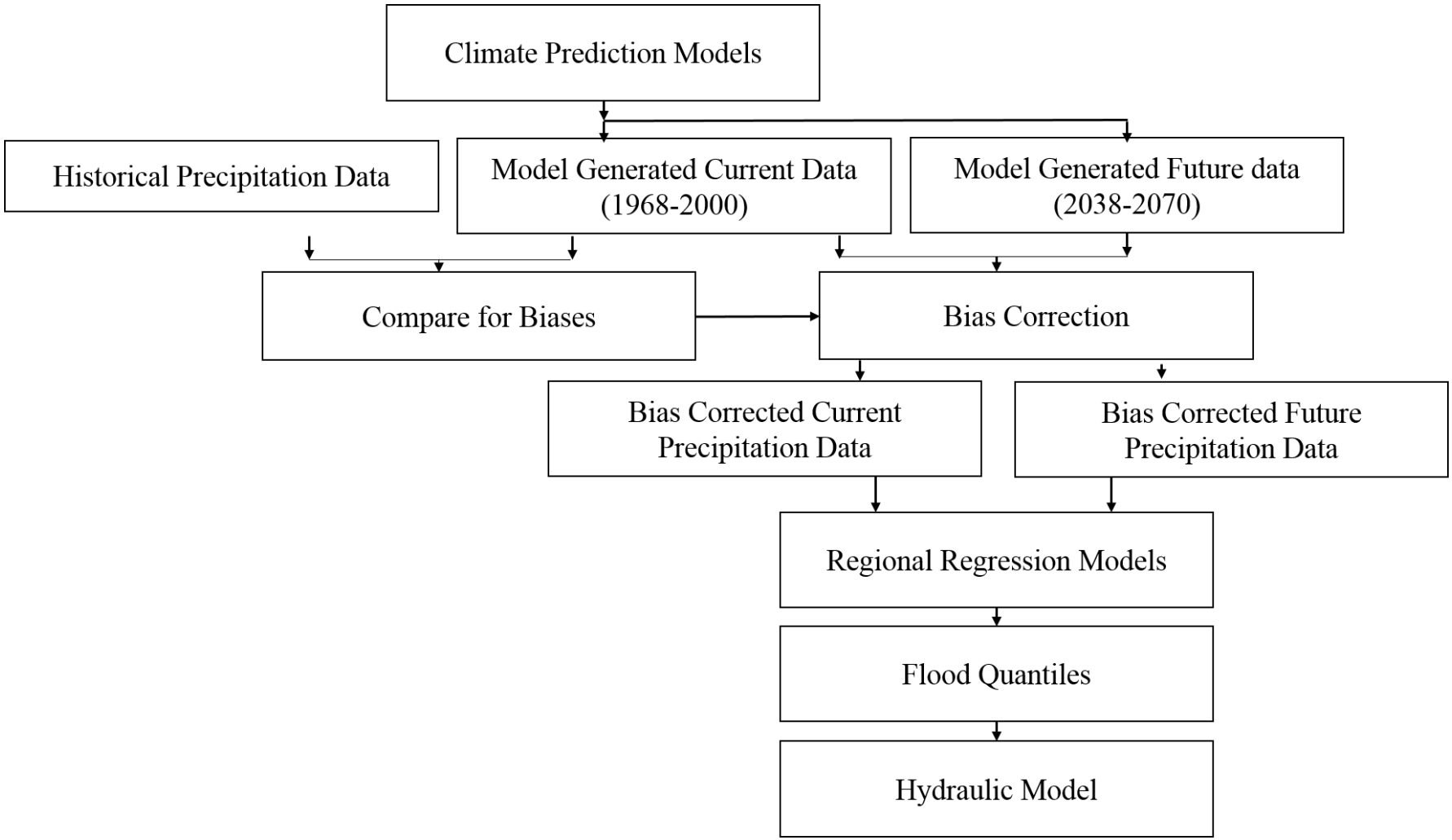

Figure 4-1 Illustration of the Methodology that has been Followed to Communicate Climate Projection Data to Hydraulic Model

4.2 HYDRAULIC MODELING

This section describes the methodology that has been applied for hydraulic modeling of the bridges. The modeling has been performed using the HEC-RAS model, established by the US Army Corps of Engineers. The modeling can be performed in one or two dimensional for steady and unsteady flow analysis of the river systems. HEC-RAS has been built with the same hydraulic principles that have been followed by most of the transportation agencies for bridge design and which have been inscribed in the HEC-18 manual by FHWA.

The hydraulic modeling using HEC-RAS can be divided into three broad parts. 1) Preprocessing or creating the geometry, 2) Inputting hydrologic data or hydrologic modeling, and 3) Hydraulic design computations. A general overview of the method is shown in ***Figure 4-2***.

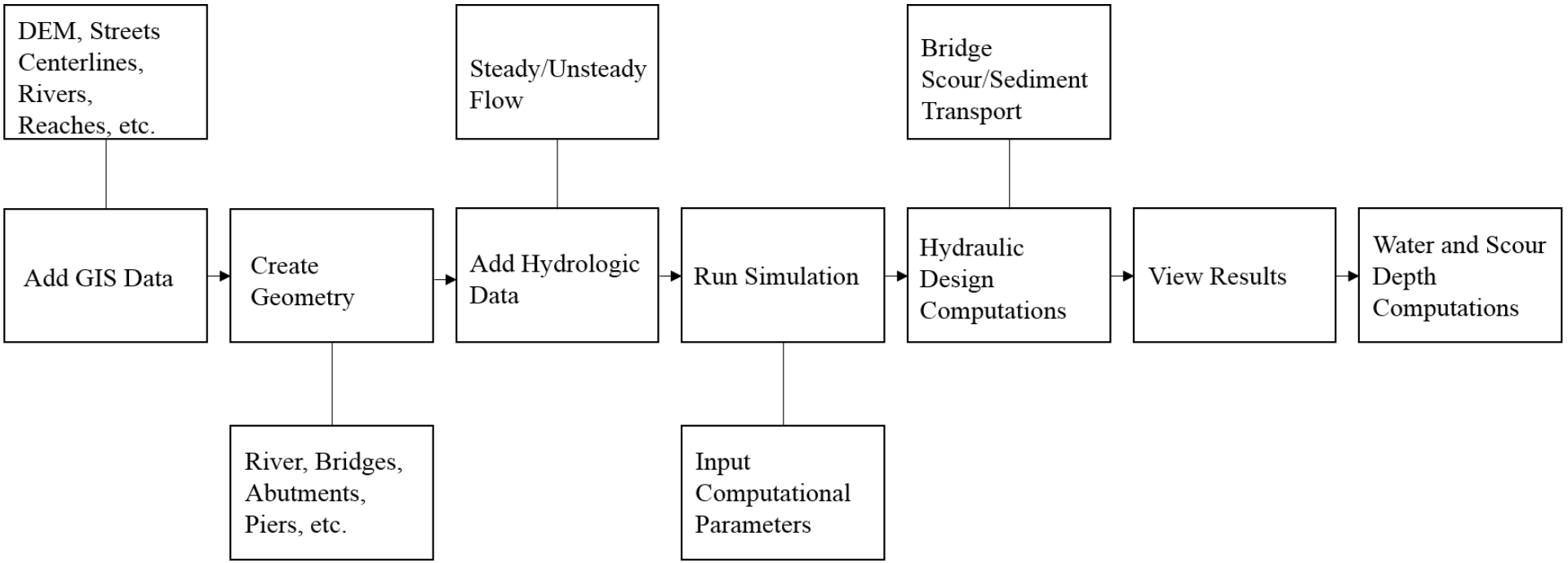

Figure 4-2 Bridge Hydraulics Analysis Using HEC-RAS

4.2.1 PRE-PROCESSING

Preprocessing of the hydraulic model or creating the terrain geometry has been done using ArcGIS. This involves collecting the Digital Elevation Model (DEM) of the study area and creating the raster file of the terrain and shapefiles for the river's reach, cross sections, bridge locations, etc. Then the raster file has been converted to the .tiff file to make it usable in RAS-mapper of HEC-RAS. **Figure *4-3*** shows the terrain file created for the Houston-Galveston area. For this a 10m DEM has been collected and processed using ArcGIS.

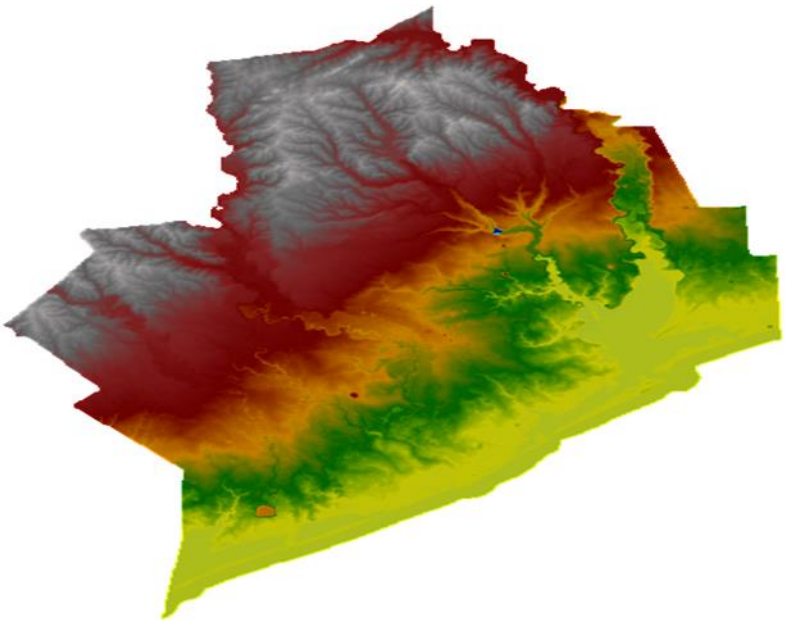

Figure 4-3 Illustration of Terrain of Houston_Galvaston area

After creating the terrain, next step is to define the river's reach and cross-sections, as well as the creating the bridge with all the required characteristic data like deck width, pier shape, and size or abutment properties, and so forth. To perform these steps, all the required data have been collected from the TxDOT BRINSAP server. The data also includes the previous routine inspection survey of the bridge condition.

To estimate vulnerability of bridges and predict the risk they may face due to climate change in future, two bridges situated in Houston (Texas) have been analyzed in this study. The bridges are US 59 crossing over West Fork San Jacinto River and SH 36 Crossing over Big Creek. Among

them, bridge US59 that has been already identified as scour-vulnerable according to the National Bridge Inventory (NBI) record (FHWA, 2016). Although SH36 is not vulnerable to scouring, it is vulnerable to overtopping. The characteristic parameters of these two bridges have been presented in this section, which has been used as the input parameters in performing hydraulic bridge analysis.

The case I: US 59 crossing West Fork San Jacinto River, Houston, Texas

The characteristics of US 59 bridge is situated in the Harris County of Houston District are included in **Table *4-1***.

Table 4-1 Case I-Characteristics of Bridge US 59

Bridge Name	**US 59**
Bridge crossing	West Fork San Jacinto River
TxDOT structural no.	12-102-0177-06-081
Bridge Coordinate	30°1'35.07"N, 95°15'32.29"W
Year built	1961
Bridge Length	1645 feet
No. of piers	25
Pier spacing	60 feet
Pier diameter	16 sq. inches
Foundation	30 feet concrete piles
Bridge Opening	60 feet

The case II: SH 36 crossing Big Creek, Houston, Texas

Similarly, the characteristics of SH 36 bridge is situated in the Fort bend county of Houston District are included in **Table *4-2***.

Table 4-2 Case-II Characteristics of Bridge SH 36

Bridge Name	**SH 36**
Bridge crossing	Big Creek
TxDOT structural no.	0188-02-023
Bridge Coordinate	29º28'35.1"N, 95º48'46.97"W
Year built	1932
Bridge Length	257 feet
No. of piers	10
Pier spacing	25 feet
Pier diameter	14 sq. inches
Foundation	25 ft to 35 ft concrete piles
Bridge Opening	15 feet

4.2.2 HYDROLOGIC MODELING

For hydraulic simulation using HEC-RAS, the streamflow data is needed, and a description of the precipitation-streamflow modeling approach is included in the following paragraphs.

Although several methods are available to perform the precipitation-streamflow simulation, a simple regional regression equation approach is used in this study. While national regression equations are available, Texas has established its own sets of regression equations for the estimation of annual peak streamflow frequency. Annual peak streamflow frequency or flood quantiles represents the peak streamflow with recurrence intervals of 2, 5, 10, 25, 50, 100, 200, 250 and 500 years.

In 2009, Asquith and Roussel (2009) in cooperation with the TxDOT established a set of equations that relate the basin characteristics to the stream flow of the basin. Although the regional regression equations are developed for 'natural basins,' the urban development does not have many effects on rainfall-runoff generation process. Thus, the used on these equations in an urban setting requires caution and a higher factor of safety (Briaud et al., 2009).

Table *4-3* shows the regional regression equations with adjusted R-factor. The flow with a given recurrence interval is related to mean annual precipitation (P [inch]), dimensionless average channel slope (S, [L/L]), Drainage area (A, [mile^2]), and a parameter Ω, that represents a generalized terrain and climate index that describes relative differences in peak streamflow

potential across the study area. The Ω can be read from the **Figure *4-4*** that illustrated the ecoregions in Texas with superimposed values of Ω values.

Table 4-3 the Regional Regression Equations (Asquith and Roussel, 2009)

Return Period	**Equations**	**R-Adjusted**
2	$Q_2 = P^{1.398} S^{0.270} 10^{[0.776\Omega + 50.98 - 50.30 A^{-0.0058}]}$	0.84
5	$Q_5 = P^{1.308} S^{0.372} 10^{[0.885\Omega + 16.62 - 15.32 A^{-0.0215}]}$	0.88
10	$Q_{10} = P^{1.203} S^{0.403} 10^{[0.918\Omega + 13..62 - 11.97 A^{-0.0289}]}$	0.89
25	$Q_{25} = P^{1.140} S^{0.446} 10^{[0.945\Omega + 11.79 - 9.819 A^{-0.0374}]}$	0.89
50	$Q_{50} = P^{1.105} S^{0.476} 10^{[0.961\Omega + 11.17 - 8.997 A^{-0.0424}]}$	0.87
100	$Q_{100} = P^{1.071} S^{0.507} 10^{[0.969\Omega + 10.82 - 8.448 A^{-0.0467}]}$	0.86
200	$Q_{200} = P^{1.034} S^{0.531} 10^{[0.975\Omega + 10.61 - 8.058 A^{-0.0504}]}$	0.84
250	$Q_{250} = P^{1.021} S^{0.541} 10^{[0.977\Omega + 10.56 - 7.943 A^{-0.0561}]}$	0.83
500	$Q_{500} = P^{0.988} S^{0.569} 10^{[0.976\Omega + 10.40 - 7.605 A^{-0.0554}]}$	0.81

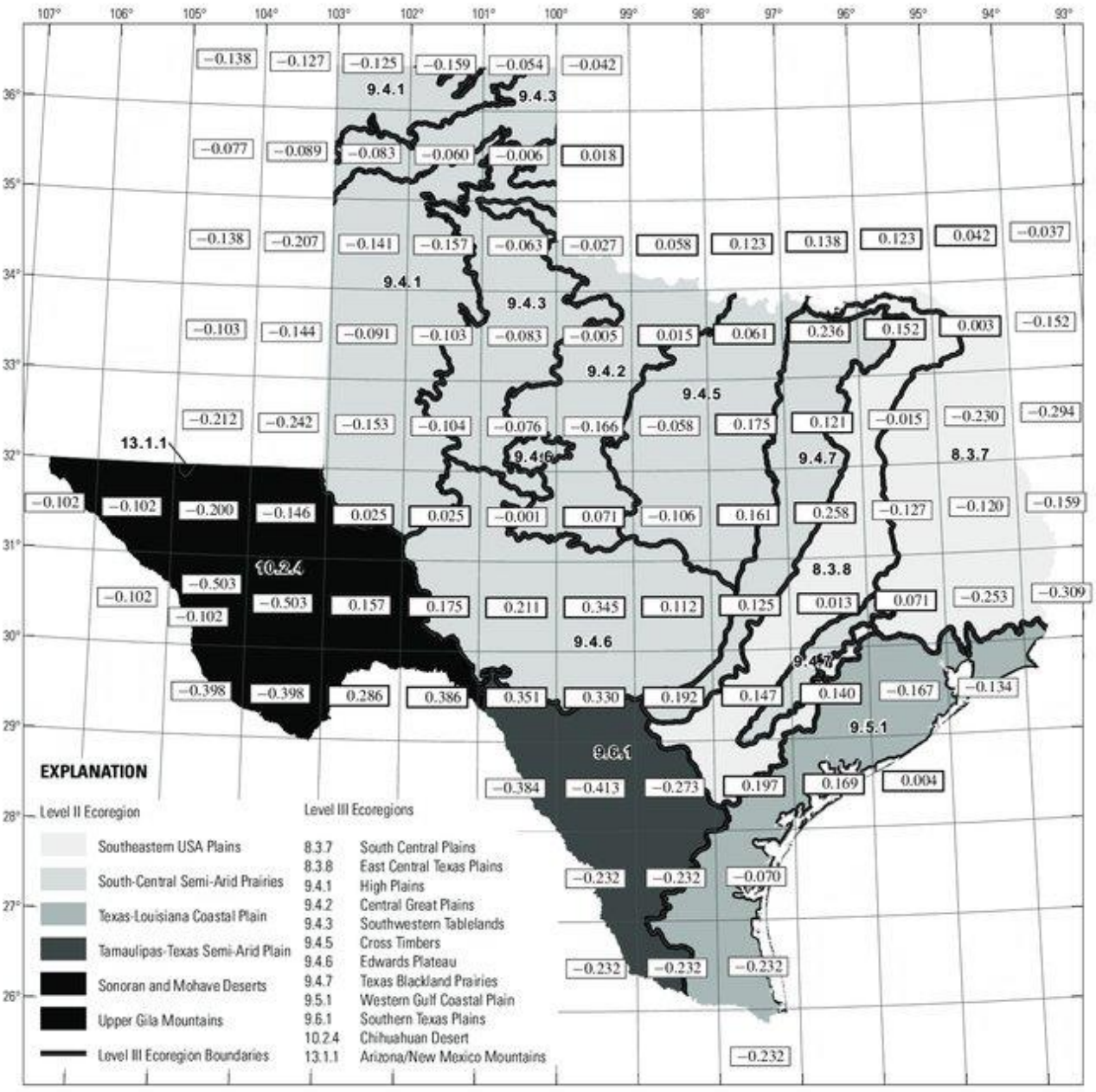

Figure 4-4 Eco-Regional Map of Texas with Superimposed Values of the Omega-Em parameter (Base from Texas Natural resources Information System digital data Ecoregions from Commission for Environmental Corporation, 1997. Scale 1:7,920,000. Albers equal area projection, datum NAD 83. Standard parallels 27º30' and 31º00', central median -100o00'. Horizontal coordinates information is referenced to the North American Datum of 1983 (NAD 83)) **(Asquith and Roussel, 2009)**

The mean annual precipitation data predicted from different climate models are incorporated in these equations, which produce the floods for different recurrence interval.

Example of Flood Quantile Estimation:

- River basin: West Fork San Jacinto River
- Area of Drainage Basin, A = 828 $mile^2$
- Slope, S = 0.003
- $\Omega = 0.14$
- Mean Annual Precipitation, P = Predicted By different models

The resulted floods for different return period have been listed in **Table *4-4***.

Table 4-4 Flood Quantiles Prediction Using Different Climate Models

	Existing	CRCM-CCSM	CRCM-CGM3	ECP2-GFDL	ECP2-HADCM3	HRM3-GFDL	HRM3-HADCM3	MM5I-CCSM	MM5I-HADCM3	RCM3-CGM3	RCM3-GFDL	WRFG-CCSM	WRFG-CGM3
P	43.2	39.23	40.78	38.24	46.56	39.80	44.90	37.90	48.00	44.48	46.57	43.80	42.71
2	20963.4	18106.8	19114.8	17471.3	23006.3	18475.7	21867.8	17254.5	24007.1	21582.3	23013.2	21122.5	20391.3
5	48983.5	42709.7	44930.2	41305.4	53436.0	43523.2	50957.9	40825.7	55608.0	50335.3	53451.1	49331.2	47731.6
10	70186.3	61873.8	64826.4	60000.3	76033.3	62956.9	72784.1	59359.1	78871.0	71965.8	76052.9	70644.4	68534.8
25	106787.6	94763.9	99043.9	92042.5	115200.0	96335.1	110529.6	91110.1	119270.5	109351.7	115228.3	107448.0	104405.1
50	140682.8	125301.3	130783.0	121811.8	151412.4	127314.5	145458.6	120615.6	156595.3	143955.8	151448.4	141525.9	137639.3
100	181663.8	162379.1	169259.9	157994.4	195077.4	164907.3	187638.0	156490.4	201546.1	185758.8	195122.2	182719.0	177853.4
200	228268.8	204829.2	213202.9	199486.8	244520.9	207907.3	235512.2	197653.1	252344.6	233234.6	244575.2	229548.7	223644.5
250	245254.3	220370.6	229264.1	214694.1	262488.7	223640.3	252937.3	212745.3	270780.1	250521.9	262546.3	246612.2	240347.8
500	301482.5	271832.2	282441.1	265053.6	321960.7	275734.1	310617.2	262725.1	331797.0	307746.3	322029.0	303097.6	295644.1

The flood of different intervals estimated using different predicted climate models is illustrated in **Figure *4-5*** and **Figure *4-6***. It shows five models predict higher flood flows than the existing one in future, while five models show flow amount can be less for different return periods. **Figure *4-5*** shows the flood flow of different return periods for the San Jacinto River. For 100-year flood, MM5I-HADCM3 predicts an increase of around 11% than the existing climatic condition, where MM5I-CCSM, which predicts around 14% less flow intensity than the existing one.

Similarly, **Figure *4-6*** shows the floods with different return periods for the predicted climate models for the Big Creek watershed. It shows MM5I-HADCM3 predicts almost 11% increase and MM5I-CCSM shows around 16% decrease in future 100-year flood flow.

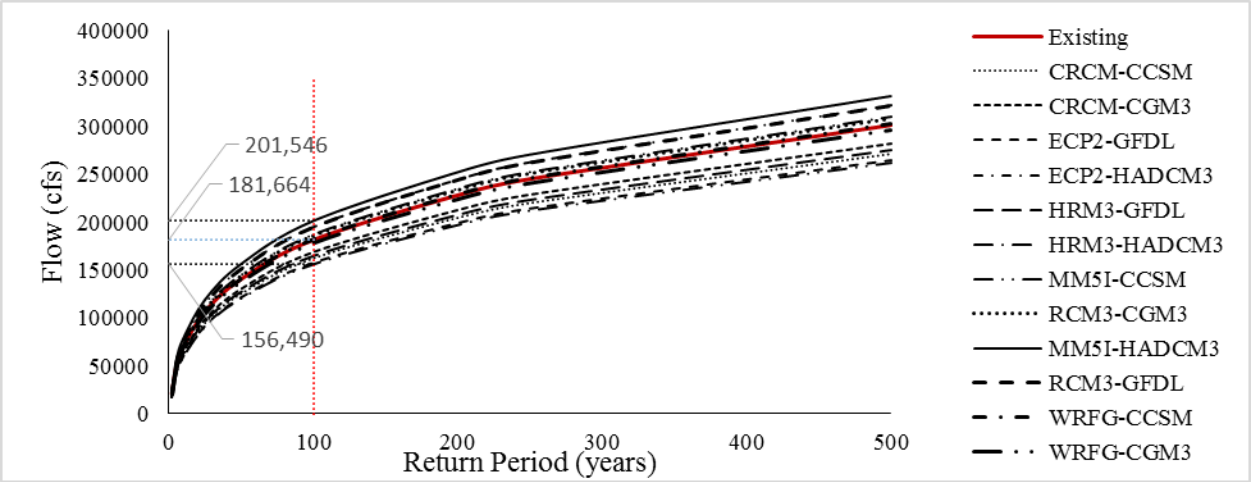

Figure 4-5 Predicted Flood Flows for Future Climate Scenarios, San Jacinto River, Houston, Texas

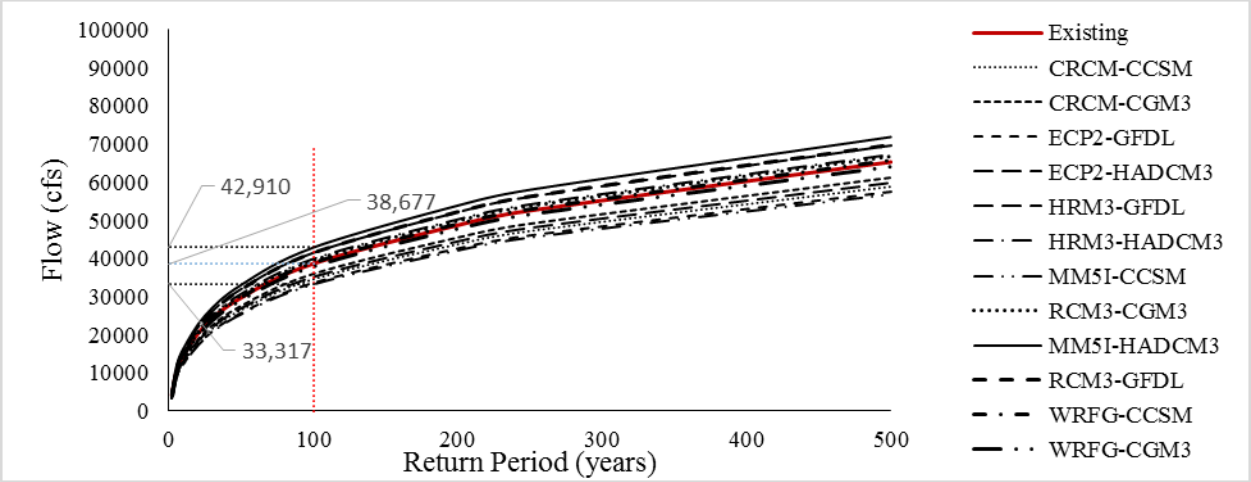

Figure 4-6 Predicted Flood Flows for Future Climate Scenarios, Big Creek, Houston, Texas

4.2.3 HYDRAULIC SIMULATIONS

The very first step in performing the hydraulic modeling in HEC-RAS is to choose the appropriate modeling approach. Several methods are available for bridge hydraulic modeling in HEC-RAS interface, for both low flow and high flow conditions.

For low flow computations:

- Energy Equation or Standard Step Method
- Momentum Balance Method
- Yarnell Equation
- FHWA WSPRO Method

For high flow computations:

- Energy Equation or Standard Step Method
- Pressure Flow Method

For low flow methods, HEC-RAS provides the opportunity to choose all the methods and compute according to the highest energy answer. However, for high flow, one has to choose either energy step method or pressure flow method. This study involves the computation of the overtopping potential, so pressure flow method is a proper choice for high flow simulations.

Although HEC-RAS provides an opportunity to perform both steady and unsteady flow analysis, a steady gradually varied flow analysis was performed in this study. To perform a steady analysis, a reach boundary condition has to be set. As from the Digital Elevation Model (DEM), the slope of the reach can be easily evaluated, and boundary conditions have been set using Normal depth of the downstream. **Figure *4-7*** shows the hydraulic simulations for 100-year flood events for bridge US 59 crossing the West Fork San Jacinto River.

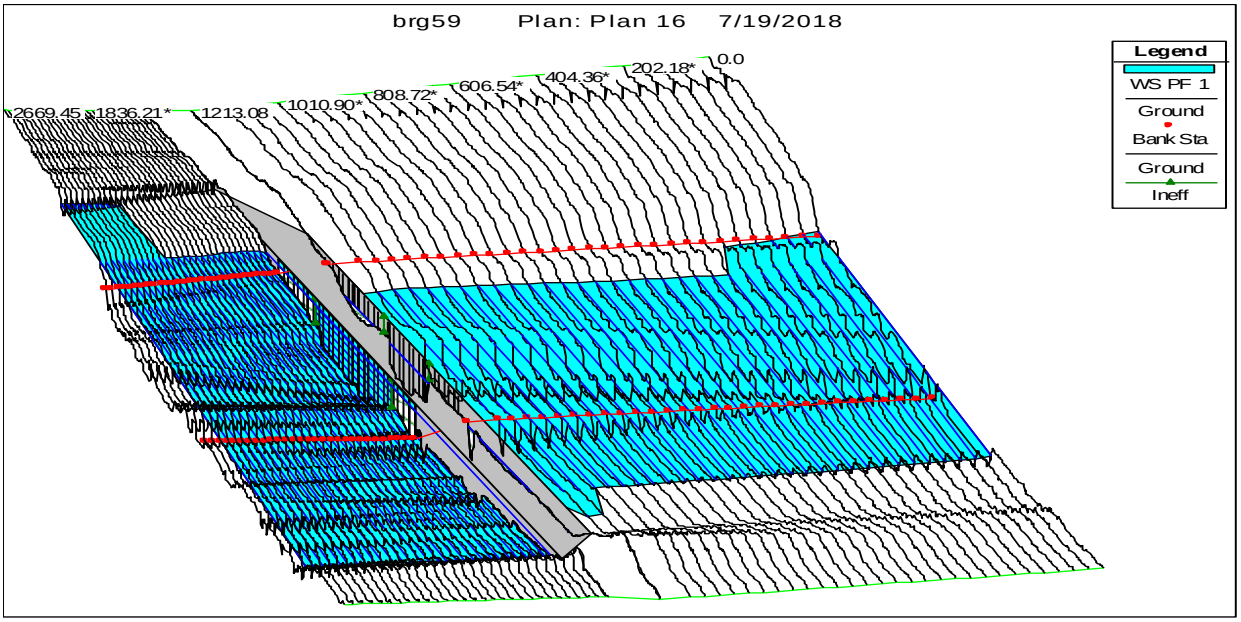

Figure 4-7 Hydraulic Simulation of the Bridge US 59 Using HEC-RAS

5. VULNERABILITY AND RISK ASSESSMENT

5.1. VULNERABILITY ASSESSMENT OF BRIDGE

Bridges are generally vulnerable to failure due to scouring of the foundation materials, overtopping, hydrodynamic forces to bridge superstructures, debris accumulation, etc. (Okeil and Cai, 2008, Parola et al., 1998, Bala et al., 2005). Bridge hydraulic design focuses primarily on flows responsible for overtopping and flows responsible for scouring. So, the evaluation of an existing bridge for the vulnerability is also focused on these two conditions. This section discusses how the future climate change will affect the overtopping and scour condition of the bridge, with respect to the existing climatic condition.

5.1.1 VULNERABILITY TO OVERTOPPING

Overtopping is an important factor of damage to the bridges especially to the approach embankments. Besides disrupting the commute networks, hydrodynamic forces occur during the submerged condition make the bridge vulnerable to failure. The drag and lift forces pose a serious threat to the stability of the bridge deck (Cigada et al., 2001, Malavasi et al., 2001, Kara et al., 2015).

Bridges are overtopped when the water depth at the peak stream flow is above the bridge high chord elevation. **Figure *5-1*** shows the water depth resulted from the flow with different return period based on existing climatic condition for the bridge the US 59 over San Jacinto River in Houston, Texas. The elevation of the bridge is 63 feet, which is taken as the threshold value or overtopping depth to analyze the graph. The hydraulic simulation of the model shows that the bridge will be overtopped in the occurrence of a 119-year flood.

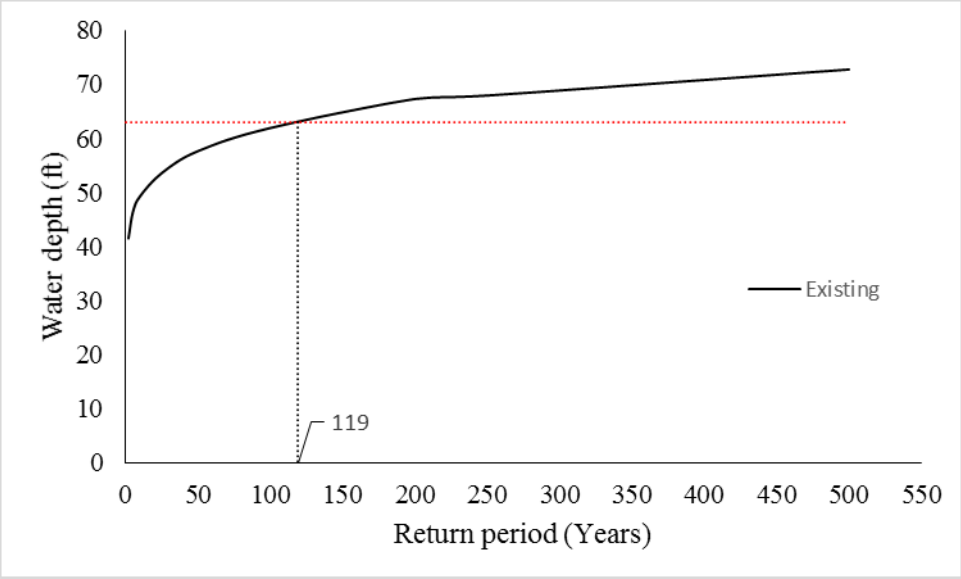

Figure 5-1 Depth of Water for Different Return Periods under Existing Climatic Condition, US59 Bridge, Houston, Texas

Climate models predict change in the flow magnitude for the future emission scenarios. Return periods or flood frequency for the overtopping depth (63') will also change for this future climate predictions. **Figure *5-2*** shows the predicted water depth for flood with different return period for the San Jacinto River. The simulation suggests the bridge will reach the overtopping depth at 90-years flood flow (predicted by MM5I-HADCM3), which is 29-years less than the existing condition.

Similarly, **Figure *5-3*** shows the simulated water depth for bridge SH 36 crossing Big Creek watershed for different climate prediction models. According to the hydraulic simulation under existing climatic condition, this bridge will be overtopped for 127-year flood flow. However, the future climate prediction shows a possibility of overtopping of the bridge for only 87-years flood flow. So for future predicted models the bridge in risk for failure due to overtopping even before the 100-year flood.

Water depth simulation results, from **Figure *5-2*** and **Figure *5-3***, also depict that the smaller water basin (big creek with 84 mile^2) shows similar trends for an increase of water depths for all models, where big basins (West Fork San Jacinto River with 842 mile^2) shows the difference in trends. This may help to conclude that the hydraulic simulation for big basins poses more biases than the smaller basin.

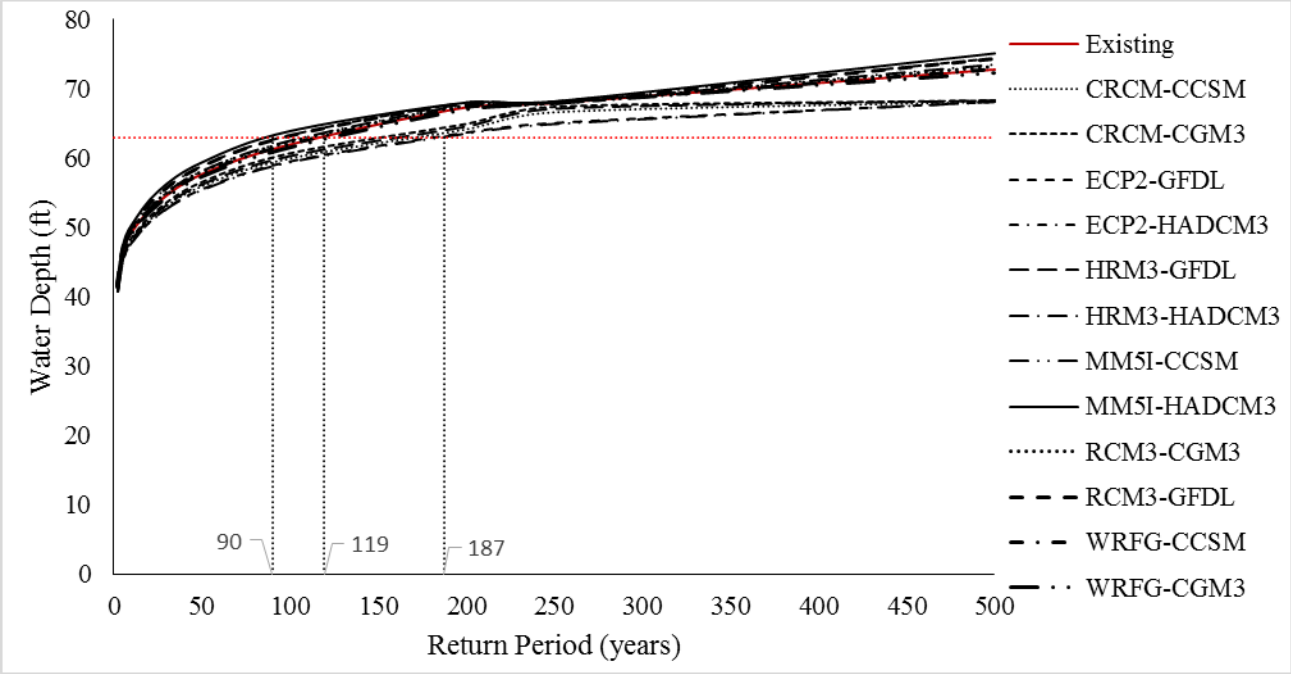

Figure 5-2 Depth of Water for Future Climate Predictions, US59 Bridge, Houston, Texas

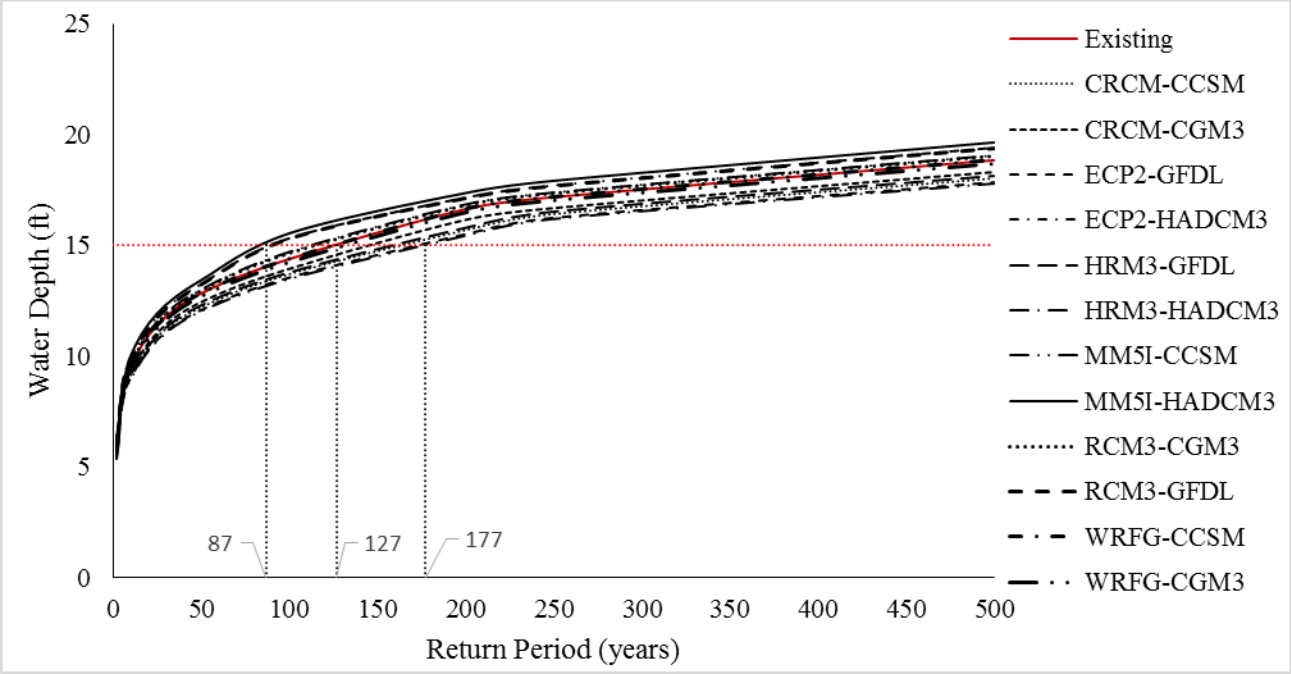

Figure 5-3 Depth of Water for Future Climate Predictions, SH36 Bridge, Houston, Texas

5.1.2 VULNERABILITY TO SCOUR

The most common reason for bridge failure is the scouring of the bed materials from the foundation of the bridge (Melville and Coleman, 2000). The scour depth is measured in this study using the HEC-18 manual, published by the Federal Highway Administration (FHWA), stated in Chapter Two. The established equations for the estimation of scour at abutment are not reliable to predict the scour depth (Briaud et al., 2009, TxDOT 2004, AASHTO LRFD 2007). So, the total scour depth comprises the scour occurred due to contraction and scour occurred underneath of the pier foundation.

This study compares the scour vulnerability of an individual bridge for different climate models as well as existing condition, concerning the allowable scour depth. Allowable scour depth is the function of depth of foundation. The standard practices estimate allowable scour depth as,

Allowable Scour Depth = ½ x Foundation Depth

Table *5-1* shows the scour depth estimated for the existing climatic condition for the flood of different return interval for the bridge the US 59 over San Jacinto River in Houston, Texas. The sour depth for the 100-year flood is 21.96 ft., where as the allowable scour depth of this bridge is 16 ft. Thus, this bridge is a scour critical bridge. **Figure *5-4*** illustrates the resulting scour depths for different floods. As per as the illustration the bridge will reach the threshold value, or allowable scour depth (16') only for a 55-year flood flow.

Table 5-1 Scour Depths for Different Flood Events, US59 Bridge, Houston, Texas

Return Period	Scour Depth (ft.)
2	3.47
5	4.59
10	6.6
25	9.89
50	15.09
100	21.96
200	15.59
250	15.63
500	14.34

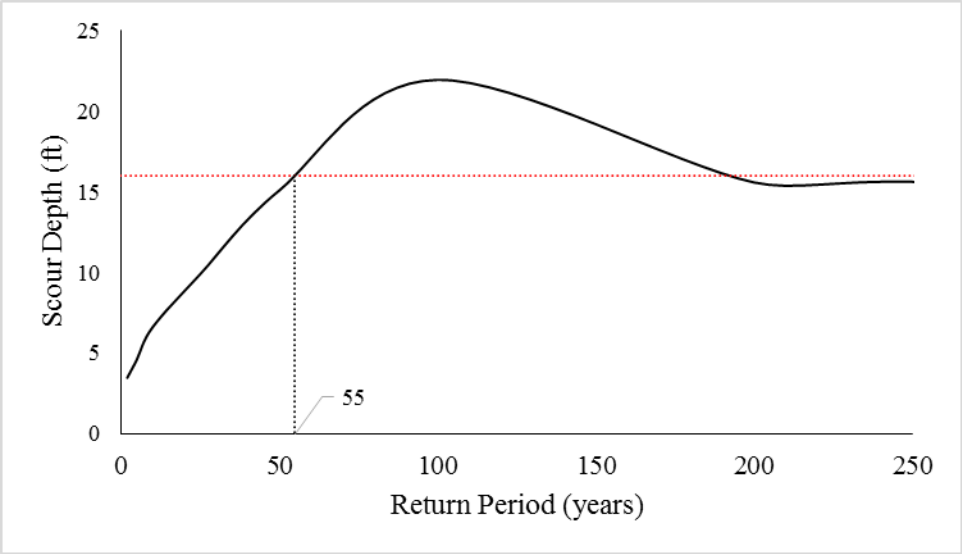

Figure 5-4 Scour Depth for Different Return Periods under Existing Climatic Condition, US59 Bridge, Houston, Texas

Figure *5-5* illustrates the scour depth resulted for different future climate models. The MM5I-HADCM3 model predicts the bridge will reach to the allowable scour depth for a 43-year flood event. Although, the highest scour depth (which is 27.33 feet) results from the flow predicted by a MM5i-CCSM climate model. So, MM5I-HADCM3 shows the scour depth will exceed the allowable scour depth earliest, but MM5I-CCSM predicts the highest amount of scour depth (for 250-year Flood), which is 6 feet higher than the highest scour depth predicted for existing climatic condition.

Similarly, bridge SH 36 is also assessed for scouring, and results are presented in **Figure *5-6***. According to NBI (National Bridge Inventory) record, this bridge is stable for the scour. The results for future climate models also suggest that this bridge will be stable for future flows.

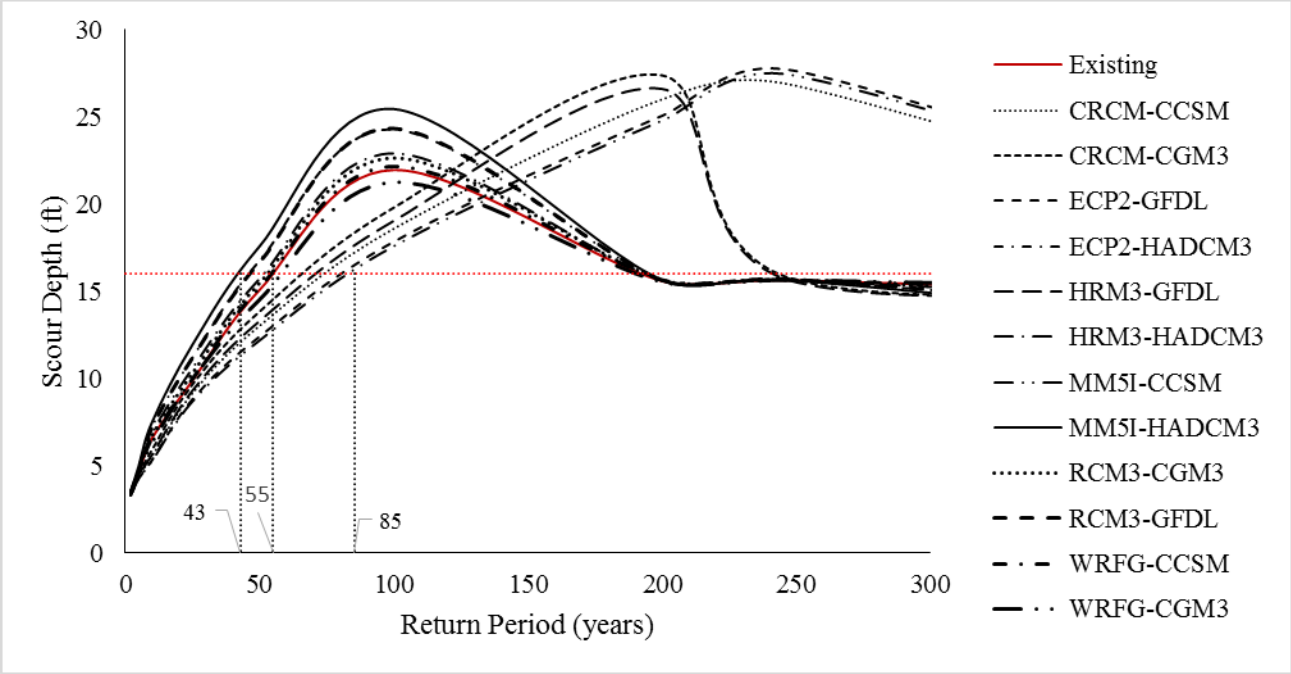

Figure 5-5 Scour Depth for Future Climate Predictions, US59 Bridge, Houston, Texas

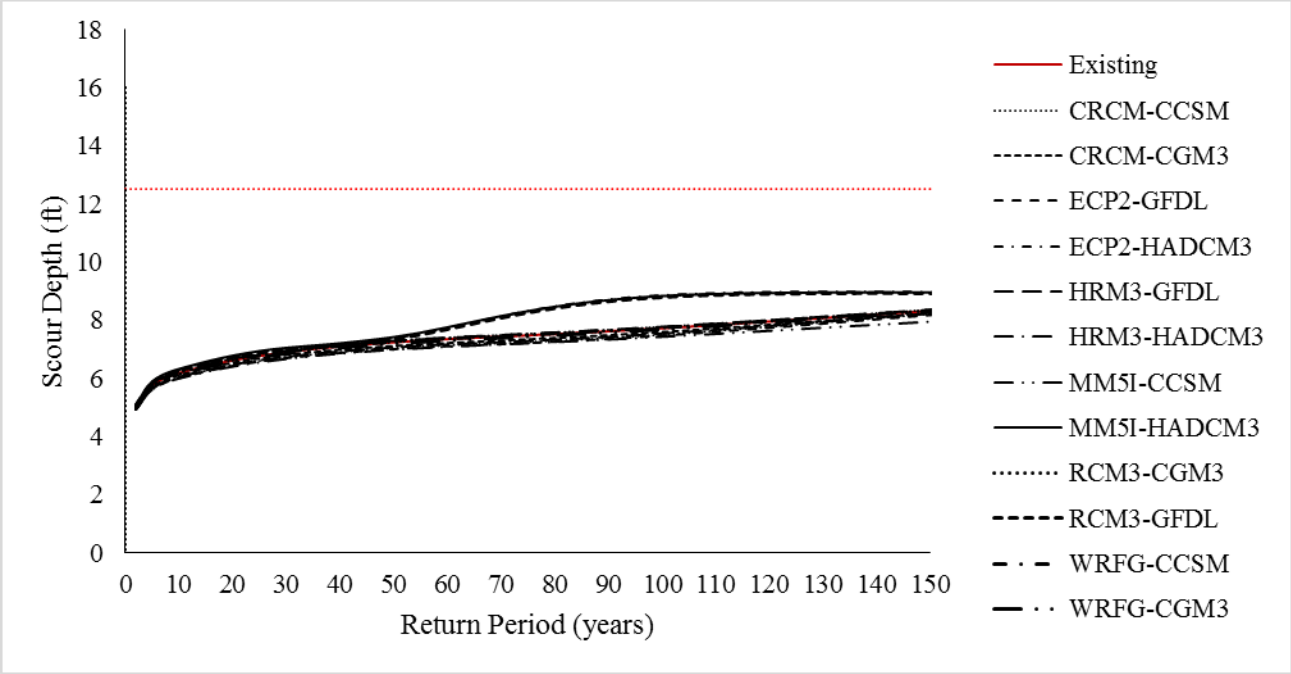

Figure 5-6 Scour Depth for Future Climate Predictions, SH36, Houston, Texas

5.2 RISK ANALYSIS

Risk can be defined as the probability that a particular climate change event occurs during a stated period causing damage to assets, including injury, and loss of life. In this study to perform risk analysis for bridges, 'HYRISK' a tool developed for FHWA was used. The tool performs a risk analysis of the bridge based on the 'probability of failure,' which accounts for the overtopping frequency and scour criticality of the bridge. HYRISK uses the NBI database and evaluates the risk of failure with the expected annual loss. According to researchers (Stein and Sedmera, 2006, Khelifa et al., 2013, Pearson et al., 2000), HYRISK is the most comprehensive method available to perform bridge risk analysis

The HYRISK model is a combination of Response model, Damage model, and Loss model (Khelifa et al., 2013). Response model estimates the probability of overtopping based on the bridge's functional class and water adequacy. Damage models estimate the probability of damage based on substructure condition, channel protection, overtopping probability, and age of the bridge. Based on the damage, the loss model estimates the total economic costs.

The economic Loss model is presented below:

$$\text{Cost} = \underbrace{(C_0 + C_1)eWL}_{\text{Rebuilding cost}} + \underbrace{[C_2\,(1\text{-}T/100) + C_3\,T/100]Dad}_{\text{Vehicle running cost}}$$

$$\underbrace{+\,[C_4O\,(1\text{-}T/100) + C_5\,T/100]Dad/S}_{\text{Time loss cost}} + \underbrace{C_6X}_{\text{Cost of life}}$$

Where, Cost = total cost of bridge failure ($), C1 = unit rebuilding cost ($/ft2), e = cost multiplier for early replacement based on average daily traffic ,W = bridge width, L = bridge length, C2 = cost of running automobile (i.e. $0.45/mi), C3 = cost of running truck ($1.30 /mi), D = detour length, A = average daily traffic (ADT), d = duration of detour, C4 = value of time per adult in passenger car ($/hr), O = average occupancy rate(typically 1.63 adults), T = average daily truck traffic (ADTT) form NBI item 109 (% of ADT), C5 = value of time for truck ($22.01/hr), S = average detour speed (typically 40 mph), C6 = cost for each life lost (typically $500,000), and X = number of deaths resulting from failure.

In the end, the final model calculates the annual risk based on the results of all these models.

$$\text{Expected annual loss} = \text{KP x Cost}$$

Where,

K = Risk adjustment factor

P = Probability of bridge failure

Data required from the NBI database to calculate the risk has been presented in **Table *5-2***. This data is for bridge US59 crossing West Fork San Jacinto River.

Table 5-2 NBI Data for Risk Analysis (FHWA, 2016)

Bridge Data		
Bridge Length	501.4	km
Bridge Width	25.2	m
Year built	1961	
Construction Type	Steel Construction	
Detour Length	2	km
Service under bridge	Waterway	
Substructure	Satisfactory Condition	
Waterway Adequacy	Bridge deck and approaches above flood elevations; remote chance of overtopping	
Scour Criticality	The bridge is scoured critically; bridge foundations determined to be unstable for calculated scour	
Average Daily Traffic	43220	
Truck Traffic (%of ADT)	10	
Route Functional Class	Urban freeway	

The cost analysis for the bridge is done using the costs embedded in the software. The basic assumptions of the calculation of the cost and the risk are listed in **Table *5-3***.

Table 5-3 Basic Assumptions for Risk Analysis

Detour speed (km/h)	64
Occupancy rate	1.57
Person Time Cost ($/h)	8
Vehicle Running Cost ($/km)	0.25
Truck Time Cost ($/h)	30
Rebuild Cost ($/m^2)	645.83

For the existing condition, the model shows the annual failure probability of the bridge is 0.03959, which results in the expected annual loss of $631600.92. The summarized results are shown in **Table *5-4***.

Table 5-4 Annual Loss for Existing Climate Condition, Bridge US59, Houston, Texas

Annual Fail Probability	0.03959
Rebuilding Cost ($)	$16,320,485.76
Running Cost ($)	$3,954,630.00
Time Cost ($)	$3,535,439.22
Total Cost ($)	$23,810,554.98
Risk ($/yr)	$631,600.92

After considering the climate prediction by the climate models, which implied a 10% increase in the annual average precipitation, the annual failure probability is also increased. To account for this increased precipitation scenario, the annual failure probability of the bridge has been calculated based on the following equation (Khelifa et al., 2013).

$$P_v^a = min\{P_v x C_a\} \quad (5\text{-}1)$$

Where, C_a is the percent increase in precipitation and P_v is the probability of bridge failure for an existing condition.

Using this method, the estimated risk becomes $694740.00, listed in **Table *5-5***, which means the annual loss increased by $63,139 for the future increased precipitation.

Table 5-5 Annual Loss for Future Predicted Climate Condition, Bridge US59, Houston, Texas

Annual Fail Probability	0.043549
Rebuilding Cost ($)	$16,320,485.76
Running Cost ($)	$3,954,630.00
Time Cost ($)	$3,535,439.22
Total Cost ($)	$23,810,554.98
Risk ($/yr)	$694,740.00

5.3 POSSIBLE ADAPTATION TO VULNERABILITY

Assessment of bridges for risk and vulnerability should follow with evaluation of possible adaptation and protection measures to counteract the problems. Agencies (State DOTs, FHWA, etc.) have guidelines for possible mitigation and protection measures to vulnerabilities. AASHTO LRFD bridge design specification guide (2005) has suggested specific sets of bridge modification that has been adopted and practiced by several agencies like the Oklahoma DOT. The modifications suggested by AAHTO LRFD bridge design specifications (2005) are as follows:

- Relocation or redesign of piers or abutments to avoid areas of deep scour or overtopping scour holes from adjacent foundation elements
- Addition of guide banks, dikes or other river training works to provide for smoother flow transitions or to control lateral movement of the channel
- Enlargement of the passing water area
- Relocation of the crossing to avoid an undesirable location

5.3.1 RAISING THE GRADE OF THE BRIDGE

One possible solution to overtopping is raising the grade of the bridges to create more waterways to pass the excess stream flow that may occur due to the future predicted climate extremes. Then the bridges can accommodate larger flood events (**Figure *5-7*** and **Figure *5-8***). These graphs show, a mere increase of one-foot height, can allow the bridges to survive for a greater flood flow. US 59, which have overtopping potential of 90-years (under MM5I-HADCM3 model), can survive 100-year flood flow after raising it by one-foot.

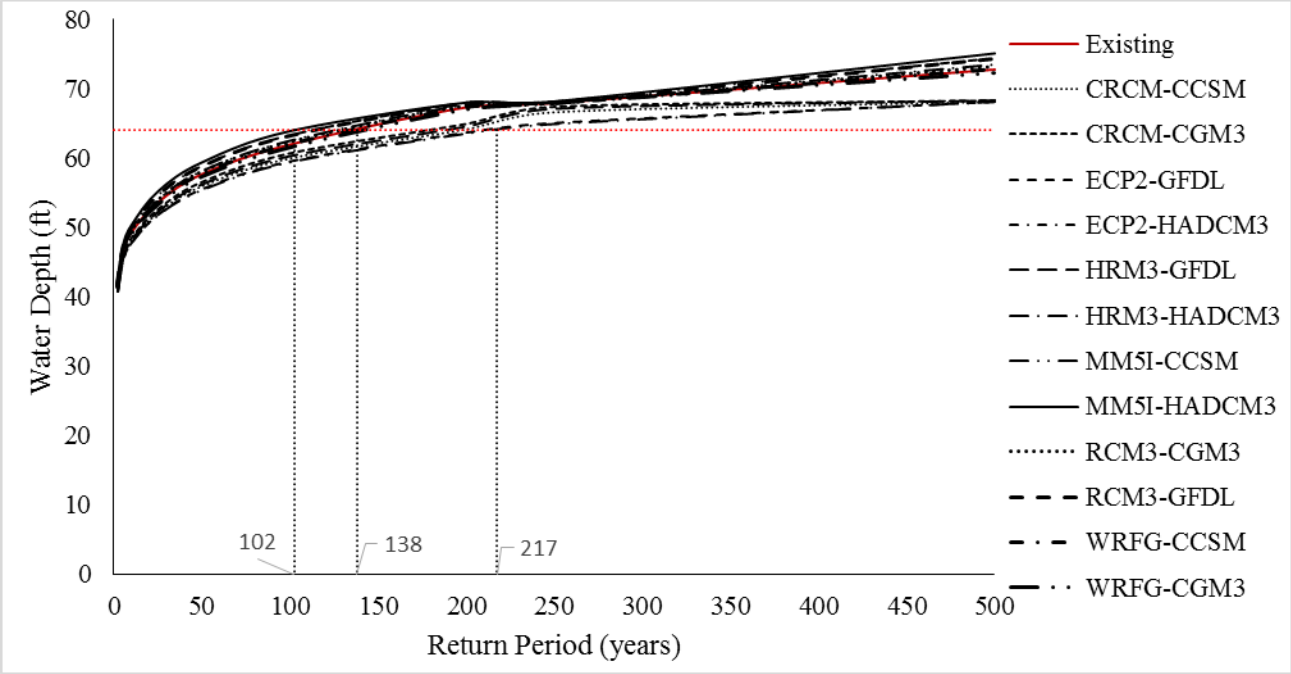

Figure 5-7 Grade Increase of the Bridge US59, Houston, Texas

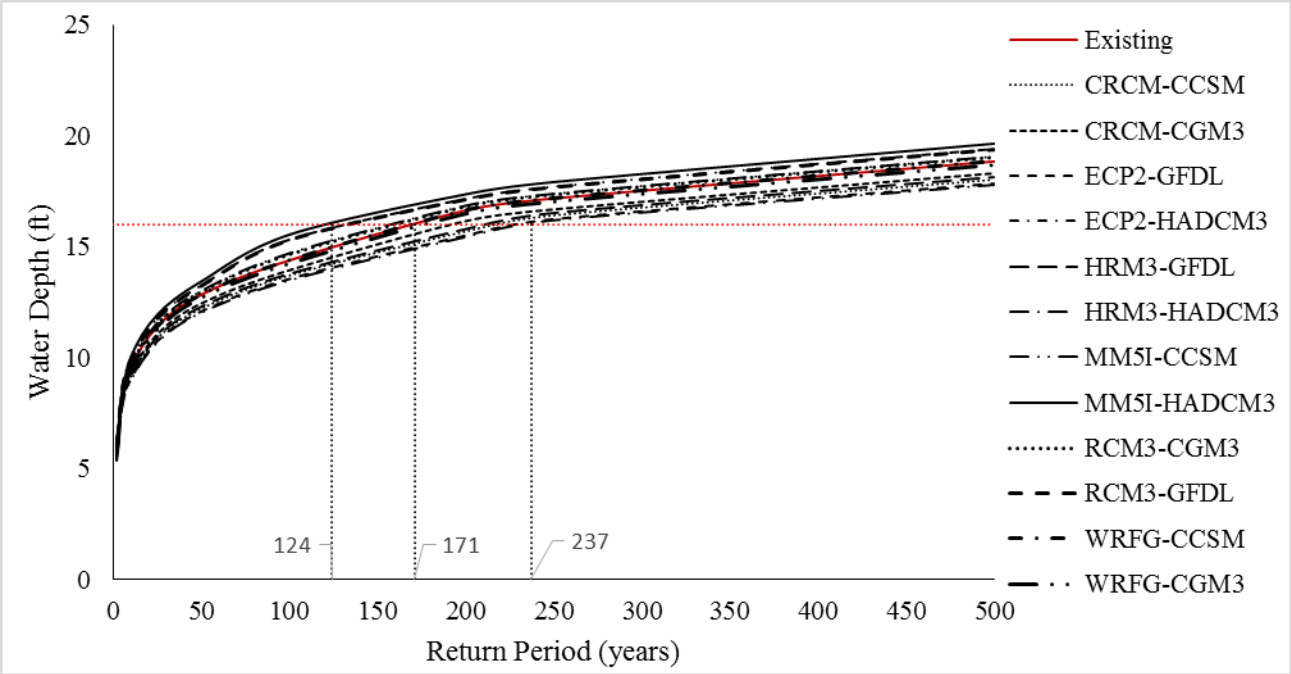

Figure 5-8 Grade Increase of the Bridge SH36, Houston, Texas

Besides, colossal cost implication, the raising of the grade may make the bridge more vulnerable to scouring as more water will pass through the bridge opening with higher pressure. Thus, the elevation increase should be associated with proper countermeasures for scouring.

5.3.2 SCOUR COUNTERMEASURES

Scour countermeasures protect the bridge foundation, pier or abutment against scouring by providing a physical barrier, such as riprap, gabions, blocks, which increases the resistance of the bed materials (Wang, Yu, and Liang, 2017). While there are several options are available for countermeasures, selection of an appropriate one depends on the following factors (Lagasse et al., 2009):

- Scour Mechanism
- Stream Characteristics
- Construction or Maintenance Requirements
- Potential for Vandalism
- Costs

To keep up with the objective of the study to be qualitative, meaning no site visit, a qualitative approach to find a select appropriate countermeasure for affected pier has been discussed below:

Lagasse et al. (2007) have provided a selection methodology of appropriate countermeasure for the protection of piers, based on establishing a Selection Index (SI). In this study, the following techniques have been analyzed:

- Standard (loose) riprap
- Partially grouted riprap
- Articulating concrete blocks
- Gabion mattresses
- Grout-filled mattresses
- Grout-filled bags

The selection index (SI) consists of five factors to consider and the technique with the highest SI value is selected as an appropriate solution for the bridge. SI is calculated as follows:

SI = (S1 x S2 x S3 x S4)/LCC

Where,

S1: Bed Materials size and transport

S2: Severity of debris or ice loading

S3: Constructability constraints

S4: Inspection and maintenance requirements

LCC: Life-cycle costs

The flow charts illustrating the selection factors are presented in ***Figure 5-9***.

Factor S1: Bed Material

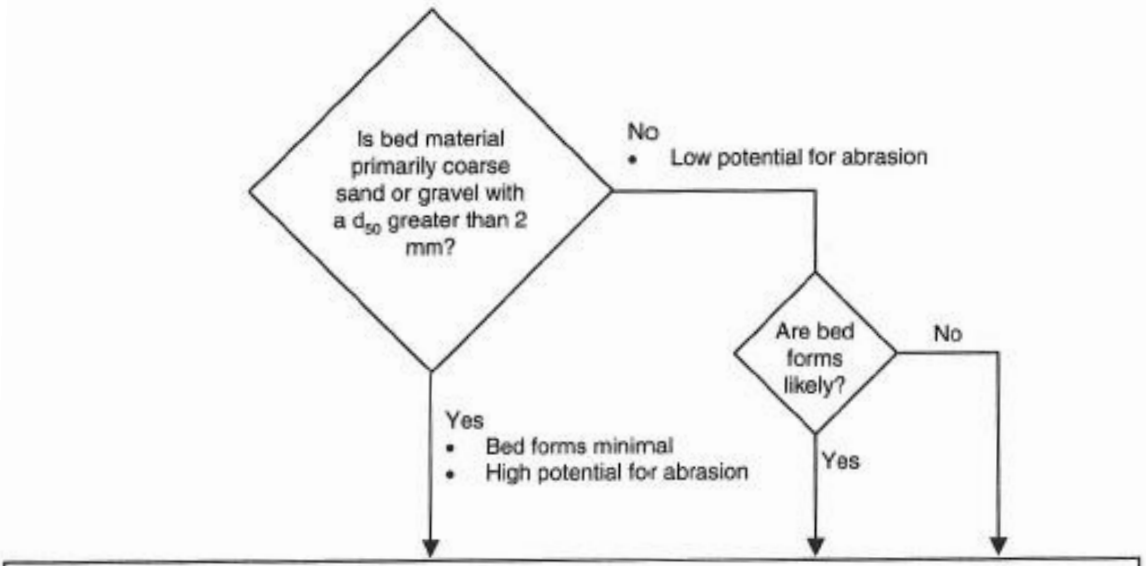

Recommended values for S1			
Riprap	5	5	5
Partially Grouted Riprap	5	4	5
Articulating Concrete Blocks	4	4	5
Grout-Filled Bags	3	3	5
Grout-Filled Mattresses	3	3	5
Gabions, Gabion Mattresses	0	4	5

(a)

Factor S2: Ice/Debris Load

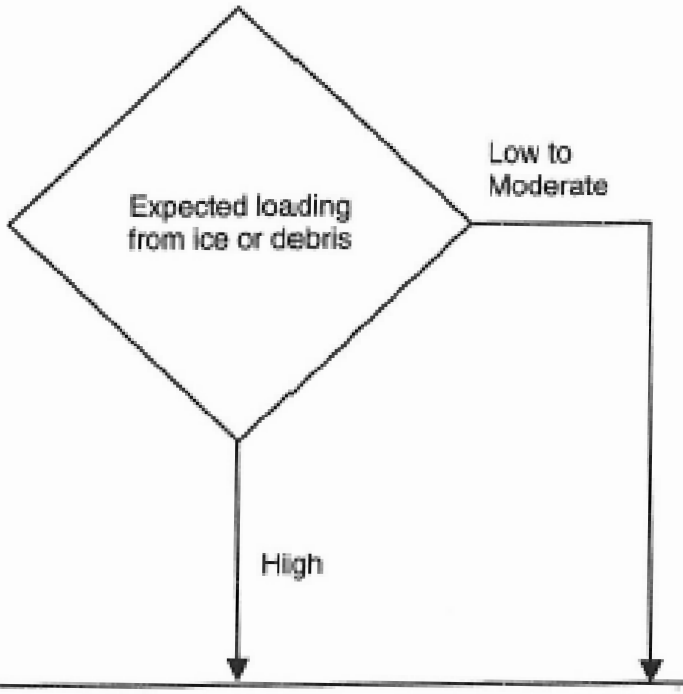

Recommended values for S2		
Riprap	3	5
Partially Grouted Riprap	4	5
Articulating Concrete Blocks	4	5
Grout-Filled Bags	3	5
Grout-Filled Mattresses	4	5
Gabions, Gabion Mattresses	1	5

(b)

Factor S3: Construction Considerations

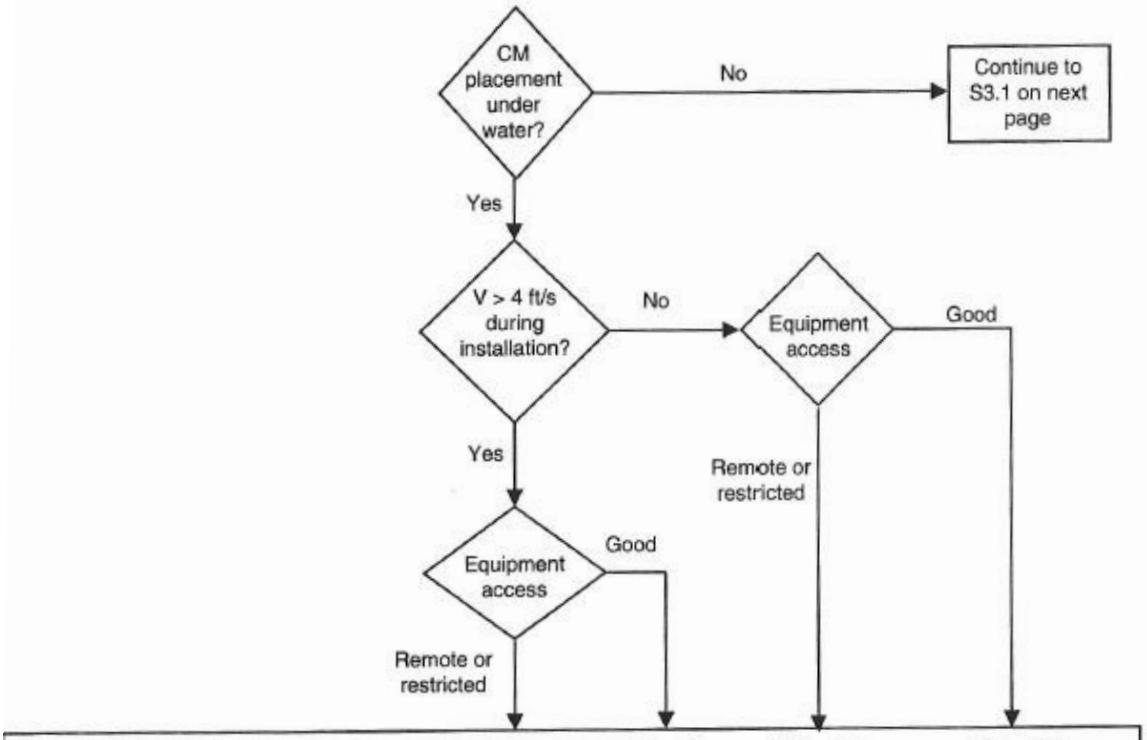

Recommended values for S3	SF*	DF	SF	DF	SF	DF	SF	DF
Riprap	0	2	1	5	1	3	2	5
Partially Grouted Riprap	0	0	0	0	2	4	0	5
Articulating Concrete Blocks	0	0	1	1	2	2	0	4
Grout-Filled Bags	0	1	1	2	1	3	1	5
Grout-Filled Mattresses	0	0	0	0	3	3	0	4
Gabions, Gabion Mattresses	0	0	0	1	1	1	0	3

*Note: Armoring countermeasures not recommended for these conditions.

SF = Shallow Pier, e.g. Spread Footing DF = Deep Footing

(c)

Factor S3.1: Construction Considerations

No Underwater Placement

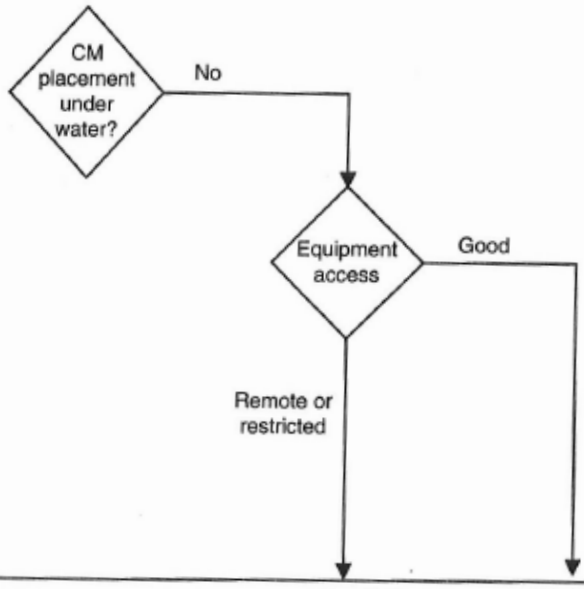

Recommended values for S3	SF	DF	SF	DF
Riprap	1	3	1	5
Partially Grouted Riprap	2	4	2	5
Articulating Concrete Blocks	2	3	5	5
Grout-Filled Bags	1	4	1	5
Grout-Filled Mattresses	3	4	5	5
Gabions, Gabion Mattresses	1	3	2	5

SF= Shallow Pier, e.g. Spread Footing DF= Deep Footing

(d)

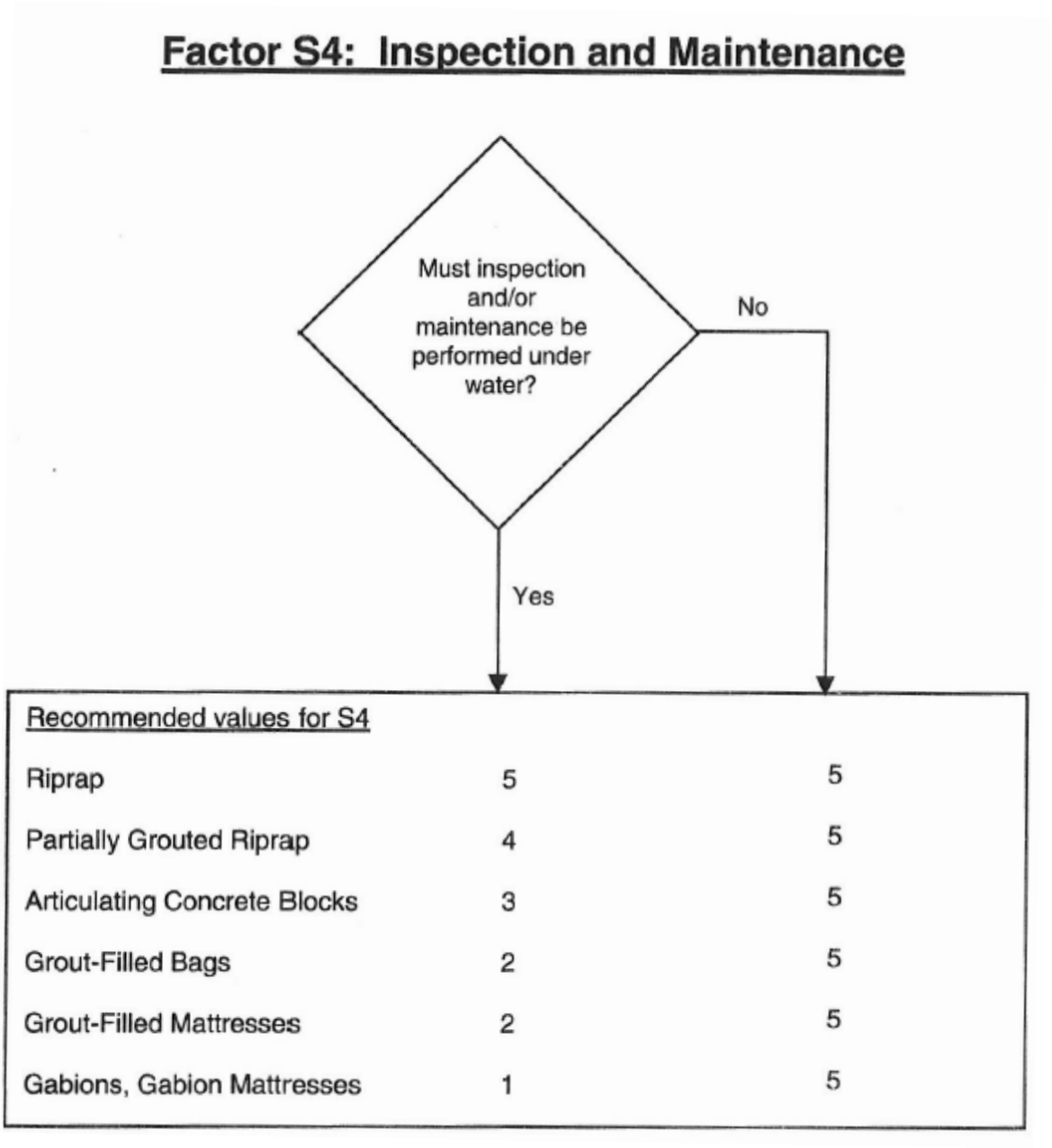

(e)

Figure 5-9 Flow Charts Illustrating Selection Factors for Scour Countermeasures (a)Based on Bed Material Characteristics (b) Based on Impact of Ice or Debris Load (c)and (d)Based on Construction Requirements and (e) Based on Inspection and Maintenance [Reprinted from Lagasse et al., (2007)

Selection of countermeasure for Bridge US 59:

Bridge: US59 crossing West Fork San Jacinto River

Size of Bed Material = 0.03 mm (No Bed Formation)

Ice/debris Loading = Low to moderate

Velocity of the river reach = 3ft/sec to 20 ft/sec

Foundation type = Deep footing

Assumptions:

- Underwater placement of the instruments
- Equipment access is good
- Inspection and maintenance operation has to be performed underwater
- Same Life-cycle costs for all techniques

Considering all the factors mentioned in the matrix, the value of SI for different techniques are as follows in ***Table 5-6***.

Table 5-6 Selection Index for bridge US59, Houston, Texas

Countermeasure	**S1**	**S2**	**S3**	**S4**	**SI**
Riprap	5	5	5	4	19
Partially Grouted Riprap	5	5	0	4	14
Articulating Concrete Blocks	5	5	1	3	14
Grout-filled Bags	5	5	2	2	14
Grout-filled Mattresses	5	5	0	2	12
Gabions, Gabion Mattresses	5	5	1	1	12

So, based on SI value, for bridge US59, Riprap is the preferable countermeasure technique. The example of riprap placing has been captured in **Figure *5-10***, which shows three placement conditions of riprap, (a) on the surface, (b) placement on excavated or scoured surface and in (c) riprap has been placed in depth in the bed.

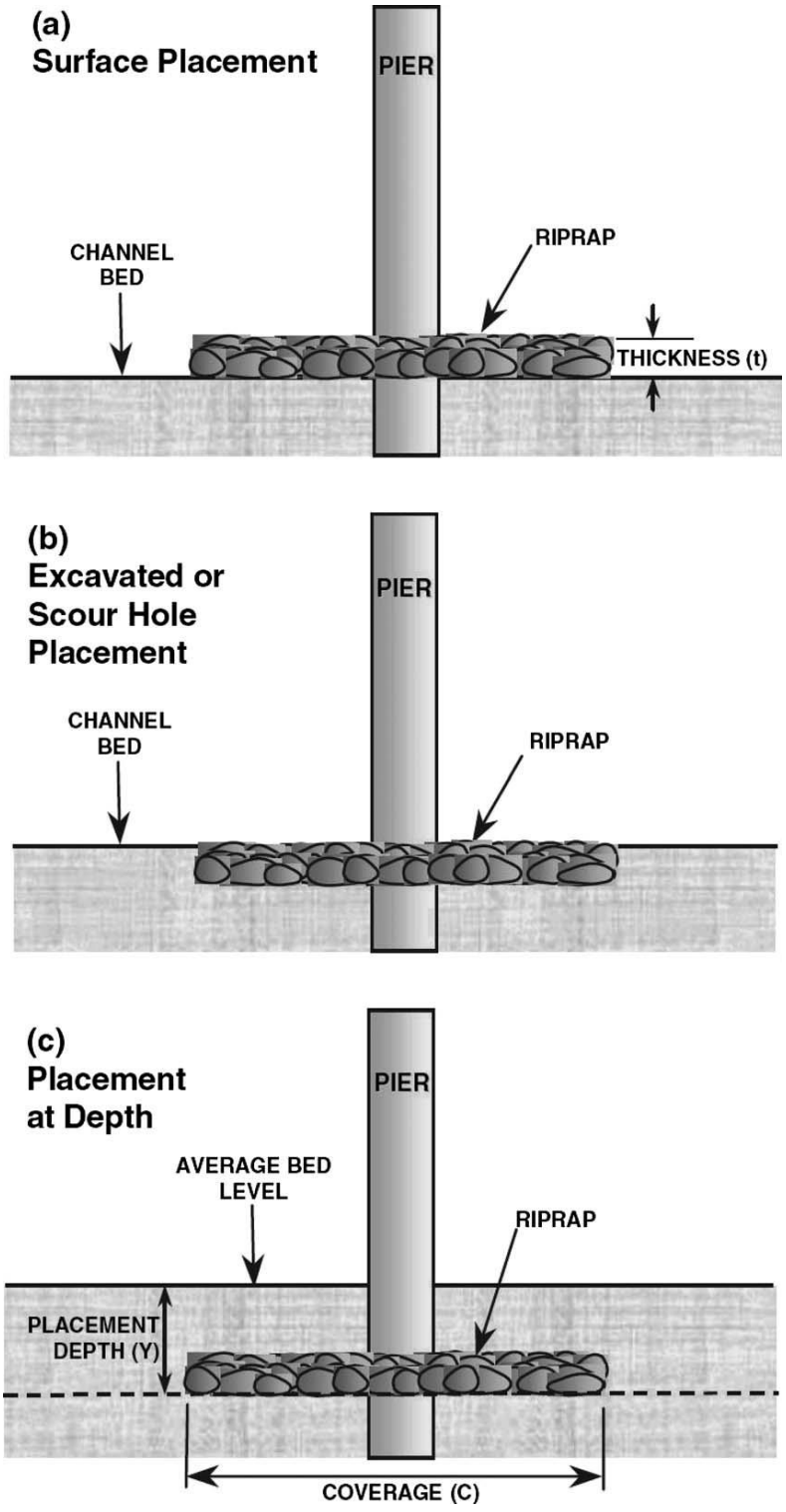

Figure 5-10 Pier Protection against Scouring Using Riprap [Reprinted from Lagasse et al., (2007)]

6. FLOOD DEPTH PREDICTION FRAMEWORK USING MACHINE LEARNING

6.1 INTRODUCTION

Machine learning is a discipline of data science that aims to train a machine to predict or anticipate the outcomes of a prescribed input. The presence of complex relationship/pattern between inputs and outputs requires the use of machine learning. Although machine learning has been used already in Civil Engineering, its application has been limited. In this study, a framework is proposed and benefits derived are demonstrated through a flood mapping example.

6.2 BACKGROUND

Machine learning is used to predict or anticipate the outcomes or pattern that traditional analytical method cannot asses. Artificial neural network is a discipline of machine learning that attempts to imitate learning similar to that of brain's neurons. Artificial neural networks use learning algorithms that require training. The training dataset consists of inputs and associated output. Machine learning can be seen as a black box model (***Figure 6-1***) where the input is a stimulus that a neuron captures, and then it passes down the information to other neurons, the final layer of neurons then provides the output. The physical relationship between input and output is not necessarily known. Random Forest algorithm is utilized as a classification/regression tool for prediction. Random forest algorithm works like a combination of decision trees that come up with rules to make a prediction based on the training dataset. Random Forest algorithm is utilized as a classification/regression tool for prediction. Random forest algorithm works like a combination of decision trees that come up with rules to make a prediction based on the training dataset.

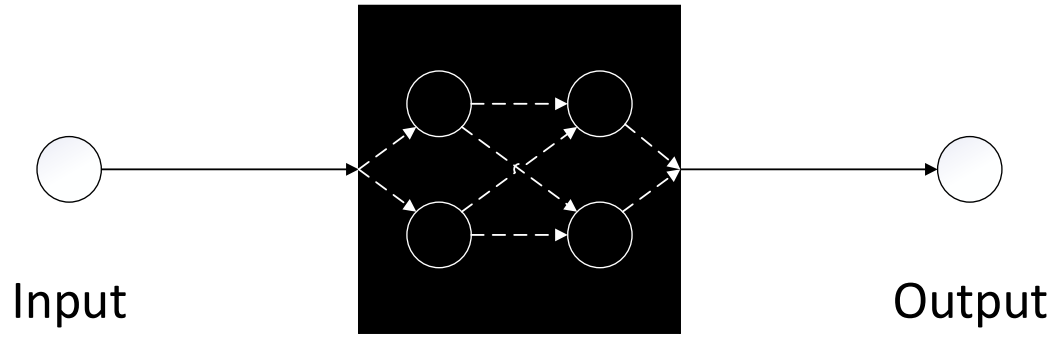

Figure 6-1 Black Box Model Diagram

6.3 METHODOLOGY

A framework for machine learning utilization in civil engineering is required to achieve optimal results. The framework can be comprised of four steps: formulating and investigating a specific problem, collect data, integrate problem, data and machine learning algorithms, and optimize machine learning usage.

Flooding in urban development is caused either due to ineffectiveness or design capacity of the drainage network. Typically, FEMA develops flood maps by utilizing hydrologic and hydraulic modeling of an area. Typical data used for hydrologic/hydraulic data are elevation, slope, flow accumulation, land use, and rainfall intensity. Traditionally, rainfall intensity has been utilized either in rainfall-runoff models (rational method) or in the stochastic processes (hydrograph analysis) to generate runoff that is later utilized in hydraulic modeling along with channel/street elevation, slope, and land use.

Flood maps can be developed by using 1D, 2D or 1D/2D hydraulic models, however, each one of them has their limitations. The 1D models do not account for water movement in any other dimensions. However, the 2D model requires more computational time. Regardless of the method used, a relationship between input and output values for prediction is needed. However, machine learning algorithms such as artificial neural networks (ANN) does not require to have a relationship between inputs and output values. ANN models use a training set containing input and output values to develop a regression or correlation that can later be utilized to predict outputs of a new set of inputs. The framework requires integration of the civil engineering problem and machine learning algorithm.

In the case of flood maps, the trend is captured using geo-locations (such as latitude and longitude) and combining them with input hydrologic and hydraulic data requirements, and flood elevations. Machine learning optimization can be achieved by changing the number of training points required for training, randomizing training point selection, and by sorting the training dataset. Although machine learning algorithms function similar to a black box model, a strategy is needed to develop procedures for optimal usage.

FEMA's geoportal allows for acquiring flood maps to use in GIS software. The layer "Base Flood Elevation" is used to determine the flood elevation at a point in a region. FEMA's flood maps use grids that are approximately 480 square miles. Once selected a region, it is required to use geoprocessing tools that allow extracting hydrologic and hydraulic information, along with geospatial descriptors.

Scikit-learn is an open-source library in python that is used to develop regression-based machine learning algorithms. The algorithm requires to have normalized inputs (latitude, longitude, elevation, slope, flow accumulation, land use) for both training and testing. The training dataset contains inputs and the associated outputs, while the testing only has the inputs. The testing dataset is used to verify the predictability of the learning algorithm. The input and output variables require to be normalized by the minimum (as in the case of longitude that has only negative values) or the maximum value. The algorithm also returns the mean squared error of the prediction and the real value.

6.4 Analysis and Results

The machine learning algorithm was utilized by analyzing the flood maps in Houston, Texas. According to USGS's flood-depth-duration maps, Houston's 100-year rainfall storm results in a precipitation of 11.5 inches. ArcMap was utilized to perform geoprocessing tools once flood maps of Houston were obtained. The inputs utilized for machine learning algorithm were latitude and longitude (in decimal degrees), elevation (in VNAD86 Datum), slope, flow accumulation, land use, precipitation, and base flood elevation. Slope and flow accumulation was calculated using ArcMap's tools Slope and Flow Accumulation.

The random forest (Scikit-learn library tool) machine learning algorithm was used to predict the flood depth in the Houston region. The algorithm was run by varying percentage of data points.

The variation of the mean squared error versus the percent of training points is shown in Figure 2 which suggests the need for only 60% training points.

The geospatial variation was assessed by comparing the flood depth variation with space of both the original and predicted points. A raster was used for this. A raster shows a georeferenced image where the pixel has a valued. In this case, the pixels represent the flood depth of the region. Figure 3 and 4 show the flood depth variation with space for both the original and predicted points, respectively.

Even though ***Figure 6-2*** shows that the mean squared error converges rapidly after using 60 % of the training points, ***Figure 6-3*** and ***Figure 6-4*** show that 80 percent of the training points are required to achieve better spatial accuracy in comparison with the original dataset.

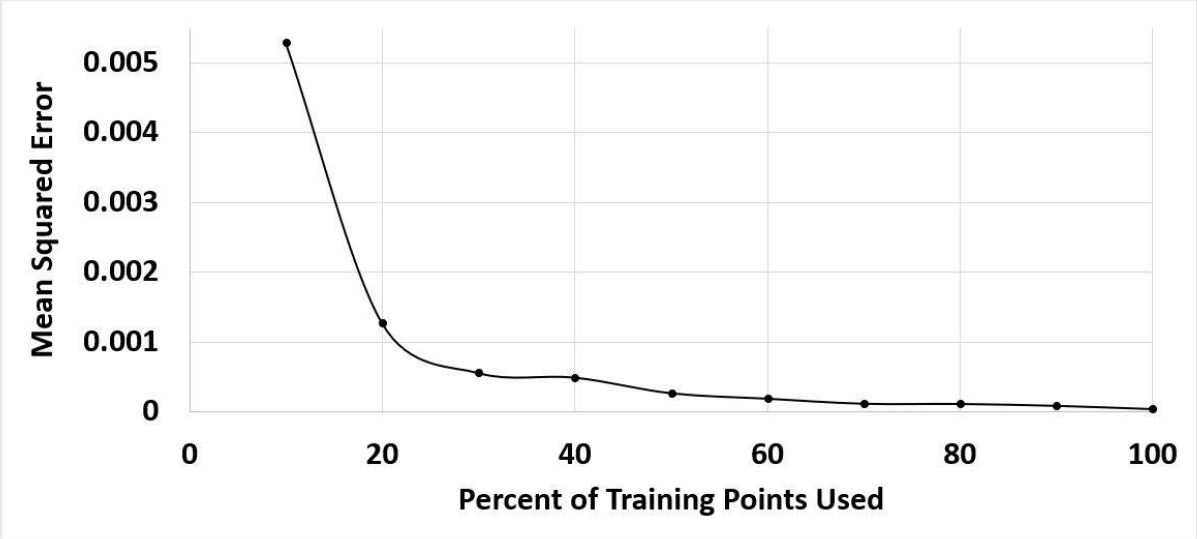

Figure 6-2 Mean Squared Error vs. Percent of Training Points

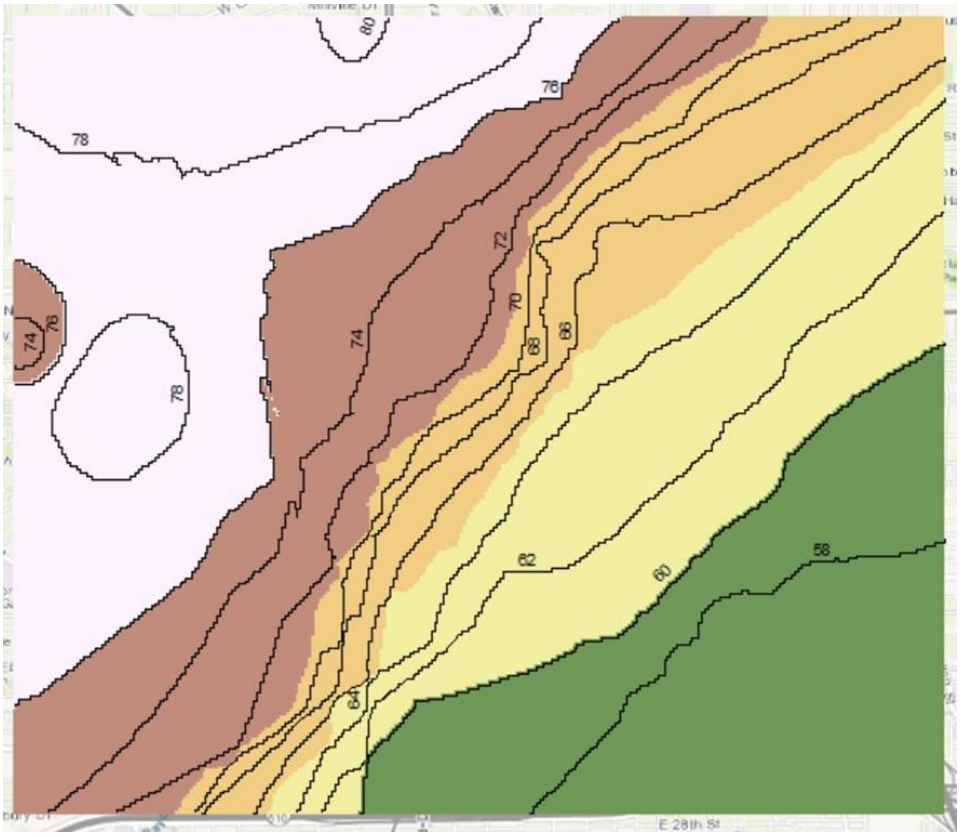

Figure 6-3 original Flood Depth Raster and Contours

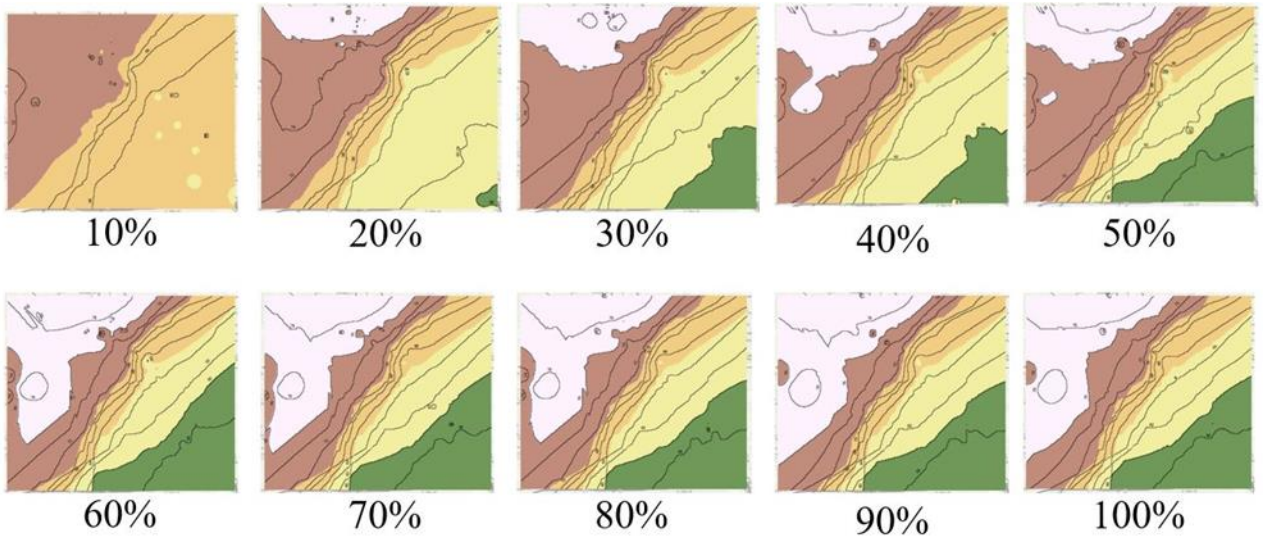

Figure 6-4 Predicted Raster and Contours

6.5 CONCLUSION

Machine learning algorithms are powerful tools that can be used when a complicated pattern or relationship defines a problem. Even though hydrologic/hydraulic modeling exists for flood map, the machine learning algorithm proves to be useful in determining the flood depth with 80 % of known points. The algorithm, in this case, does not provide for randomization and does not take into account if there is any bias regarding minimum or maximum values. Further studies should be conducted to assess the reliability of machine learning algorithms by selecting random training points based on statistical patterns.

7. CLOSURE

7.1 SUMMARY

Global climates are significantly changing over the years and are causing an increased number of extreme weather events. These changes of climate have a significant effect on the highway infrastructures, such as bridges. Hydraulic design of bridges is primarily focused on the flood frequency for plausible vulnerability such as overtopping and scouring. Climate change causes the change in the frequency of these flood events. This study was done to find out the future climate change predicted from climate models extracted from NARCCAP database and using them to quantify the vulnerability of bridges in the Houston-Galveston area of Texas. For this, a hydraulic model has been developed using HEC-RAS. This study also evaluates the annual economic loss for bridge failure and suggests possible adaptation measures.

7.2 CONCLUSIONS

The findings from this study are as follows:

- Most of the climate models predict increased precipitation in future for cities of Texas and New Mexico. But not significant changes are predicted for cities of Louisiana, Arkansas, and Oklahoma.
- Climate prediction by the climate models varies with location. For instance, in Texas MM5I-HADCM3 predicts more precipitation than the existing one, but in Oklahoma, the same model predicts less than the existing precipitation.
- For Houston (Texas), climate models predict the highest increase of precipitation of 10.2%, which results in 11% more streamflow in West Fork San Jacinto River.
- The increased amount of flow in future will increase overtopping potential for bridges. Bridges will be overtopped for earlier flood events. For example, US59 Bridge will be overtopped for 90-years flood event instead of 119-years flood event and SH36 Bridge will be overtopped at 87-year flood event instead of a 127-year flood event.
- Scour condition will also worsen under the increased precipitation scenario. Bridge US 59 is a scour critical bridge as per as the NBI record and the allowable scour depth for

this bridge will reach for 55-year flood events under existing climatic condition. However, for future climate data, the bridge will undergo the exceeding of allowable scour depth for 43-year flood events, which is 12-years earlier than the existing climatic condition.

- The model predicted increased precipitation poses a risk of $63,139 more annual loss for the bridge US59.
- Raising the grade of the bridge can solve the overtopping problem. Increasing the grade of the bridge by only one-foot for bridge US59 will allow 12-years more intense flood events through the bridge without overtopping.
- Proper choice of scour countermeasures can be made by a site visit and clear understanding of the field condition of the bridge and the channel.

7.3 LIMITATIONS AND FUTURE WORK

This study has been performed using different models, such as climate models, hydrologic models, hydraulic model, scour model, etc. All of these models have some limitations due to inherent uncertainties. The uncertainties associated with the models have been stated below:

- The uncertainties in climate models primarily come from three main sources, such as the unpredicted nature of the climatic systems (natural variability), the inability to model the earth's many complex processes (model uncertainty) and the inability to project future societal choices such as energy use (scenario uncertainty). Proper bias correction or ensembles can reduce the amount of uncertainty in climate prediction (Dikanski et al., 2018). Although climate uncertainty cannot be eliminated completely, and it remains as a barrier to effective adaptation (Green et al., 2014 and Reeder et al. 2011).
- Estimation of flood frequency using hydrologic models such as regional regression models possesses their source of uncertainty. Like in this study, USGS regional regression equations have been used, which have been generated based on 683-gauge station data and the characteristic of the catchment area has been defined with a single parameter 'omega.'
- In bridge scour assessment most, common practice is using the empirical models. 22 empirical models have been found for scouring estimation by Sheppard et al. (2014).

Uncertainty arises using these models, as scour depends on the non-linear interaction between water flow and sediment transport, which can be evaluated with high-resolution geomorphological simulation models (Dikanski et al.,2018). Lagasee et al. (2013), has evaluated HEC-18 models' uncertainty by comparing model simulated results to observational field data. Results show that uncertainties of models may vary based on the flow conditions. The study also found that local scour is less sensitive to the flow conditions than the contraction scour, which lead to the conclusion by Dikanski et al. (2018), contraction scour is more sensitive to climate change compared to local scour.

Recommendations for future research are stated below:

- Comparative analysis between climate prediction data sources, e.g., CMIP3, CMIP5, etc. should be performed to identify most suitable climate prediction models to be incorporated in bridge hydraulics study.
- For installation or adaptation of countermeasures for scour, a detailed field survey should be performed for analyzing the suitability of the technique.

8. REFERENCES

Almodovar-Rosario, Natalia, Chris Dorney, Mike Flood, Justin Lennon, and J. T. Lockman. "MnDOT Flash Flood Vulnerability and Adaptation Assessment Pilot Project." (2014).

American Association of State Highway and Transportation Officials (AASHTO). AASHTO LRFD Bridge Design Specifications. 4th Ed., AASHTO, Washington, DC. 2007.Anderson, C.J., Claman, D., and Mantilla, R. *Iowa's Bridge and Highway Climate Change and Extreme Weather Vulnerability Assessment Pilot*, Institute for Transportation Iowa State University, 2015.

Arneson, L. A., L. W. Zevenbergen, P. F. Lagasse, and P. E. Clopper. "Evaluating Scour at Bridges, Hydraulic Engineering Circular No. 18 (HEC-18)." *Publication No. FHWA-HIF-12-003*(2012).

Arkansas State Highway and Transportation Department (ASHTD). Drainage manual, Hydraulics Section, ASHTD, Arkansas.1982.

Asquith, William H., and Meghan C. Roussel. *Regression equations for estimation of annual peak-streamflow frequency for undeveloped watersheds in Texas using an L-moment-based, PRESS-Minimized, residual-adjusted approach*. No. FHWA/TX-09/0-5521-1. US Geological Survey, 2009.

Asquith, W. H., & Roussel, M. C. Atlas of Depth-Duration Frequency of Precipitation Annual Maxima for Texas. Austin, Texas, United States of America.2004.

Bala, Sujit Kumar, M. Mozammel Hoque, and S. M. U. Ahmed. "Failure of a Bridge Due to Flood in Bangladesh-A Case Study." *UAP Journal of Civil and Environmental Engineering* 1, no. 1 (2005): 38-44.

Brekke, L., B. L. Thrasher, E. P. Maurer, and T. Pruitt. Downscaled CMIP3 and CMIP5 climate and hydrology projections: Release of downscaled CMIP5 climate projections, comparison with preceding information, and summary of user needs. US Army Corps of Engineers, US Geological Survey, 2013.

Briaud, Jean-Louis, Anand V. Govindasamy, Dongkyun Kim, Paolo Gardoni, Francisco Olivera, Hamn-Ching Chen, Christopher Mathewson, and Kenneth Elsbury. *Simplified method for estimating scour at bridges*. No. FHWA/TX-09/0-5505-1. 2009.

Brunner, G.W., *HEC-RAS River Analysis System User's Manual Version 4.0*. Report CPD-68 (Davis, CA: US Army Corps of Engineers, Hydrologic Engineering Center), 2008.

Carriere, P., Mohaghegh, S., & Gaskari, R. Performance of a Virtual Runoff Hydrograph System. Journal of Water Resources Planning and Management, 421-427.1996.

Chiew, Y.-M., and Lim, S.-Y. "Protection of bridge piers using a sacrificial sill." *Proc. Inst. Civ. Eng.*, Waters. Maritime Energ.,156(1), 53–62.2003.

Cigada, Alfredo, Stefano Malavasi, and M. Vanalil. "Direct force measurements on a submerged bridge model." *WIT Transactions on the Built Environment* 56 (2001).

CMIP5 Coupled Model Intercomparison Project, Program for Climate Model Diagnosis and Intercomparison, World Climate Research Program,

http://cmip-pcmdi.llnl.gov/cmip5/forcing.html

Deng, Lu, and C. S. Cai. "Bridge scour: Prediction, modeling, monitoring, and countermeasures." Practice periodical on structural design and construction 15, no. 2 (2009): 125-134.

Dikanski, Hristo, Boulent Imam, and Alex Hagen-Zanker. "Effects of uncertain asset stock data on the assessment of climate change risks: A case study of bridge scour in the UK." Structural Safety 71 (2018): 1-12.

FHWA "Climate Change and Extreme Weather Vulnerability Assessment Framework,"FHWA-2012:HEP-13-005,
http://www.fhwa.dot.gov/environment/climate_change/adaptation/resources_and_publications/v ulnerability_assessment_framework/index.cfm

Filosa, Gina, and Alexandra Oster. *International practices on climate adaptation in transportation: findings from a virtual review*. No. DOT-VNTSC-FHWA-15-01; FHWA-HEP-15-012. John A. Volpe National Transportation Systems Center (US), 2015.

Gangopadhyay, S., Raj Gautam, T., & Das Gupta, A. Subsurface Characterization Using Artificial Neural Network and GIS. Journal of Computing in Civil Engineering, 153-161.1999.

Green, Michael, and E. K. Weatherhead. "Coping with climate change uncertainty for adaptation planning: An improved criterion for decision making under uncertainty using UKCP09." Climate Risk Management 1 (2014): 63-75.

Gutowski Jr, William J., Raymond W. Arritt, Sho Kawazoe, David M. Flory, Eugene S. Takle, Sébastien Biner, Daniel Caya et al. "Regional extreme monthly precipitation simulated by NARCCAP RCMs." *Journal of Hydrometeorology* 11, no. 6 (2010): 1373-1379.

Guo, J. C. A Semivirtual Watershed Model by Neural Networks. Computer-Aided Civil and Infrastructure Engineering, 106-111.2001.

Hayhoe, K., and A. Stoner. "Gulf Coast Study, Phase 2 Temperature and Precipitation Projections for the Mobile Bay Region." *US DOT Center for Climate Change and Environmental Forecasting Final Rep* (2012).

Hempel, S., K. Frieler, L. Warszawski, J. Schewe, and F. Piontek. A trend-preserving bias correction–the ISI-MIP approach. Earth System Dynamics, 4(2), 219-236, 2013.

Hogan, Michael, David Elder, and Stephanie Molden. "Connecticut Department of Transportation Climate Change and Extreme Weather Vulnerability Pilot Project Final Report." (2014).

IPCC - Intergovernmental Panel on Climate Change,

http://www.ipcc.ch/ . Accessed June 16, 2018.

Intergovernmental Panel on Climate Change. Working Group III. Emissions Scenarios: Summary for Policymakers. A Special Report of IPCC Working Group III. Intergovernmental Panel on Climate Change, 2000.

IPCC (2013). Summary for Policymakers. In: Climate Change 2013: The Physical Science Basis. The contribution of Working Group I to the Fifth Assessment Report of the Intergovernmental Panel on Climate Change [Stocker, T.F., D. Qin, G.-K. Plattner, M.

Tignor, S.K. Allen, J. Boschung, A. Nauels, Y. Xia, V. Bex and P.M. Midgley (eds.)]. Cambridge University Press, Cambridge, United Kingdom and New York, NY, USA.2013,

http://www.climatechange2013.org/images/report/WG1AR5_SPM_FINAL.pdf

Kara, Sibel, Thorsten Stoesser, Terry W. Sturm, and Saad Mulahasan. "Flow dynamics through a submerged bridge opening with overtopping." *Journal of Hydraulic Research* 53, no. 2 (2015): 186-195.

Karl, Thomas R., Gerald A. Meehl, Christopher D. Miller, Susan Joy Hassol, Anne M. Waple, and William L. Murray. Weather and climate extremes in a changing climate. US Climate Change Science Program, 2008.

Khelifa, A., Garrow, L. A., Higgins, M. J., & Meyer, M. D. Impacts of climate change on scour-vulnerable bridges: Assessment based on HYRISK. *Journal of Infrastructure Systems*, (2013):19(2), 138-146.

Kilgore, Roger T., George Rudy Herrmann, Wilbert O. Thomas Jr, and David B. Thompson. *Highways in the river environment—Floodplains, extreme events, risk, and resilience*. No. FHWA-HIF-16-018. 2016.

Kumar, V., Ranga Raju, K. G., and Vittal, N. "Reduction of local scour around bridge piers using slots and collars." *J. Hydraul. Eng.*,125(12), 1302–1305.1999.

Lagasse, Peter Frederick. *Countermeasures to protect bridge piers from scour*. Vol. 593. Transportation Research Board, 2007.

Lagasse, P. F., P. E. Clopper, J. E. Pagán-Ortiz, L. W. Zevenbergen, L. A. Arneson, J. D. Schall, and L. G. Girard. *Bridge scour and stream instability countermeasures: experience, selection, and design guidance: Volume 1*. No. FHWA-NHI-09-111. National Highway Institute (US), 2009.

Lauchlan, C. S., and Melville, B. W. "Riprap protection at bridge piers." J. Hydraul. Eng., 127(5), 412–418.2001.

Laursen, Emmett M. "An analysis of relief bridge scour." *Journal of the Hydraulics Division* 89, no. 3 (1963): 93-118.

Li, H., Barkdoll, B. D., Kuhnle, R., and Alonso, C. "Parallel walls as an abutment scour countermeasure." J. Hydraul. Eng., 132(5), 510–520.2006.

MACA Statistically Downscaled Climate Data from CMIP5, University of Idaho., http://maca.northwestknowledge.net/index.php

Malavasi, Stefano, Monica Riva, Marcello Vanali, and Enrico Larcan. "Hydrodynamic forces on a submerged bridge." *WIT Transactions on The Built Environment* 56 (2001).

Markus, Momcilo, James Angel, Gregory Byard, Sally McConkey, Chen Zhang, Ximing Cai, Michael Notaro, and Moetasim Ashfaq. "Communicating the impacts of projected climate change on heavy rainfall using a weighted ensemble approach." *Journal of Hydrologic Engineering* 23, no. 4 (2018): 04018004.

Mearns, L. O., W. J. Gutowski, R. Jones, L.-Y. Leung, S. McGinnis, A. M. B. Nunes, and Y. Qian. A regional climate change assessment program for North America. EOS, Vol. 90, No. 36, 2009, pp. 311-312.

Mearns, L. O., W. J. Gutowski, R. Jones, L.-Y. Leung, S. McGinnis, A. M. B. Nunes, and Y. Qian. The North American Regional Climate Change Assessment Program dataset. National Center for Atmospheric Research Earth System Grid data portal, Boulder, CO. 2007, updated 2014, Data downloaded 2015-10-23.

Mearns, L. O., W. J. Gutowski, R. Jones, L.-Y. Leung, S. McGinnis, A. M. B. Nunes, and Y. Qian. The North American Regional Climate Change Assessment Program dataset. National Center for Atmospheric Research Earth System Grid data portal, Boulder, CO. 2007, updated 2014, Data downloaded 2015-10-23.

Melville, Bruce W., and Stephen E. Coleman. Bridge scour. Water Resources Publication, 2000.

National Climate Change Viewer (NCCV), Climate Research and Development Program, USGS, https://www2.usgs.gov/climate_landuse/clu_rd/nccv.asp

New Mexico Department of Transportation (NMDOT). Drainage Manual, Volume II-Hydraulics, Sedimentation and Erosion, Drainage Section, NMDOT, Albuquerque, NM.1998.

Nakicenovic, Nebojsa, and Rob Swart. "Emissions scenarios. Special report of the Intergovernmental panel on climate change." (2000).

NORTH AMERICAN REGIONAL REANALYSIS: A long-term, consistent, high-resolution climate dataset for the North American domain, as a major improvement upon the earlier global reanalysis datasets in both resolution and accuracy, Fedor Mesinger et. al, submitted to BAMS 2004.

Odgaard, A. J., and Wang, Y. "Scour prevention at bridge piers." *Proc., 1987 National Conf. on Hydraulic Engineering*, New York, 523–527.1987.

Okeil, Ayman M., and C. S. Cai. "Survey of short-and medium-span bridge damage induced by Hurricane Katrina." *Journal of Bridge Engineering* 13, no. 4 (2008): 377-387.

Parker, G., Toro-Escobar, C., and Voight, R. L., Jr. "Countermeasures to protect bridge piers from scour." Users' Guide (revised 1999) and Final Report, NCHRP Project No. 24-7, Prepared for National Cooperative Highway Research Program, Transportation Research Board by St. Anthony Falls Hydraulic Laboratory, Univ. of Minnesota, Minn.1998.

Parola, Arthur C., and Arthur C. Parola. *Highway infrastructure damage caused by the 1993 upper Mississippi River basin flooding*. No. 417. Transportation Research Board, 1998.

Pearson, David, J. Jones, and Stuart Stein. "Risk-based design of bridge scour countermeasures." *Transportation Research Record: Journal of the Transportation Research Board* 1696 (2000): 229-235.

Räty, Olle, Jouni Räisänen, and Jussi S. Ylhäisi. "Evaluation of delta change and bias correction methods for future daily precipitation: intermodel cross-validation using ENSEMBLES simulations." *Climate dynamics* 42, no. 9-10 (2014): 2287-2303.

Reeder, Tim, and Nicola Ranger. "How do you adapt in an uncertain world?: lessons from the Thames Estuary 2100 project." (2011).

Roads, J., S-C. Chen, and M. Kanamitsu. "US regional climate simulations and seasonal forecasts." *Journal of Geophysical Research: Atmospheres* 108, no. D16 (2003).

Savonis, M. J., V. Burkett, and J. R. Potter. Impacts of climate change and variability on transportation systems and infrastructure: Gulf coast study, Phase I. U.S. Climate Change Science Program and Global Change Research. 2008.

Schuring, John R., Robert Dresnack, and Eugene Golub. *Design and Evaluation of Scour for Bridges Using HEC-18*. No. FHWA-NJ-2017-011. New Jersey Department of Transportation, 2017.

Shan, Haoyin, Zhaoding Xie, Cezary Bojanowski, Oscar Suaznabar, Steven Lottes, Jerry Shen, and Kornel Kerenyi. *Submerged flow bridge scour under clear water conditions*. No. FHWA-HRT-12-034. 2012.

Sheppard, D. M., Bruce Melville, and H. Demir. "Evaluation of existing equations for local scour at bridge piers." Journal of Hydraulic Engineering 140, no. 1 (2013): 14-23.

State of Louisiana Department of Transportation and Development (LDOT). Hydraulics manual, Baton Rouge, Louisiana.2011.

Stein, Stuart, and Karsten Sedmera. *Risk-based management guidelines for scour at bridges with unknown foundations*. Transportation Research Board of the National Academies, 2006.

Stocker, T. F., D. Qin, G.K. Plattner, M. Tignor, S. K. Allen, J. Boschung, A. Nauels, Y. Xia, V. Bex, and P. M. Midgley. Climate change 2013: The physical science basis. Cambridge University Press, New York, 2014.

Texas Department of Transportation (TxDOT). Hydraulic design manual, Design Division, TxDOT, Austin, Tex.2004.

Thirumalaiah, K., & Deo, M. C. Real-Time Flood Forecasting Using Neural Networks. Computer-Aided Civil and Infrastructure Engineering, 101-111.1998.

Wang, Chen, Xiong Yu, and Fayun Liang. "A review of bridge scour: mechanism, estimation, monitoring and countermeasures." *Natural Hazards* 87, no. 3 (2017): 1881-1906.

Warren, F. J, R. Schwartz, J., Andrey, B. Mills, and D. Riedel. Climate Change Impacts and Adaptation: A Canadian Perspective. In Climate Change Impacts and Adaptation Directorate, Natural Resources Canada, Ottawa, Ontario, 2004. ISBN: 0-662-33123-0.

Wardhana, Kumalasari, and Fabian C. Hadipriono. "Analysis of recent bridge failures in the United States." *Journal of performance of constructed facilities* 17, no. 3 (2003): 144-150.

Zarrati, A. R., Nazahira, M., and Mashahir, M. B. "Reduction of local scour in the vicinity of bridge pier groups using collars and riprap." *J. Hydraul. Eng.*, 132(2), 154–162.2006.

Zevenbergen, L. W., L. A. Arneson, J. H. Hunt, and Arthur Carl Miller. *Hydraulic design of safe bridges*. No. FHWA-HIF-12-018. 2012

A. CLIMATE DATA

Bias Correction for Amarillo, Texas:

Table A-1 Bias Corrected Precipitation Data, Amarillo, Texas

Climate Models	Future Simulation (in)	Current Simulation (in)	Bias Corrected (in)
CRCM-CCSM	17.9	18.2	18.1
CRCM-CGCM3	19.7	18.9	19.2
ECP2-GFDL	21.4	24.5	16.1
ECP2-HADCM3	15.3	17.6	15.9
HRM3-GFDL	27.0	29.7	16.7
HRM3-HADCM3	21.5	23.1	17.1
MM5I-CCSM	17.1	17.9	17.6
MM5I-HADCM3	21.3	21.7	18.0
RCM3-CGCM3	20.0	21.7	16.9
RCM3-GFDL	29.0	29.7	18.0
WRFG-CCSM	14.5	14.5	18.4
WRFG-CGCM3	15.1	13.6	20.4

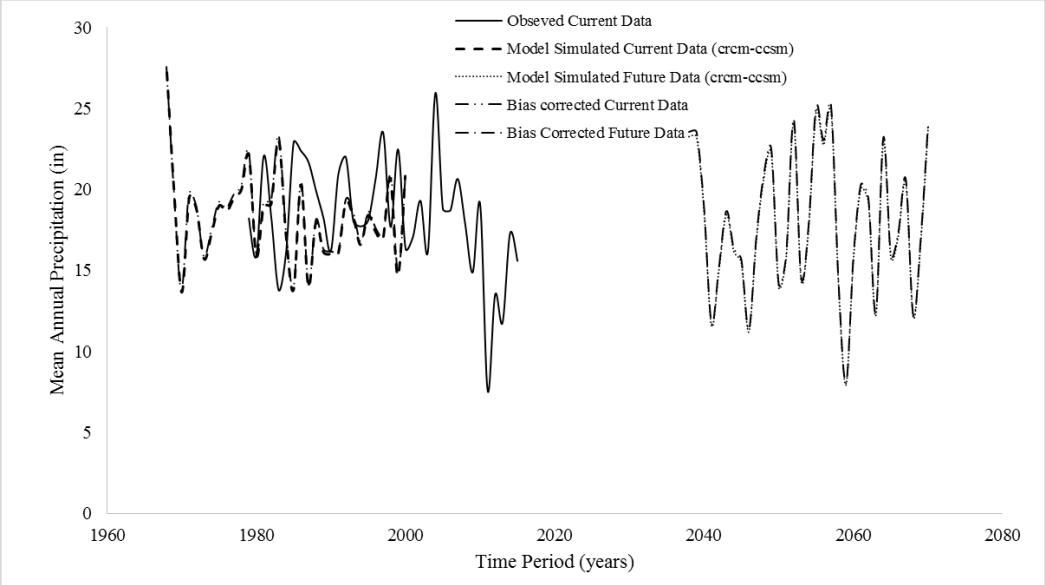

Figure A-1 Bias Correction for Mean Annual Precipitation, Amarillo, Texas

Bias Correction for Austin, Texas:

Table A-2 Bias Corrected Precipitation Data, Austin, Texas

Climate Models	Future Simulation (in)	Current Simulation (in)	Bias Corrected (in)
CRCM-CCSM	18.6	20.7	28.4
CRCM-CGCM3	27.7	27.7	31.7
ECP2-GFDL	33.4	36.7	28.7
ECP2-HADCM3	41.0	37.5	34.6
HRM3-GFDL	34.7	37.6	29.2
HRM3-HADCM3	42.4	38.6	34.7
MM5I-CCSM	17.2	19.2	28.2
MM5I-HADCM3	37.5	32.9	36.1
RCM3-CGCM3	35.3	34.5	32.3
RCM3-GFDL	43.2	43.4	31.5
WRFG-CCSM	24.3	24.4	31.5
WRFG-CGCM3	28.2	27.0	33.0

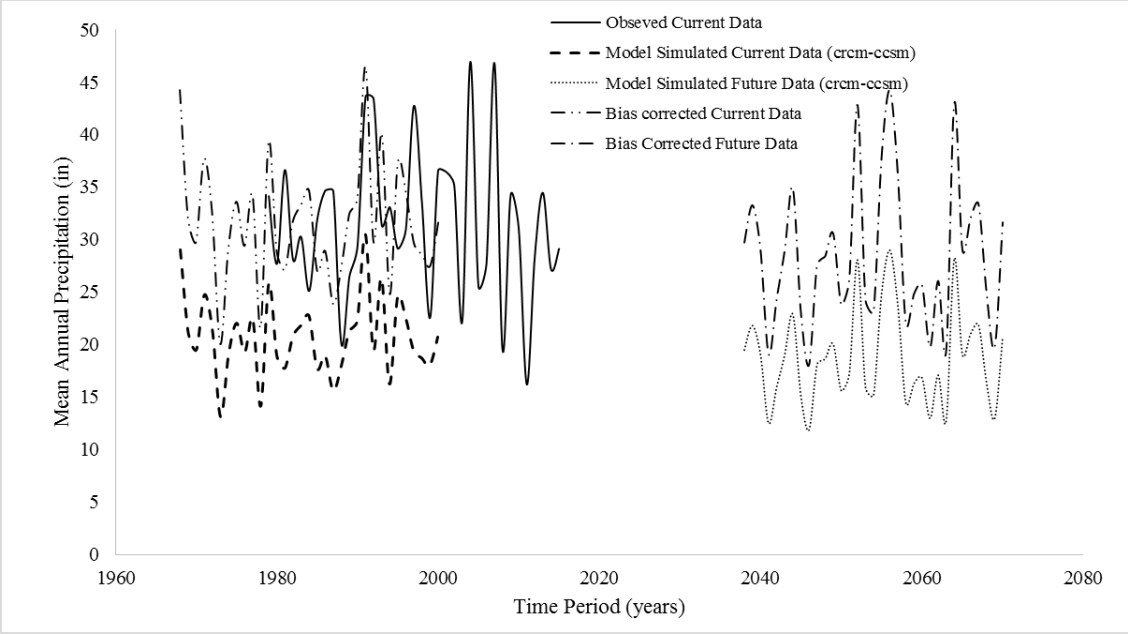

Figure A-2 Bias Correction for Mean Annual Precipitation, Austin, Texas

Bias Correction for Dallas, Texas:

Table A-3 Bias Corrected Precipitation Data, Dallas, Texas

Climate Models	Future Simulation (in)	Current Simulation (in)	Bias Corrected (in)
CRCM-CCSM	21.0	22.0	33.2
CRCM-CGCM3	27.6	26.8	35.8
ECP2-GFDL	32.2	37.1	30.2
ECP2-HADCM3	33.3	33.2	34.9
HRM3-GFDL	36.8	37.1	34.5
HRM3-HADCM3	36.3	34.7	36.4
MM5I-CCSM	21.9	23.2	32.9
MM5I-HADCM3	31.0	29.5	36.5
RCM3-CGCM3	30.9	31.8	33.9
RCM3-GFDL	37.8	37.2	35.3
WRFG-CCSM	25.0	22.7	38.4
WRFG-CGCM3	25.3	25.3	34.8

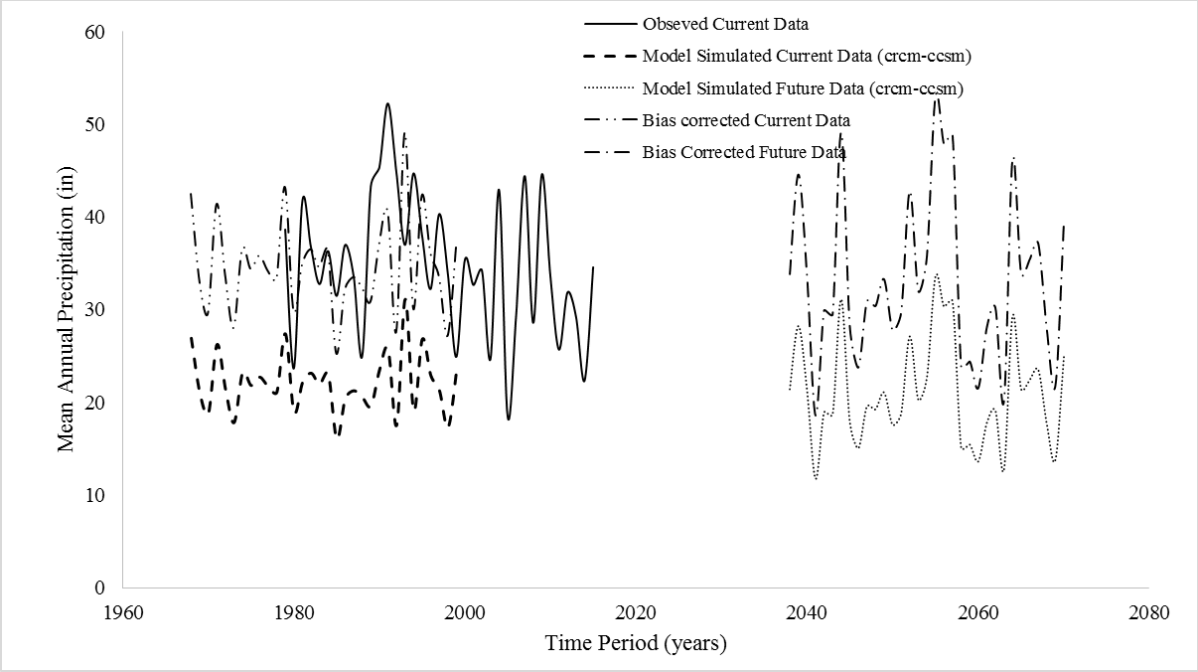

Figure A-3 Bias Correction for Mean Annual Precipitation, Dallas, Texas

Bias Correction for El Paso, Texas:

Table A-4 Bias Corrected Precipitation Data, El Paso, Texas

Climate Models	Future Simulation (in)	Current Simulation (in)	Bias Corrected (in)
CRCM-CCSM	13.2	15.6	8.1
CRCM-CGCM3	11.6	12.5	8.8
ECP2-GFDL	16.7	16.8	9.4
ECP2-HADCM3	8.4	9.0	8.9
HRM3-GFDL	21.9	23.8	8.7
HRM3-HADCM3	12.2	15.1	7.7
MM5I-CCSM	9.3	11.7	7.5
MM5I-HADCM3	12.7	11.1	10.9
RCM3-CGCM3	34.3	35.3	9.2
RCM3-GFDL	41.6	42.3	9.3
WRFG-CCSM	9.8	10.9	8.5
WRFG-CGCM3	7.1	7.1	9.5

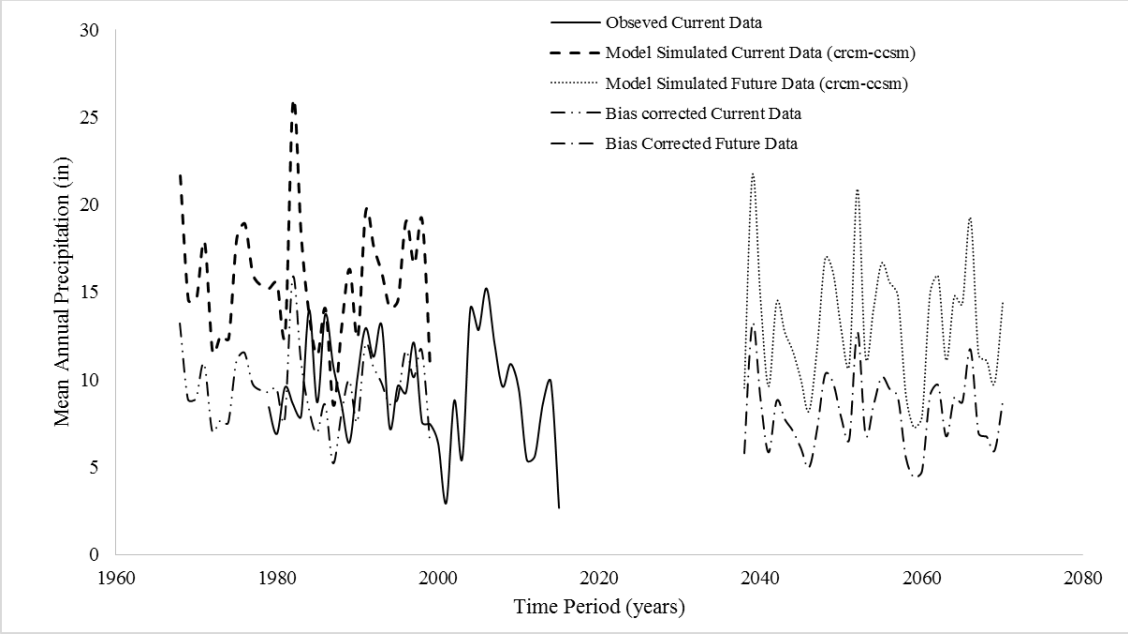

Figure A-4 Bias Correction for Mean Annual Precipitation, El Paso, Texas

Bias Correction for Fort Worth, Texas:

Table A-5 Bias Corrected Precipitation Data, Fort Worth, Texas

Climate Models	Future Simulation (in)	Current Simulation (in)	Bias-Corrected (in)
CRCM-CCSM	19.8	20.6	32.8
CRCM-CGCM3	22.0	24.4	30.8
ECP2-GFDL	31.0	36.1	29.2
ECP2-HADCM3	32.0	31.6	34.5
HRM3-GFDL	36.4	37.9	32.7
HRM3-HADCM3	35.2	33.7	35.7
MM5I-CCSM	21.0	21.9	32.8
MM5I-HADCM3	28.2	27.1	35.5
RCM3-CGCM3	21.5	30.1	24.3
RCM3-GFDL	36.0	36.1	34.0
WRFG-CCSM	22.6	20.6	37.3
WRFG-CGCM3	22.0	21.6	34.7

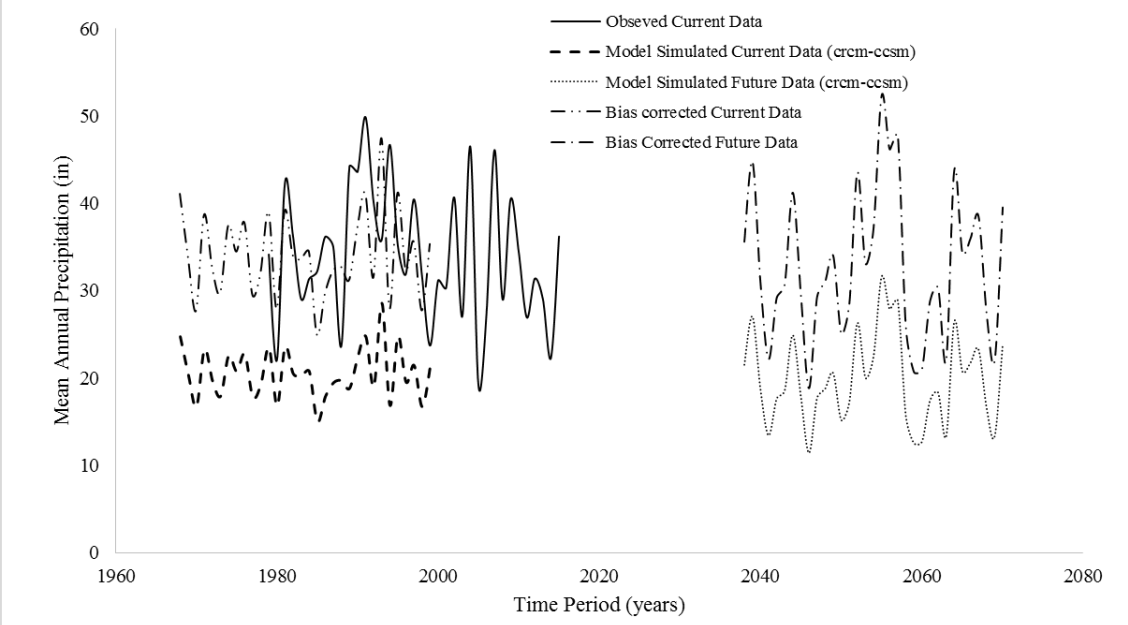

Figure A-5 Bias Correction for Mean Annual Precipitation, Fort Worth, Texas

Bias Correction for McAllen, Texas:

Table A-6 Bias Corrected Precipitation Data, McAllen, Texas

Climate Models	Future Simulation (in)	Current Simulation (in)	Bias-Corrected (in)
CRCM-CCSM	24.0	29.2	14.9
CRCM-CGCM3	42.5	44.1	17.5
ECP2-GFDL	33.0	38.5	15.5
ECP2-HADCM3	46.1	35.4	23.6
HRM3-GFDL	24.2	27.4	16.0
HRM3-HADCM3	39.6	34.7	20.7
MM5I-CCSM	10.7	15.6	12.4
MM5I-HADCM3	44.5	46.3	17.5
RCM3-CGCM3	51.1	49.7	18.6
RCM3-GFDL	69.7	69.4	18.2
WRFG-CCSM	21.4	25.0	15.5
WRFG-CGCM3	32.0	34.7	16.8

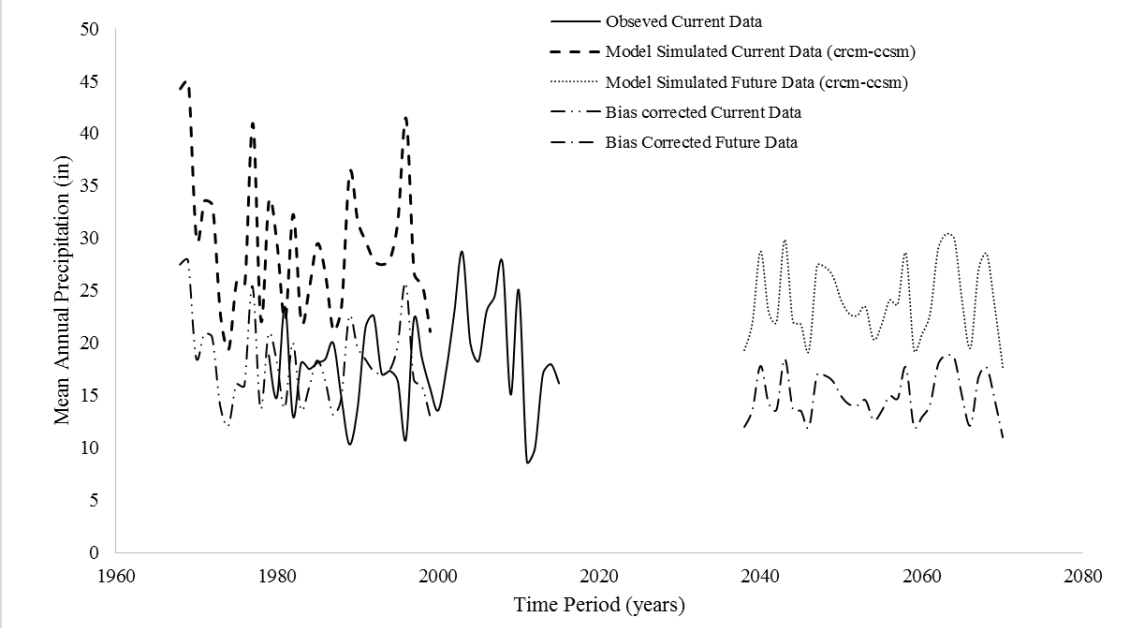

Figure A-6 Bias Correction for Mean Annual Precipitation, McAllen, Texa

Bias Correction for San Antonio, Texas:

Table A-7 Bias Corrected Precipitation Data, San Antonio, Texas

Climate Models	Future Simulation (in)	Current Simulation (in)	Bias-Corrected (in)
CRCM-CCSM	17.1	19.5	26.5
CRCM-CGCM3	27.0	27.0	30.2
ECP2-GFDL	29.4	34.6	25.7
ECP2-HADCM3	39.1	34.3	34.5
HRM3-GFDL	30.3	32.6	28.1
HRM3-HADCM3	39.1	32.9	35.9
MM5I-CCSM	14.7	16.1	27.5
MM5I-HADCM3	34.4	30.2	34.5
RCM3-CGCM3	33.3	32.5	31.0
RCM3-GFDL	41.7	42.0	30.0
WRFG-CCSM	24.0	24.4	29.8
WRFG-CGCM3	25.4	24.8	30.9

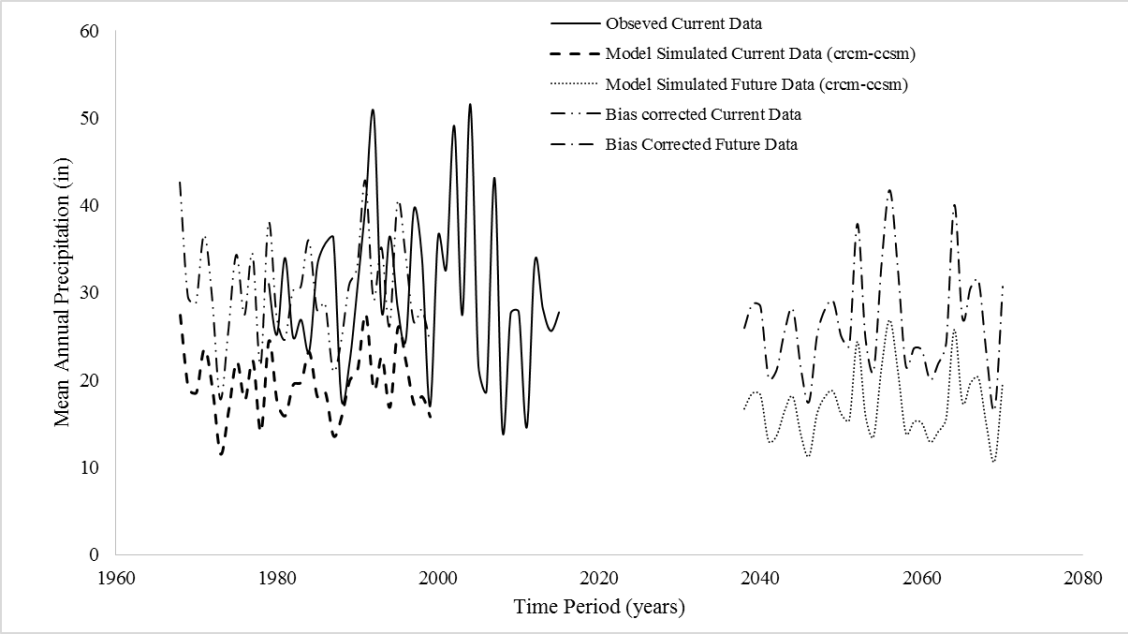

Figure A-7 Bias Correction for Mean Annual Precipitation, San Antonio, Texas

Bias Correction for Albuquerque, New Mexico:

Table A-8 Bias Corrected Precipitation Data, Albuquerque, New Mexico

Climate Models	Future Simulation (in)	Current Simulation (in)	Bias Corrected (in)
CRCM-CCSM	13.1	14.6	9.2
CRCM-CGCM3	11.3	11.5	10.1
ECP2-GFDL	22.8	19.8	11.8
ECP2-HADCM3	9.4	10.1	9.4
HRM3-GFDL	22.9	24.4	9.6
HRM3-HADCM3	15.4	17.7	8.9
MM5I-CCSM	9.4	11.1	8.7
MM5I-HADCM3	15.8	15.7	10.3
RCM3-CGCM3	12.0	14.3	8.6
RCM3-GFDL	25.4	26.2	9.9
WRFG-CCSM	14.5	14.6	10.2
WRFG-CGCM3	12.6	13.3	9.7

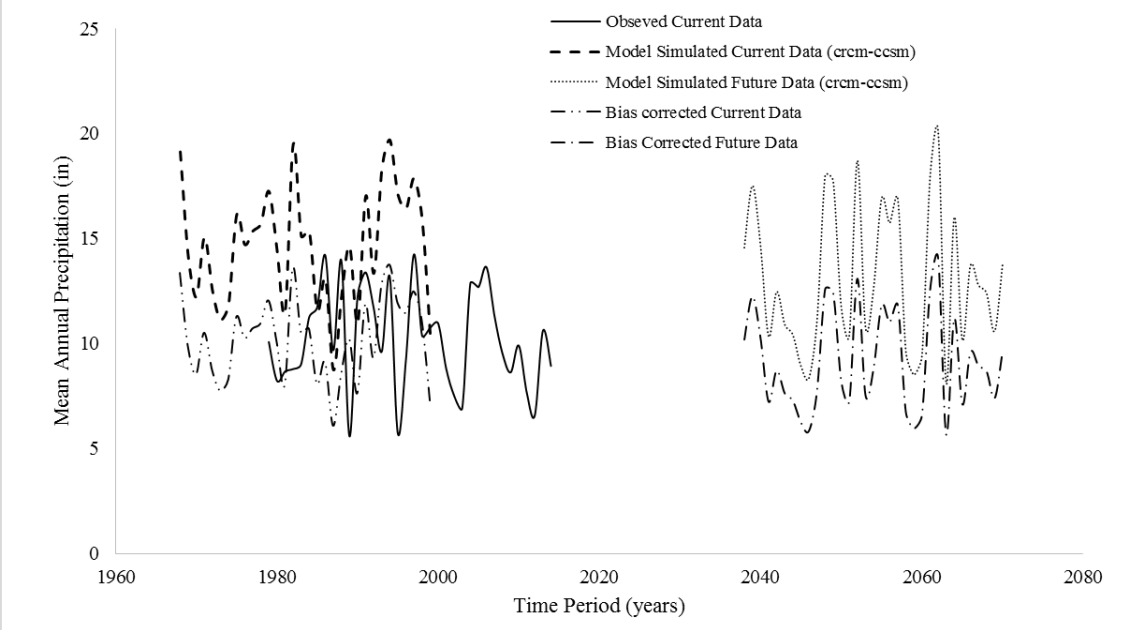

Figure A-8 Bias Correction for Mean Annual Precipitation, Albuquerque, New Mexico

Bias Correction for Las Cruces, New Mexico:

Table A-9 Bias Corrected Precipitation Data, Las Cruces, New Mexico

Climate Models	Future Simulation (in)	Current Simulation (in)	Bias Corrected (in)
CRCM-CCSM	16.1	18.4	9.0
CRCM-CGCM3	14.3	15.3	9.7
ECP2-GFDL	16.7	15.9	10.8
ECP2-HADCM3	7.2	8.2	9.2
HRM3-GFDL	25.6	28.9	9.2
HRM3-HADCM3	15.4	19.3	8.2
MM5I-CCSM	9.7	11.9	8.4
MM5I-HADCM3	12.9	11.5	11.6
RCM3-CGCM3	8.6	9.1	9.8
RCM3-GFDL	19.2	20.7	9.6
WRFG-CCSM	11.0	11.8	9.6
WRFG-CGCM3	8.9	8.7	10.6

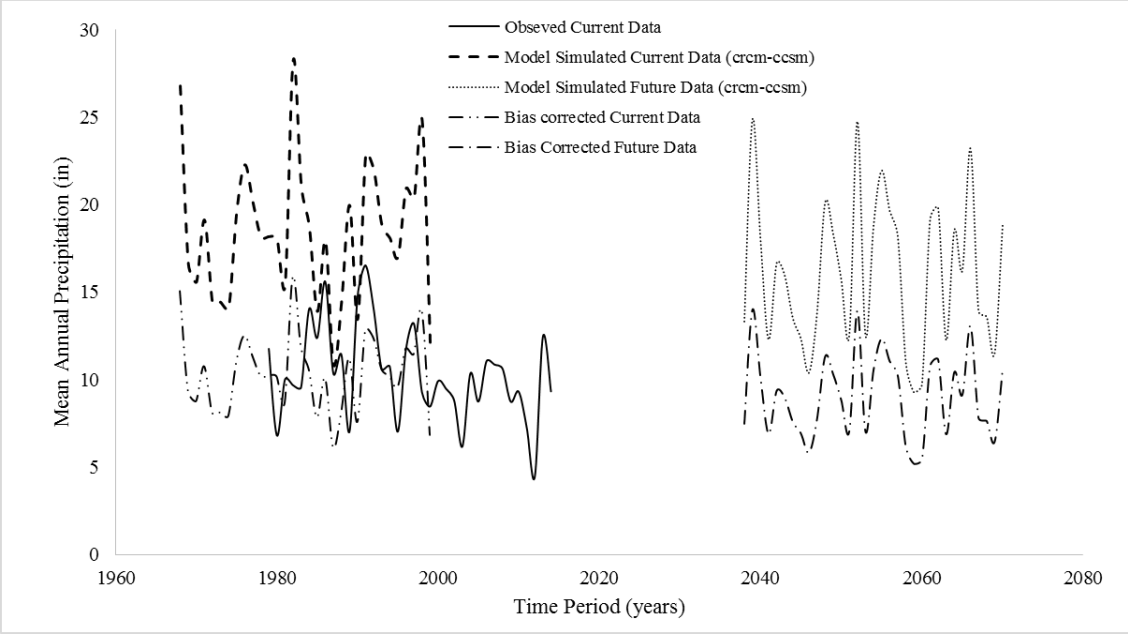

Figure A-9 Bias Correction for Mean Annual Precipitation, Las Cruces, New Mexico

Bias Correction for Taos, New Mexico:

Table A-10 Bias Corrected Precipitation Data, Taos, New Mexico

Climate Models	Future Simulation (in)	Current Simulation (in)	Bias-Corrected (in)
CRCM-CCSM	17.2	18.3	14.6
CRCM-CGCM3	15.6	16.1	15.0
ECP2-GFDL	35.3	42.0	13.0
ECP2-HADCM3	26.3	29.7	13.7
HRM3-GFDL	33.6	36.1	14.4
HRM3-HADCM3	26.0	28.9	14.0
MM5I-CCSM	17.2	21.8	12.2
MM5I-HADCM3	34.1	32.6	16.2
RCM3-CGCM3	31.3	31.8	15.3
RCM3-GFDL	41.4	40.6	15.8
WRFG-CCSM	17.5	17.9	15.2
WRFG-CGCM3	16.9	18.4	14.3

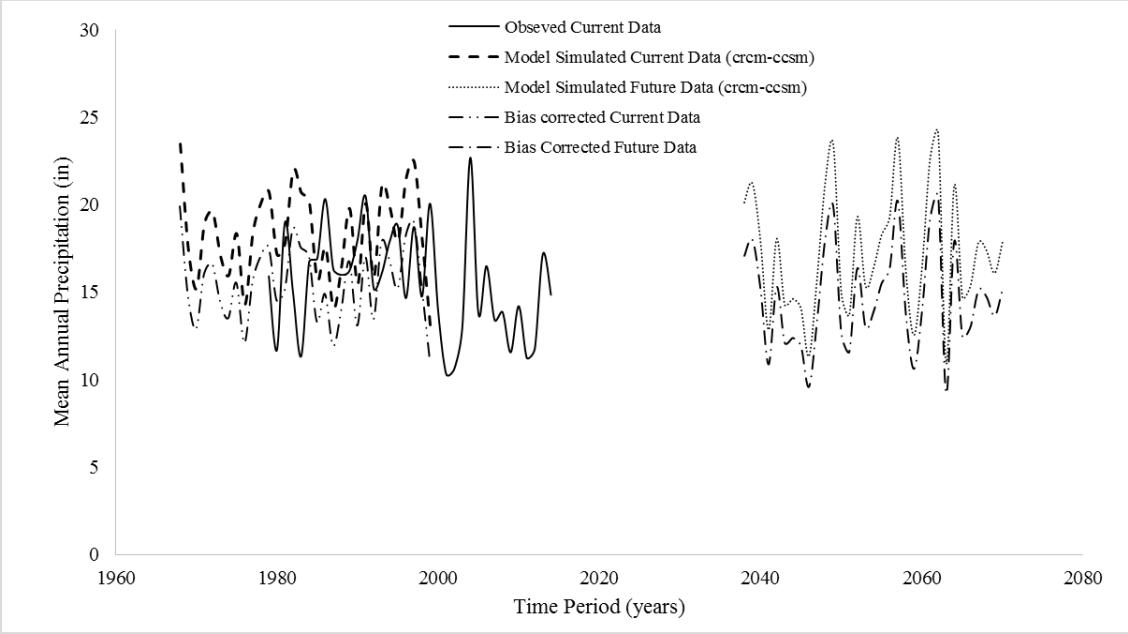

Figure A-10 Bias Correction for Mean Annual Precipitation, Taos, New Mexico

Bias Correction for Santa Fe, New Mexico:

Table A-11 Bias Corrected Precipitation Data, Santa Fe, New Mexico

Climate Models	Future Simulation (in)	Current Simulation (in)	Bias-Corrected (in)
CRCM-CCSM	18.5	20.0	12.2
CRCM-CGCM3	16.6	17.1	12.8
ECP2-GFDL	32.2	32.7	13.0
ECP2-HADCM3	19.6	21.6	12.0
HRM3-GFDL	21.9	23.6	12.3
HRM3-HADCM3	15.5	17.6	11.6
MM5I-CCSM	13.3	16.1	10.9
MM5I-HADCM3	25.2	24.0	13.8
RCM3-CGCM3	15.3	18.1	11.1
RCM3-GFDL	30.9	30.9	13.2
WRFG-CCSM	16.2	16.8	12.7
WRFG-CGCM3	15.0	15.7	12.6

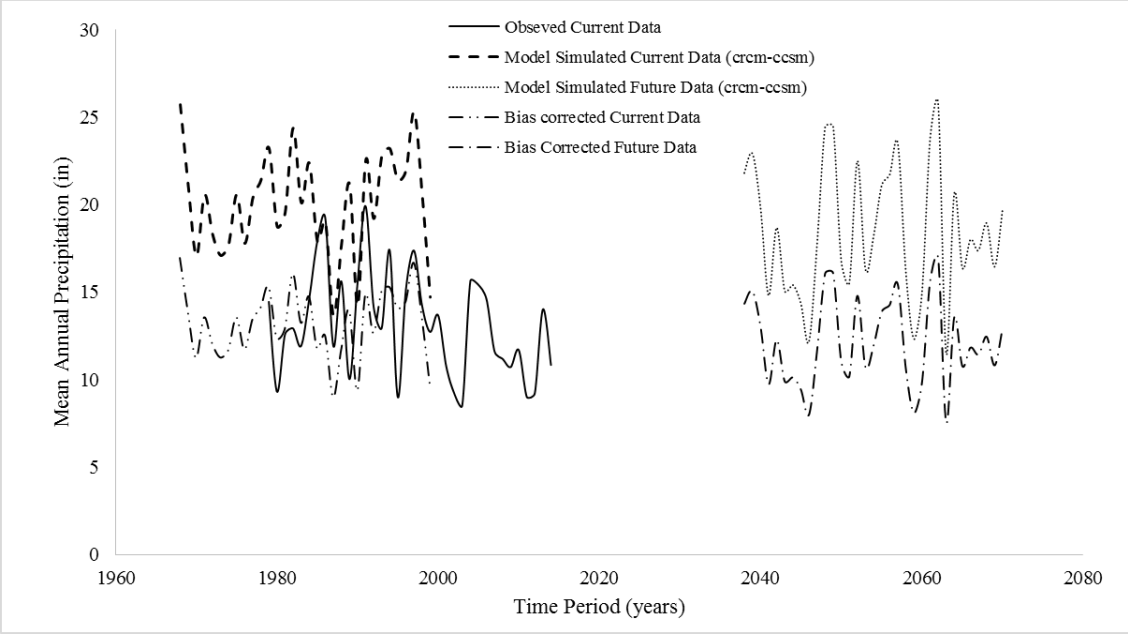

Figure A-11 Bias Correction for Mean Annual Precipitation, Santa Fe, New Mexico

Bias Correction for Roswell, New Mexico:

Table A-12 Bias Corrected Precipitation Data, Roswell, New Mexico

Climate Models	Future Simulation (in)	Current Simulation (in)	Bias-Corrected (in)
CRCM-CCSM	14.9	15.4	11.4
CRCM-CGCM3	13.8	14.5	11.2
ECP2-GFDL	17.3	16.8	12.2
ECP2-HADCM3	7.7	8.7	10.4
HRM3-GFDL	20.4	23.8	10.1
HRM3-HADCM3	13.1	15.8	9.8
MM5I-CCSM	10.6	10.7	11.6
MM5I-HADCM3	13.0	11.4	13.4
RCM3-CGCM3	14.7	16.0	10.8
RCM3-GFDL	25.8	27.3	11.1
WRFG-CCSM	13.9	14.1	11.6
WRFG-CGCM3	13.9	12.3	13.4

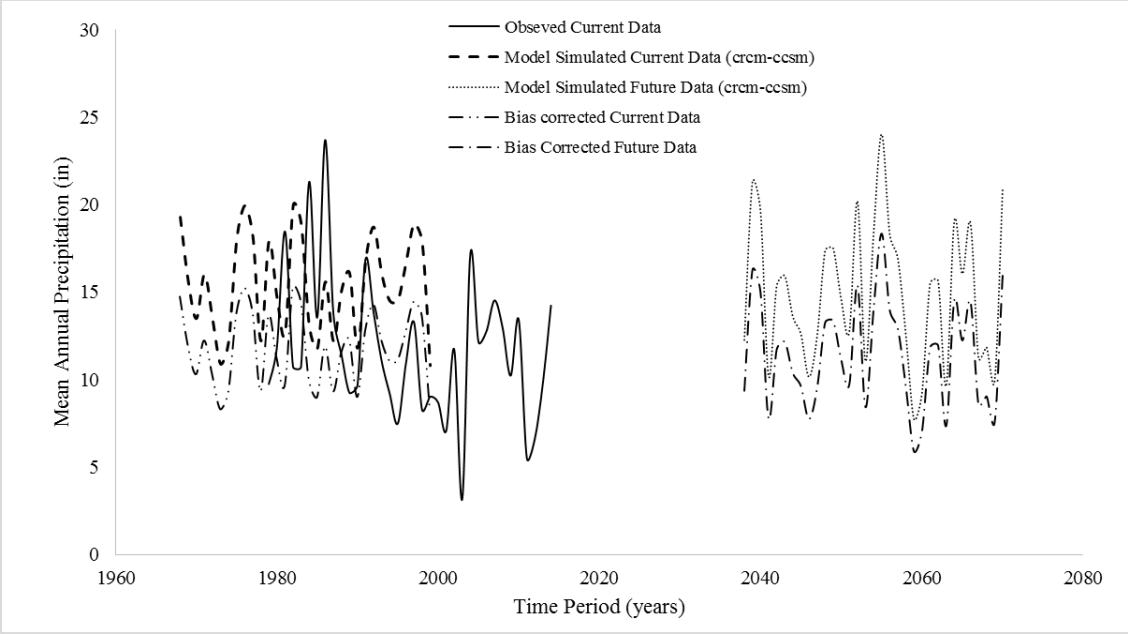

Figure A-12 Bias Correction for Mean Annual Precipitation, Roswell, New Mexico

Bias Correction for Farmington, New Mexico:

Table A-13 Bias Corrected Precipitation Data, Farmington, New Mexico

Climate Models	Future Simulation (in)	Current Simulation (in)	Bias-Corrected (in)
CRCM-CCSM	17.4	19.7	8.2
CRCM-CGCM3	14.2	14.6	9.0
ECP2-GFDL	29.9	27.0	10.3
ECP2-HADCM3	15.3	15.8	9.0
HRM3-GFDL	15.6	16.5	8.8
HRM3-HADCM3	10.2	12.0	7.9
MM5I-CCSM	10.5	12.4	7.9
MM5I-HADCM3	17.3	17.5	9.2
RCM3-CGCM3	16.9	19.0	8.2
RCM3-GFDL	34.0	34.1	9.3
WRFG-CCSM	12.5	13.1	8.9
WRFG-CGCM3	11.3	11.7	9.0

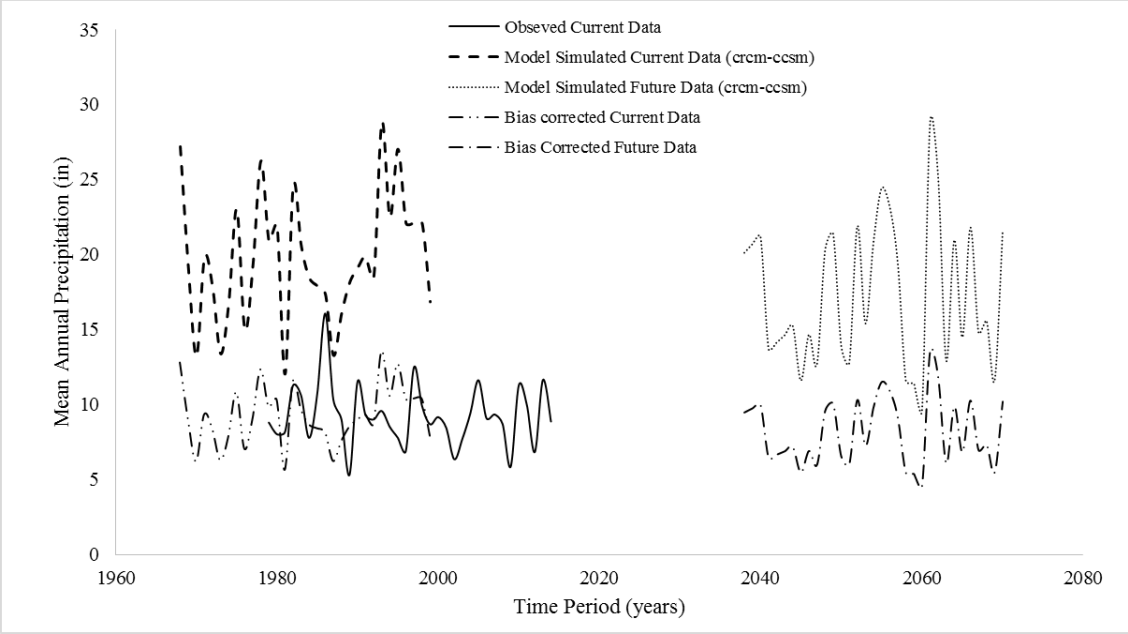

Figure A-13 Bias Correction for Mean Annual Precipitation, Farmington, New Mexico

Bias Correction for Lordsburg, New Mexico:

Table A-14 Bias Corrected Precipitation Data, Lordsburg, New Mexico

Climate Models	Future Simulation (in)	Current Simulation (in)	Bias-Corrected (in)
CRCM-CCSM	12.6	16.1	9.8
CRCM-CGCM3	10.7	11.0	12.2
ECP2-GFDL	22.8	20.5	13.9
ECP2-HADCM3	11.1	11.3	12.3
HRM3-GFDL	25.5	28.2	11.3
HRM3-HADCM3	12.8	15.1	10.6
MM5I-CCSM	9.4	13.3	8.9
MM5I-HADCM3	14.7	13.2	13.9
RCM3-CGCM3	9.5	10.1	11.8
RCM3-GFDL	22.6	24.6	11.5
WRFG-CCSM	10.4	13.3	9.8
WRFG-CGCM3	8.9	8.6	13.0

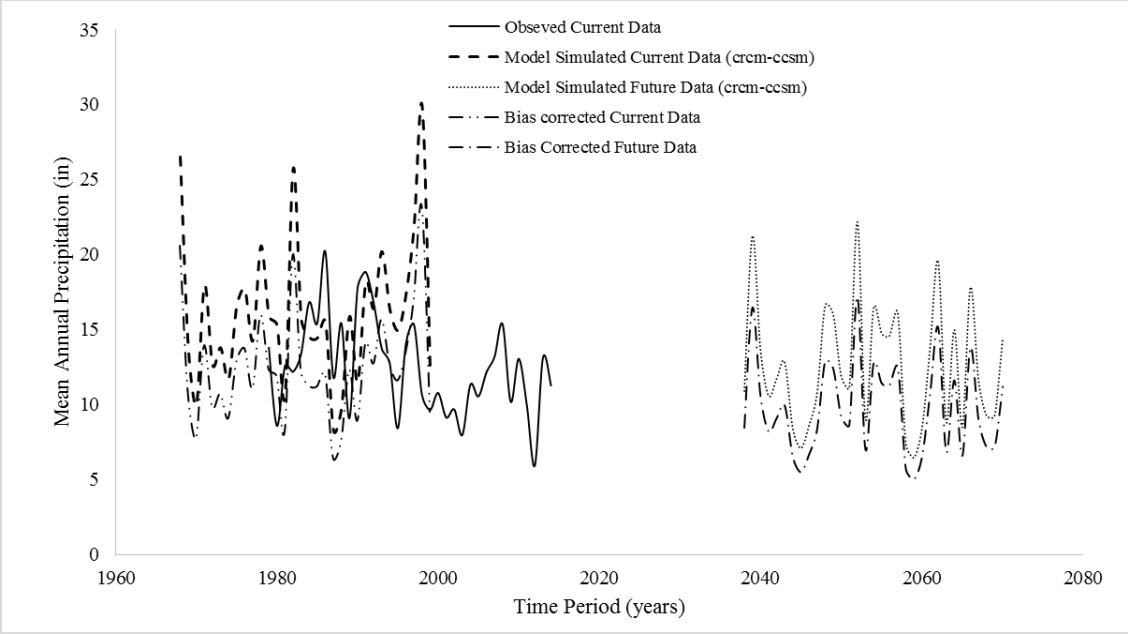

Figure A-14 Bias Correction for Mean Annual Precipitation, Lordsburg, New Mexico

Bias Correction for Lafayette, Louisiana:

Table A-15 Bias Corrected Precipitation Data, Lafayette, Louisiana

Climate Models	Future Simulation (in)	Current Simulation (in)	Bias Corrected (in)
CRCM-CCSM	24.1	26.4	54.0
CRCM-CGCM3	41.8	41.5	59.8
ECP2-GFDL	37.8	40.5	55.3
ECP2-HADCM3	48.0	45.9	62.1
HRM3-GFDL	36.2	40.3	53.2
HRM3-HADCM3	48.8	48.1	60.1
MM5I-CCSM	30.6	32.7	55.5
MM5I-HADCM3	60.1	55.1	64.6
RCM3-CGCM3	58.7	57.5	60.6
RCM3-GFDL	56.2	55.5	60.1
WRFG-CCSM	28.5	31.1	54.3
WRFG-CGCM3	53.3	51.3	61.7

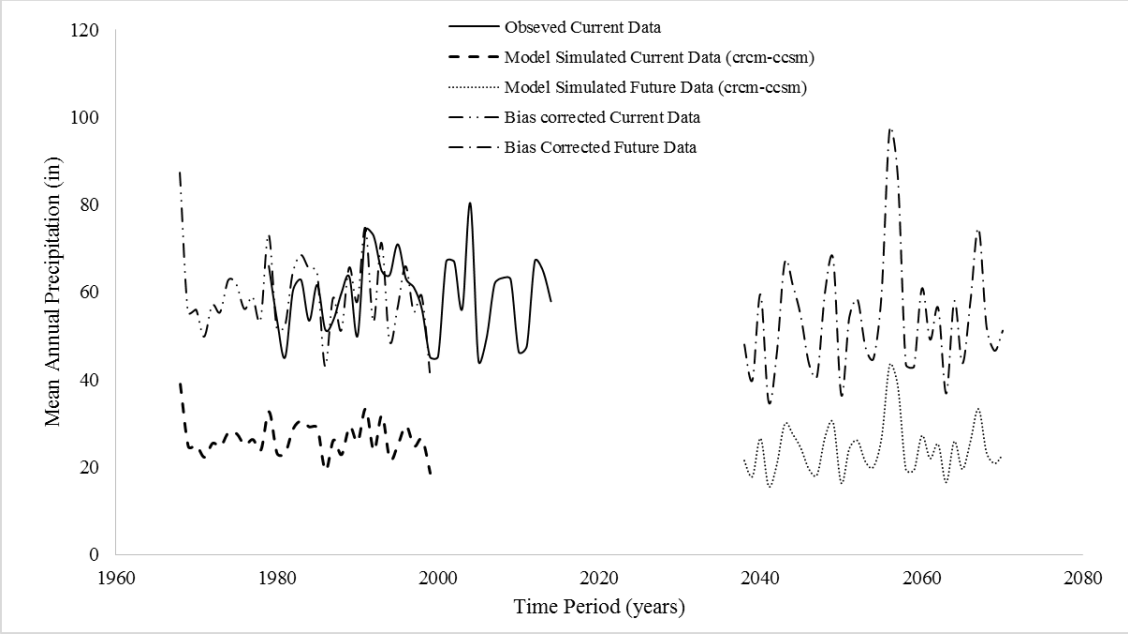

Figure A-15 Bias Correction for Mean Annual Precipitation, Lafayette, Louisiana

Bias Correction for Baton Rouge, Louisiana:

Table A-16 Bias Corrected Precipitation Data, Baton Rouge, Louisiana

Climate Models	Future Simulation (in)	Current Simulation (in)	Bias Corrected (in)
CRCM-CCSM	23.7	26.1	55.0
CRCM-CGCM3	40.1	38.2	63.5
ECP2-GFDL	51.5	58.1	53.6
ECP2-HADCM3	65.2	64.4	61.3
HRM3-GFDL	38.6	43.0	54.3
HRM3-HADCM3	49.8	49.2	61.3
MM5I-CCSM	32.9	34.8	57.2
MM5I-HADCM3	61.5	56.1	66.4
RCM3-CGCM3	60.8	59.0	62.4
RCM3-GFDL	58.0	56.2	62.5
WRFG-CCSM	29.5	32.8	54.4
WRFG-CGCM3	58.1	54.5	64.6

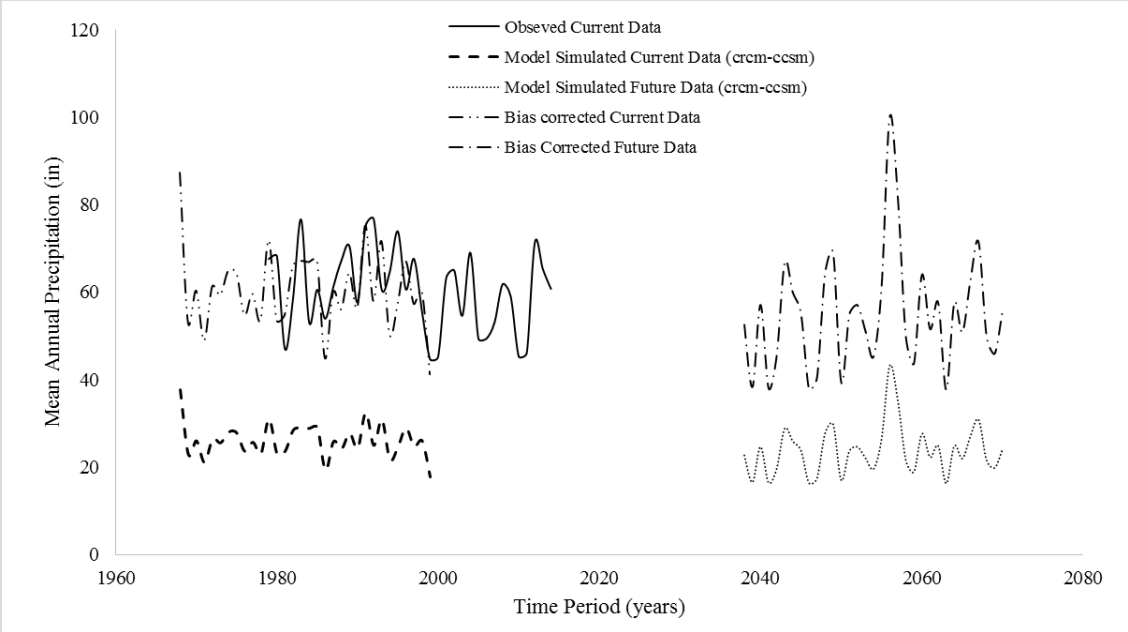

Figure A-16 Bias Correction for Mean Annual Precipitation, Lafayette, Louisiana

Bias Correction for New Orleans, Louisiana:

Table A-17 Bias Corrected Precipitation Data, New Orleans, Louisiana

Climate Models	Future Simulation (in)	Current Simulation (in)	Bias-Corrected (in)
CRCM-CCSM	24.1	26.7	49.7
CRCM-CGCM3	42.3	41.4	56.1
ECP2-GFDL	58.1	60.2	53.0
ECP2-HADCM3	76.9	64.6	65.3
HRM3-GFDL	38.6	42.4	50.0
HRM3-HADCM3	49.8	50.0	54.7
MM5I-CCSM	24.7	27.1	50.1
MM5I-HADCM3	106.2	71.4	81.7
RCM3-CGCM3	70.6	66.7	58.1
RCM3-GFDL	64.2	64.5	54.7
WRFG-CCSM	32.8	36.1	49.9
WRFG-CGCM3	66.7	66.7	54.9

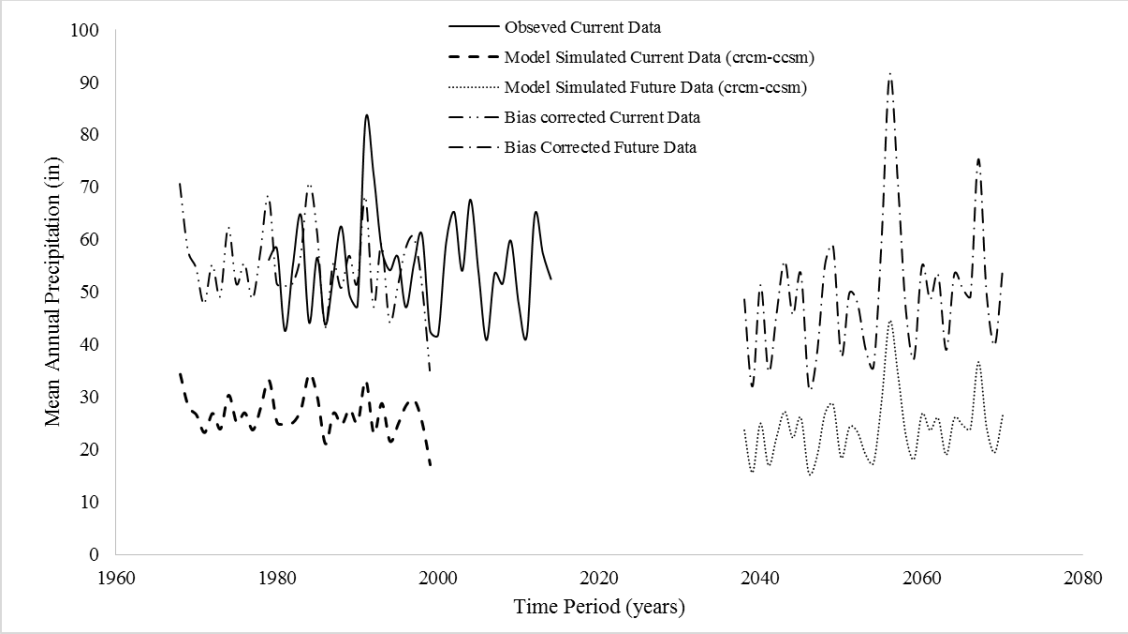

Figure A-17 Bias Correction for Mean Annual Precipitation, New Orleans, Louisiana

Bias Correction for Shreveport, Louisiana:

Table A-18 Bias Corrected Precipitation Data, Shreveport, Louisiana

Climate Models	Future Simulation (in)	Current Simulation (in)	Bias-Corrected (in)
CRCM-CCSM	26.1	27.7	44.9
CRCM-CGCM3	36.6	34.9	49.9
ECP2-GFDL	45.9	48.2	45.3
ECP2-HADCM3	45.1	46.3	46.4
HRM3-GFDL	41.6	44.8	44.1
HRM3-HADCM3	43.5	44.1	46.9
MM5I-CCSM	28.4	30.6	44.1
MM5I-HADCM3	43.8	41.6	50.1
RCM3-CGCM3	38.4	40.6	45.0
RCM3-GFDL	45.0	45.4	47.2
WRFG-CCSM	26.3	27.3	45.8
WRFG-CGCM3	36.3	35.4	48.8

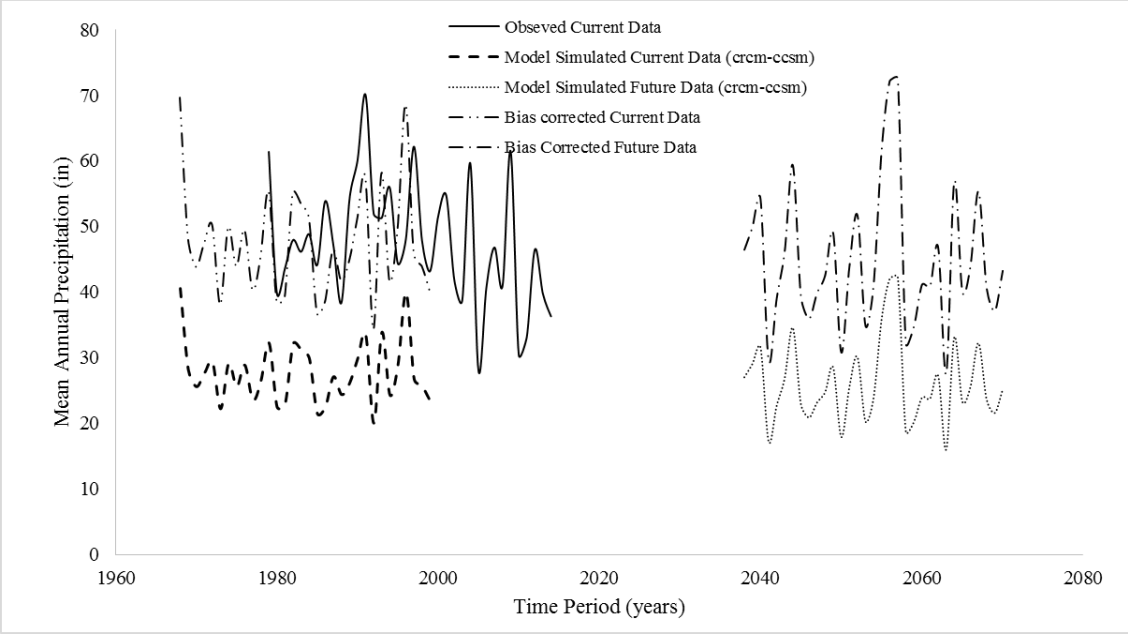

Figure A-18 Bias Correction for Mean Annual Precipitation, Shreveport, Louisiana

Bias Correction for Oklahoma City, Oklahoma:

Table A-19 Bias Corrected Precipitation Data, Oklahoma City, Oklahoma

Climate Models	Future Simulation (in)	Current Simulation (in)	Bias-Corrected (in)
CRCM-CCSM	21.2	21.0	35.7
CRCM-CGCM3	26.2	24.7	37.5
ECP2-GFDL	28.9	32.5	31.5
ECP2-HADCM3	23.1	25.9	31.5
HRM3-GFDL	34.8	37.7	32.6
HRM3-HADCM3	32.3	31.7	36.0
MM5I-CCSM	23.7	23.0	36.4
MM5I-HADCM3	26.4	24.9	37.5
RCM3-CGCM3	27.8	30.2	32.5
RCM3-GFDL	35.1	34.7	35.8
WRFG-CCSM	19.9	18.6	37.9
WRFG-CGCM3	19.7	18.7	37.1

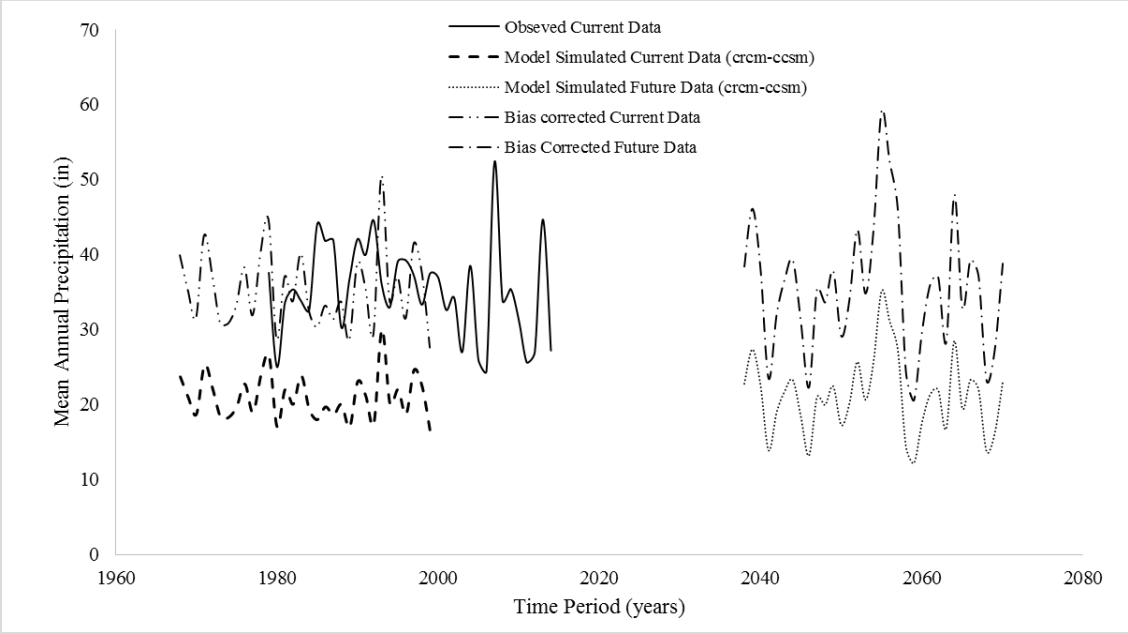

Figure A-19 Bias Correction for Mean Annual Precipitation, Oklahoma City, Oklahoma

Bias Correction for Tulsa, Oklahoma:

Table A-20 Bias Corrected Precipitation Data, Tulsa, Oklahoma

Climate Models	Future Simulation (in)	Current Simulation (in)	Bias Corrected (in)
CRCM-CCSM	27.2	27.6	38.5
CRCM-CGCM3	33.9	31.5	42.2
ECP2-GFDL	32.1	36.2	34.7
ECP2-HADCM3	26.8	29.7	35.3
HRM3-GFDL	41.2	43.3	37.2
HRM3-HADCM3	38.0	37.8	39.2
MM5I-CCSM	28.3	27.9	39.6
MM5I-HADCM3	31.5	29.1	42.3
RCM3-CGCM3	32.7	34.6	36.9
RCM3-GFDL	39.8	40.4	38.5
WRFG-CCSM	21.0	20.3	40.5
WRFG-CGCM3	25.3	21.8	45.3

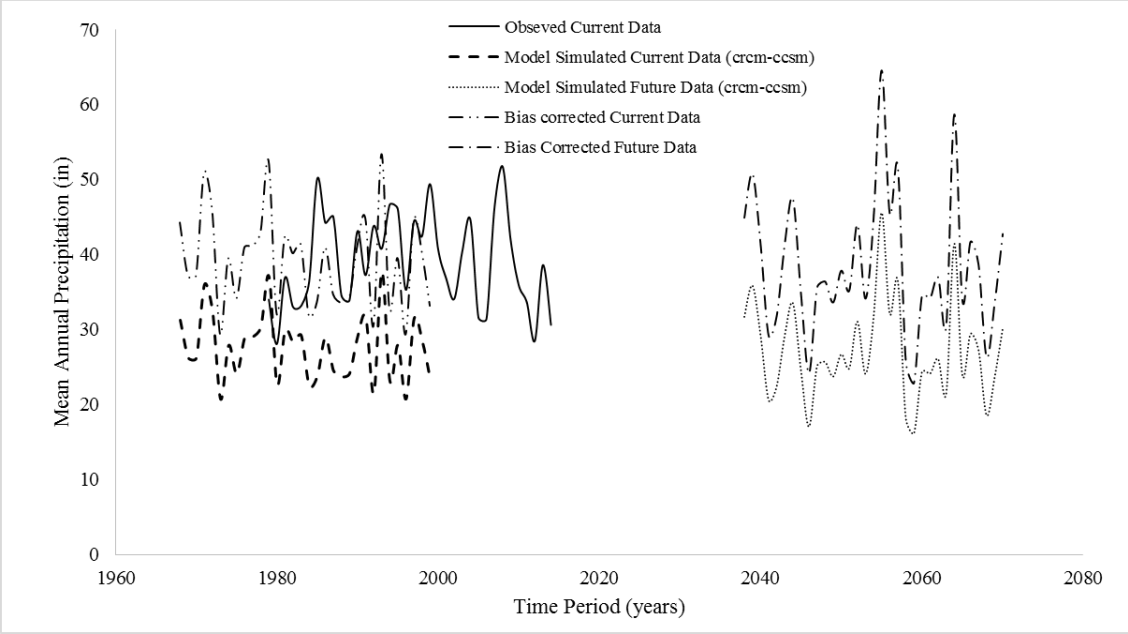

Figure A-20 Bias Correction for Mean Annual Precipitation, Tulsa, Oklahoma

Bias Correction for Stillwater, Oklahoma:

Table A-21 Bias Corrected Precipitation Data, Stillwater, Oklahoma

Climate Models	Future Simulation (in)	Current Simulation (in)	Bias-Corrected (in)
CRCM-CCSM	23.7	23.3	36.7
CRCM-CGCM3	28.9	26.9	38.6
ECP2-GFDL	29.8	32.8	32.6
ECP2-HADCM3	23.4	26.4	31.8
HRM3-GFDL	36.9	39.2	33.8
HRM3-HADCM3	33.7	33.8	35.9
MM5I-CCSM	23.9	24.1	35.7
MM5I-HADCM3	27.6	25.7	38.5
RCM3-CGCM3	29.5	32.0	33.2
RCM3-GFDL	37.3	37.1	36.2
WRFG-CCSM	17.9	17.9	36.0
WRFG-CGCM3	21.2	18.4	41.4

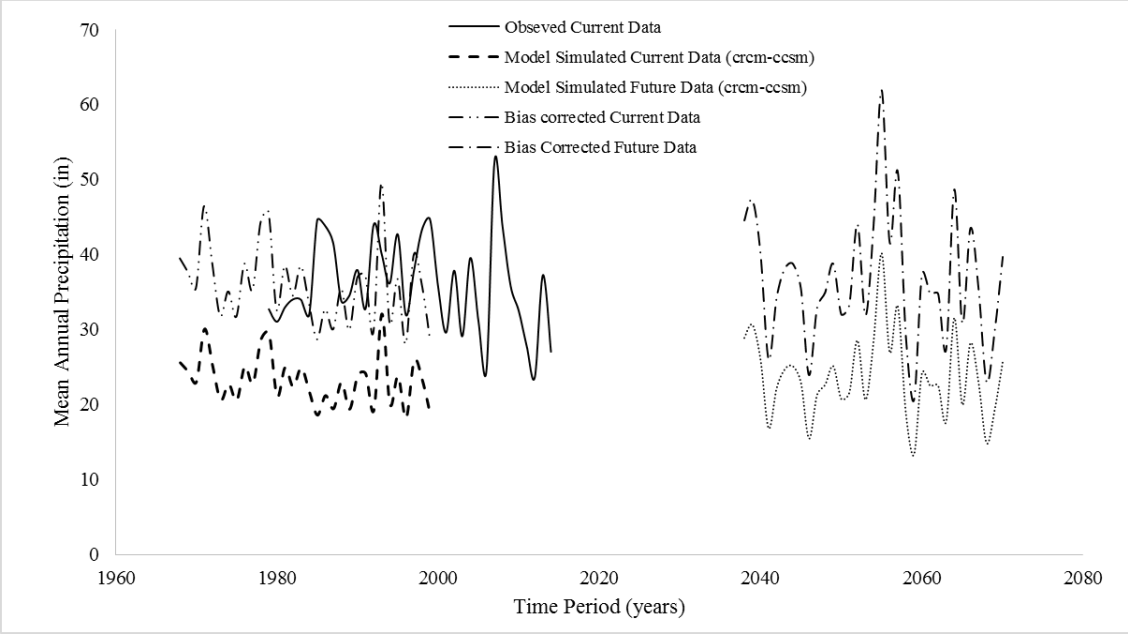

Figure A-21 Bias Correction for Mean Annual Precipitation, Stillwater, Oklahoma

Bias Correction for Lawton, Oklahoma:

Table A-22 Bias Corrected Precipitation Data, Lawton, Oklahoma

Climate Models	Future Simulation (in)	Current Simulation (in)	Bias-Corrected (in)
CRCM-CCSM	20.0	20.2	30.1
CRCM-CGCM3	24.7	23.3	32.3
ECP2-GFDL	25.1	29.2	26.1
ECP2-HADCM3	20.2	22.4	27.4
HRM3-GFDL	18.2	20.1	27.6
HRM3-HADCM3	15.1	14.8	31.0
MM5I-CCSM	20.9	20.2	31.5
MM5I-HADCM3	24.4	23.0	32.3
RCM3-CGCM3	23.7	23.8	30.3
RCM3-GFDL	29.3	30.4	29.3
WRFG-CCSM	17.7	16.5	32.8
WRFG-CGCM3	17.3	16.4	32.2

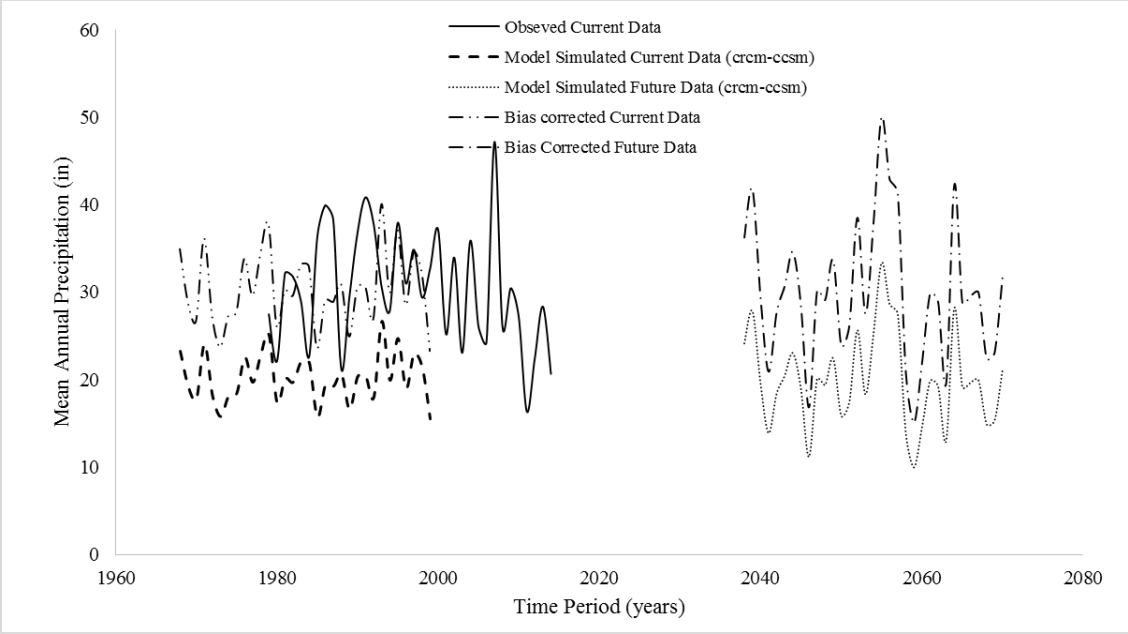

Figure A-22 Bias Correction for Mean Annual Precipitation, Lawton, Oklahoma

Bias Correction for Ardmore, Oklahoma:

Table A-23 Bias Corrected Precipitation Data, Ardmore, Oklahoma

Climate Models	Future Simulation (in)	Current Simulation (in)	Bias-Corrected (in)
CRCM-CCSM	22.2	22.6	29.8
CRCM-CGCM3	27.9	26.9	31.4
ECP2-GFDL	28.5	33.5	25.8
ECP2-HADCM3	25.9	27.7	28.4
HRM3-GFDL	37.6	42.4	26.9
HRM3-HADCM3	36.4	35.9	30.8
MM5I-CCSM	25.1	23.6	32.3
MM5I-HADCM3	28.5	27.3	31.7
RCM3-CGCM3	28.5	29.9	29.0
RCM3-GFDL	35.6	35.2	30.7
WRFG-CCSM	20.5	19.9	31.3
WRFG-CGCM3	21.5	20.6	31.7

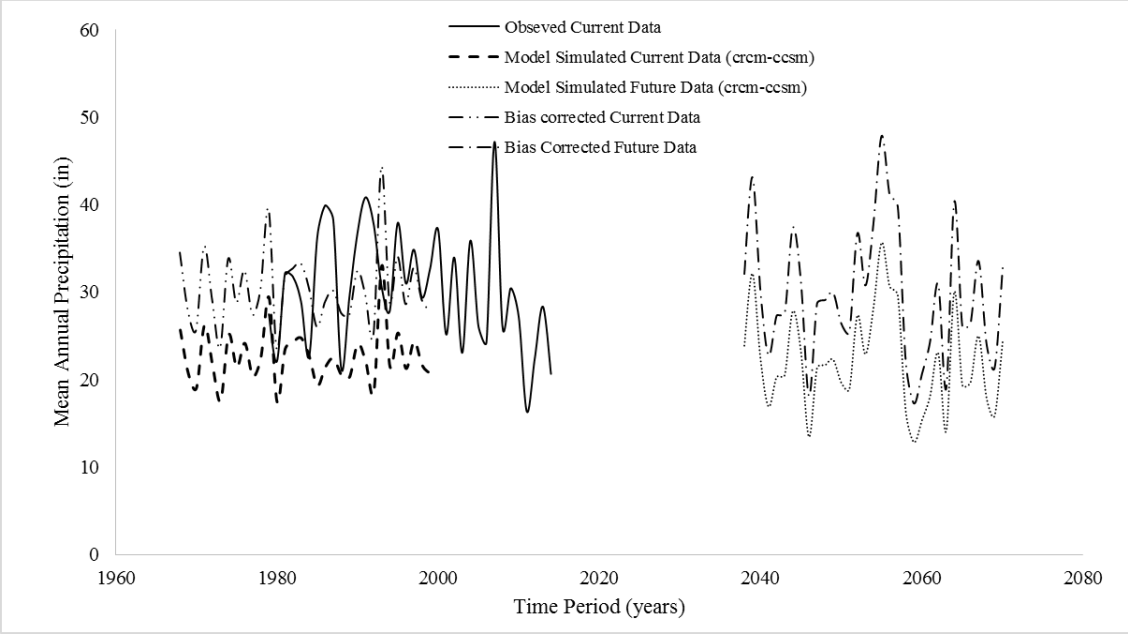

Figure A-23 Bias Correction for Mean Annual Precipitation, Ardmore, Oklahoma

Bias Correction for Fayetteville, Arkansas:

Table A-24 Bias Corrected Precipitation Data, Fayetteville, Arkansas

Climate Models	Future Simulation (in)	Current Simulation (in)	Bias-Corrected (in)
CRCM-CCSM	31.8	32.0	44.6
CRCM-CGCM3	38.6	36.7	47.2
ECP2-GFDL	39.8	45.1	39.6
ECP2-HADCM3	36.0	37.1	43.6
HRM3-GFDL	46.7	47.7	43.9
HRM3-HADCM3	43.8	42.2	46.6
MM5I-CCSM	32.5	32.0	45.5
MM5I-HADCM3	35.1	33.0	47.7
RCM3-CGCM3	37.9	39.3	43.3
RCM3-GFDL	43.0	41.8	46.1
WRFG-CCSM	25.6	24.9	46.1
WRFG-CGCM3	31.3	27.9	50.2

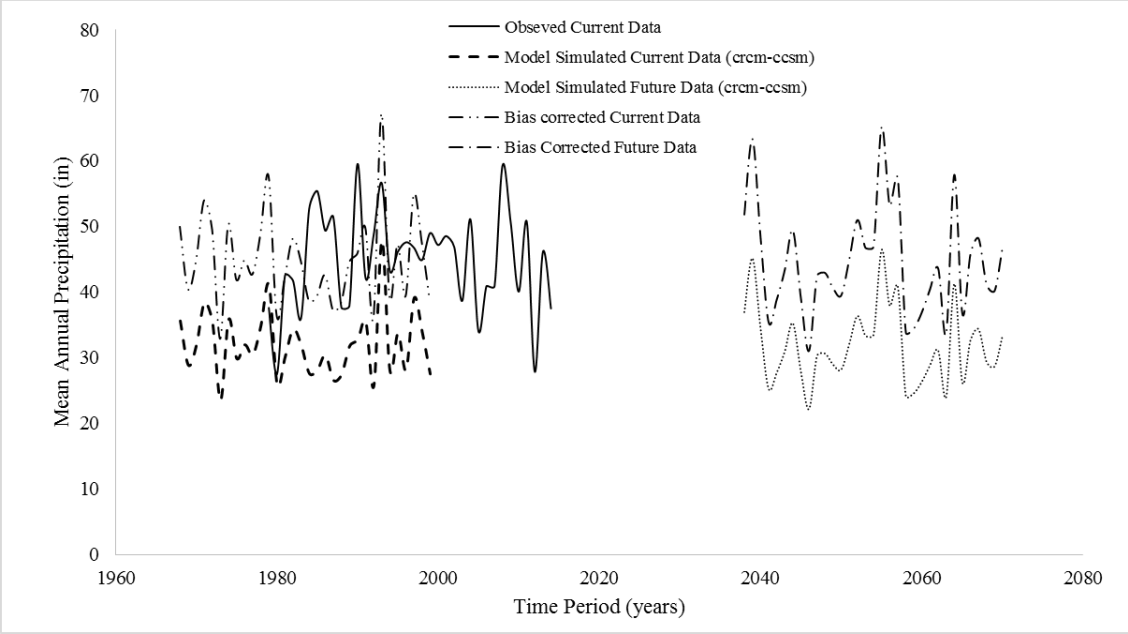

Figure A-24 Bias Correction for Mean Annual Precipitation, Fayetteville, Arkansas

Bias Correction for Fort Smith, Arkansas:

Table A-25 Bias Corrected Precipitation Data, Fort Smith, Arkansas

Climate Models	Future Simulation (in)	Current Simulation (in)	Bias-Corrected (in)
CRCM-CCSM	29.0	29.7	44.4
CRCM-CGCM3	36.5	35.6	46.7
ECP2-GFDL	38.2	42.8	40.6
ECP2-HADCM3	34.5	35.6	44.1
HRM3-GFDL	38.6	38.4	45.7
HRM3-HADCM3	34.7	33.3	47.4
MM5I-CCSM	29.7	30.2	44.7
MM5I-HADCM3	33.5	31.5	48.5
RCM3-CGCM3	36.8	39.6	42.3
RCM3-GFDL	41.4	41.0	45.9
WRFG-CCSM	27.5	26.1	47.9
WRFG-CGCM3	30.8	29.6	47.4

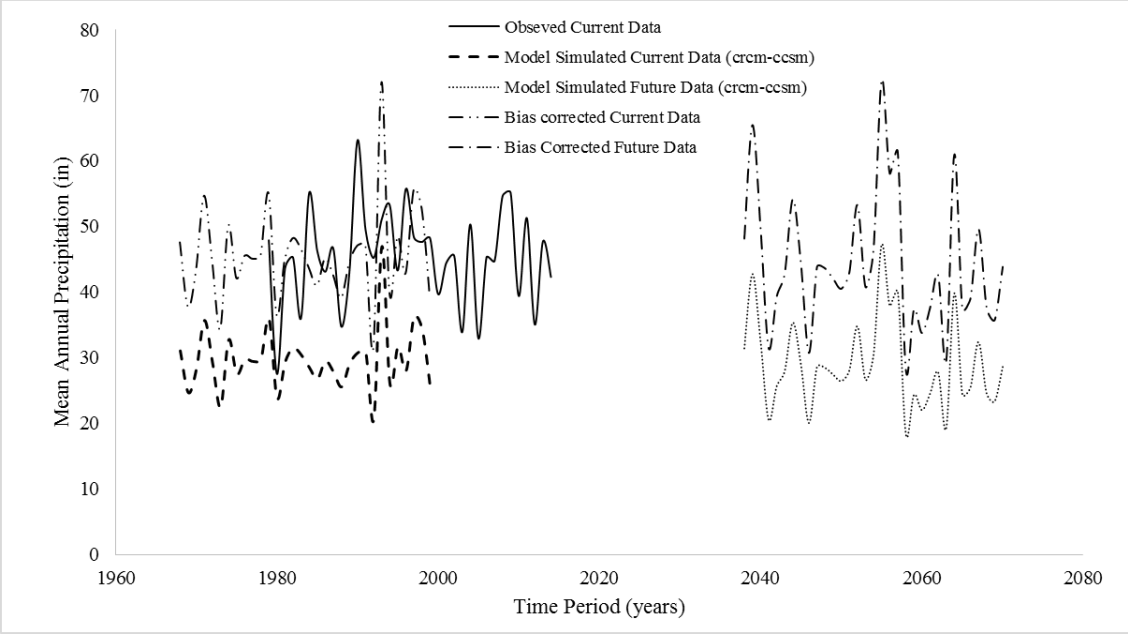

Figure A-25 Bias Correction for Mean Annual Precipitation, Fort Smith, Arkansas

Bias Correction for Conway, Arkansas:

Table A-26 Bias Corrected Precipitation Data, Conway, Arkansas

Climate Models	Future Simulation (in)	Current Simulation (in)	Bias-Corrected (in)
CRCM-CCSM	30.0	30.3	45.3
CRCM-CGCM3	38.4	37.2	47.2
ECP2-GFDL	43.0	47.2	41.8
ECP2-HADCM3	41.0	40.2	46.7
HRM3-GFDL	29.9	33.4	41.1
HRM3-HADCM3	39.3	34.9	51.7
MM5I-CCSM	34.0	34.6	45.1
MM5I-HADCM3	42.7	38.0	51.4
RCM3-CGCM3	42.0	42.0	45.8
RCM3-GFDL	43.7	43.6	46.0
WRFG-CCSM	32.0	31.7	46.4
WRFG-CGCM3	39.4	37.0	48.8

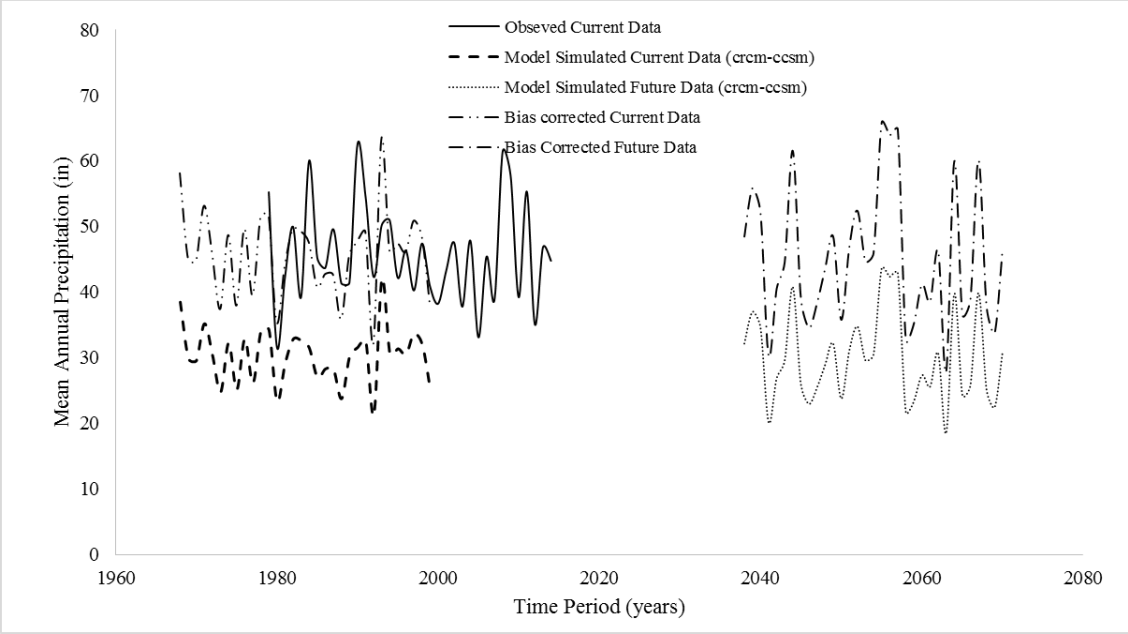

Figure A-26 Bias Correction for Mean Annual Precipitation, Conway, Arkansas

Bias Correction for Hot Springs, Arkansas:

Table A-27 Bias Corrected Precipitation Data, Hot Springs, Arkansas

Climate Models	Future Simulation (in)	Current Simulation (in)	Bias-Corrected (in)
CRCM-CCSM	28.1	29.2	50.7
CRCM-CGCM3	37.0	36.6	53.2
ECP2-GFDL	44.3	48.7	47.8
ECP2-HADCM3	41.6	42.4	51.7
HRM3-GFDL	26.3	29.1	47.5
HRM3-HADCM3	34.9	30.8	59.7
MM5I-CCSM	34.9	36.0	51.1
MM5I-HADCM3	44.2	39.9	58.3
RCM3-CGCM3	41.4	42.0	51.8
RCM3-GFDL	45.4	45.2	52.8
WRFG-CCSM	30.4	30.2	53.0
WRFG-CGCM3	38.6	36.3	56.0

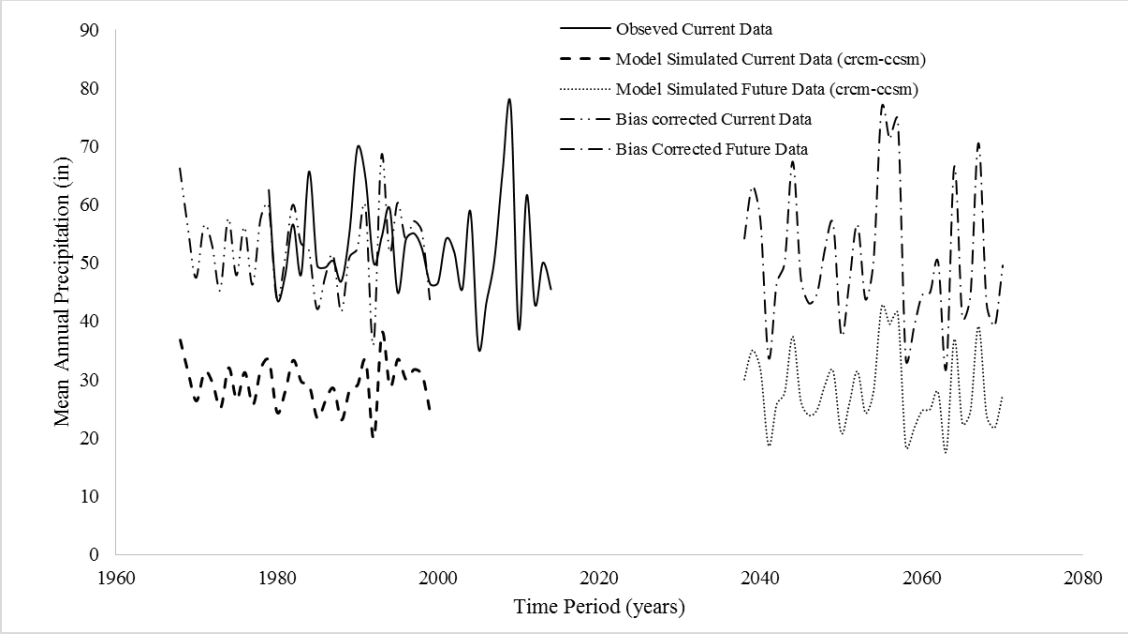

Figure A-27 Bias Correction for Mean Annual Precipitation, Hot Springs, Arkansas

Bias Correction for Pine Bluff, Arkansas:

Table A-28 Bias Corrected Precipitation Data, Pine Bluff, Arkansas

Climate Models	Future Simulation (in)	Current Simulation (in)	Bias-Corrected (in)
CRCM-CCSM	30.4	31.2	45.3
CRCM-CGCM3	39.1	37.6	48.5
ECP2-GFDL	44.6	49.0	42.5
ECP2-HADCM3	44.0	44.6	46.1
HRM3-GFDL	45.1	48.0	43.8
HRM3-HADCM3	45.0	44.2	47.5
MM5I-CCSM	34.2	34.9	45.7
MM5I-HADCM3	45.1	39.5	53.2
RCM3-CGCM3	43.5	43.6	46.5
RCM3-GFDL	45.6	45.5	46.7
WRFG-CCSM	30.0	30.2	46.3
WRFG-CGCM3	38.7	36.9	48.9

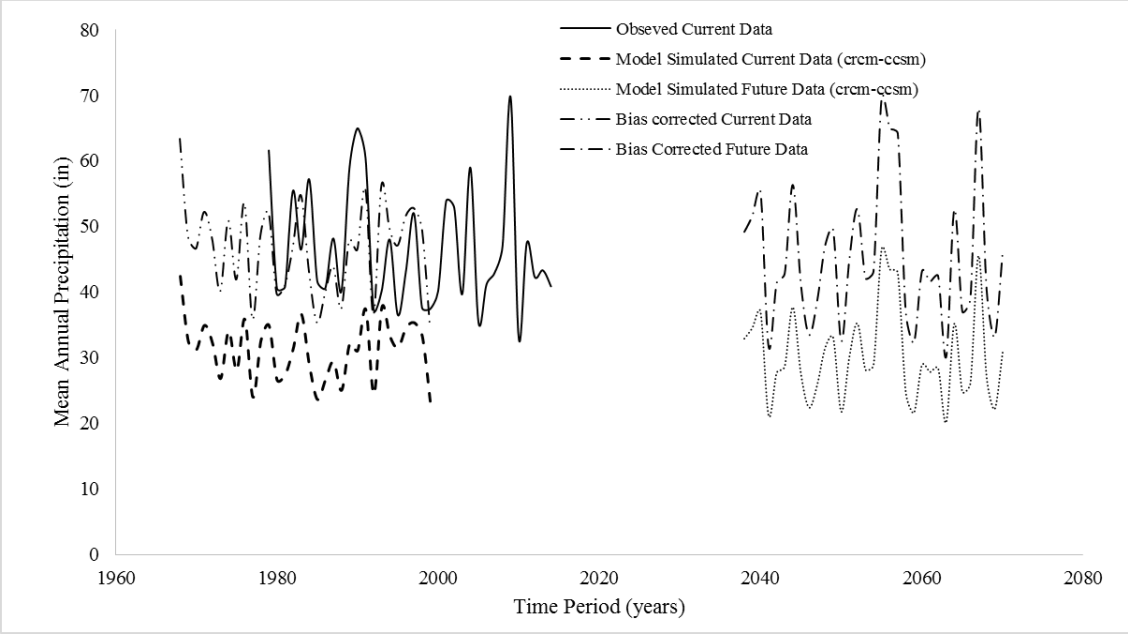

Figure A-28 Bias Correction for Mean Annual Precipitation, Pine Bluff, Arkansas